Adv Polym Sci (2005) 175: 1–128
DOI 10.1007/b100116

Emulsion Polymerization: Kinetic and Mechanistic Aspects

Mamoru Nomura (✉) · Hidetaka Tobita · Kiyoshi Suzuki

Department of Materials Science and Engineering, Fukui University, Fukui, Japan
nomuram@matse.fukui-u.ac.jp, tobita@matse.fukui-u.ac.jp, suzuki@matse.fukui-u.ac.jp

Abstract The current understanding of the kinetics and mechanisms of batch and continuous emulsion polymerizations is summarized from the viewpoints of particle formation and growth and polymer structure development. There are numerous factors that affect these processes; among them, studies on the radical transfer and monomer partitioning between phases, which are key factors for particle formation and growth, are reviewed and discussed. Attention is also focused on the effects of initiator type, additives and impurities in the recipe ingredients, and agitation, each of which sometimes exert crucial influences on the processes of particle formation and growth. In relation to polymer structure development, important aspects of the molecular weight distribution and branched/crosslinked polymer formation are highlighted.

Keywords Emulsion polymerization · Kinetics · Particle nucleation · Particle growth · Molecular weight distribution · Nonlinear polymers

Abbreviations

AA	acrylic acid
AAm	acrylamide
AN	acrylonitrile
APS	ammonium persulfate
AIBN	2,2′-azobis-isobutyronitrile
BA	butyl acrylate
Bu	butadiene
CCTVFR	continuous Couette-Taylor vortex flow reactor
CLTR	continuous loop-tubular reactor
CMC	critical micellar concentration
CSTR	continuous stirred tank reactor
CTR	continuous tubular reactor
DVB	divinylbenzene
E	ethylene
KPS	potassium persulfate
MA	methyl acrylate
MAA	methacrylic acid
MC	Monte Carlo
MMA	methyl methacrylate
MWD	molecular weight distribution
NaLS	sodium laurylsulfate
n-BA	*n*-butyl methacrylate
PSD	particle size distribution
PSPC(R)	pulsed sieve plate column (reactor)
PT(R)	pulsed tubular (reactor)
S-E	Smith and Ewart
SEC	size exclusion chromatography
St	styrene
VAc	vinyl acetate
VCl	vinyl chloride
A_m	total surface area of micelles per unit volume of water
A_p	total surface area of polymer particles per unit volume of water
a_s	surface area occupied by a unit amount of emulsifier
d_m	diameter of a micelle
d_p	diameter of a polymer particle
D_w	diffusion coefficient for radicals in the aqueous phase

D_p	diffusion coefficient for radicals inside a polymer particle
$E(t)$	residence time distribution function
F	absorption efficiency factor defined in Eq. 8
f	initiator efficiency
f_i	fraction of i-radicals in the polymer particle phase
I_0, $[I_0]$	initial initiator concentration
k_d	rate constant for initiator decomposition
k_{em}	mass transfer coefficient for micelles defined by Eq. 7
k_{ep}	mass transfer coefficient for polymer particles defined by Eq. 7
k_f	rate coefficient for radical desorption per particle
k_{mf}	chain transfer rate constant to monomer
k_{tw}	rate coefficient for bimolecular radical termination in the aqueous phase
k_{Tf}	chain transfer rate constants to chain transfer agent (CTA)
m_d	partition coefficient for monomer (monomeric radicals) between particle and aqueous phases defined by $m_d=[M]_p/[M]_m$
M_m	aggregation number of emulsifier molecules per micelle
M_0	initial monomer concentration
$[M]_{pc}$	constant monomer concentration in polymer particles at saturation swelling
$[M]_w$	monomer concentration in the aqueous phase
$\bar{n}_A$	average number of A-radicals per polymer particle
N_n	number of polymer particles containing n radicals
R_p	rate of polymerization
$[R_w^\bullet]$	radical concentration in the aqueous phase
S_0	initial emulsifier concentration
S_m	concentration of emulsifier forming micelles
v_p	volume of a polymer particle
X_{Mc}	critical monomer conversion where monomer droplets disappear from the aqueous phase
α_w	nondimensional parameter defined by $\rho_w v_p/k_{tp}N_T$
ε	defined by $(k_{ep}/k_{em})M_m$ in Eq. 37
λ	partition coefficient for radicals between particle and water phase
μ	volumetric growth rate per polymer particle
θ	mean residence time
ρ	radical entry rate per polymer particle defined by Eq. 12
ρ_e	overall rate of radical entry into polymer particles
ρ_p	polymer density
ρ_w	rate of radical generation per unit volume of water

1 Introduction

There are four main types of liquid-phase heterogeneous free-radical polymerization; microemulsion polymerization, emulsion polymerization, miniemulsion polymerization and dispersion polymerization, all of which can produce nano- to micron-sized polymeric particles. Emulsion polymerization is sometimes called macroemulsion polymerization. In recent years, these heterophase polymerization reactions have become more and more important

technologically and commercially, not only as methods for producing high-performance polymeric materials, but also from an environmental point of view. It is well known that microemulsion, miniemulsion and dispersion polymerizations bare many similarities to emulsion polymerization in the kinetics of particle nucleation and growth and in polymer structure development. Therefore, for optimal design and operation of these heterophase free radical polymerizations, it is important to have detailed knowledge of the kinetics and mechanisms of emulsion polymerization. In this article, recent developments in emulsion polymerization are reviewed from kinetic and mechanistic perspectives.

Between 1995 and 1997, three excellent books on emulsion polymerization were published and provide extensive reviews of the subject up to 1995 [1–3]. Therefore, this review article will focus on research work that has appeared since ~1996. We will also include historically important work from before 1995 in this review article.

2
Emulsion Polymerization Kinetics

2.1
Generally Accepted Kinetics Scheme

Emulsion polymerization takes place over a number of steps, where various chemical and physical events take place simultaneously during the process of particle formation and growth. Figure 1 depicts the generally accepted scheme for the kinetics of emulsion polymerization.

Three major mechanisms for particle formation have been proposed to date. Figure 1a shows the proposed scheme for particle formation in emulsion polymerization initiated by water-soluble initiators. Particle formation is considered to take place when either: (1) a free radical in the aqueous phase enters a monomer-swollen emulsifier micelle and propagation proceeds therein (*micellar nucleation*); (2) the chain length of a free radical growing in the aqueous phase exceeds its solubility limit and precipitates to form a particle nucleus (*homogeneous nucleation*), or; (3) a free radical growing in the aqueous phase enters a monomer droplet and propagation proceeds therein (*droplet nucleation*). However, if the resultant polymer particles are not stable enough, the final number of polymer particles produced, regardless of the mechanism of particle formation, is determined by coagulation between the existing particles (*coagulative nucleation*).

In the process of particle growth, various chemical and physical events occur in both the aqueous and particle phases, as illustrated in Fig. 1b [1]. We now know that the polymerization takes place exclusively in the resultant polymer particle phase, wherever the free radicals are generated. Smith and Ewart [4] were the first to establish a quantitative description of the processes of parti-

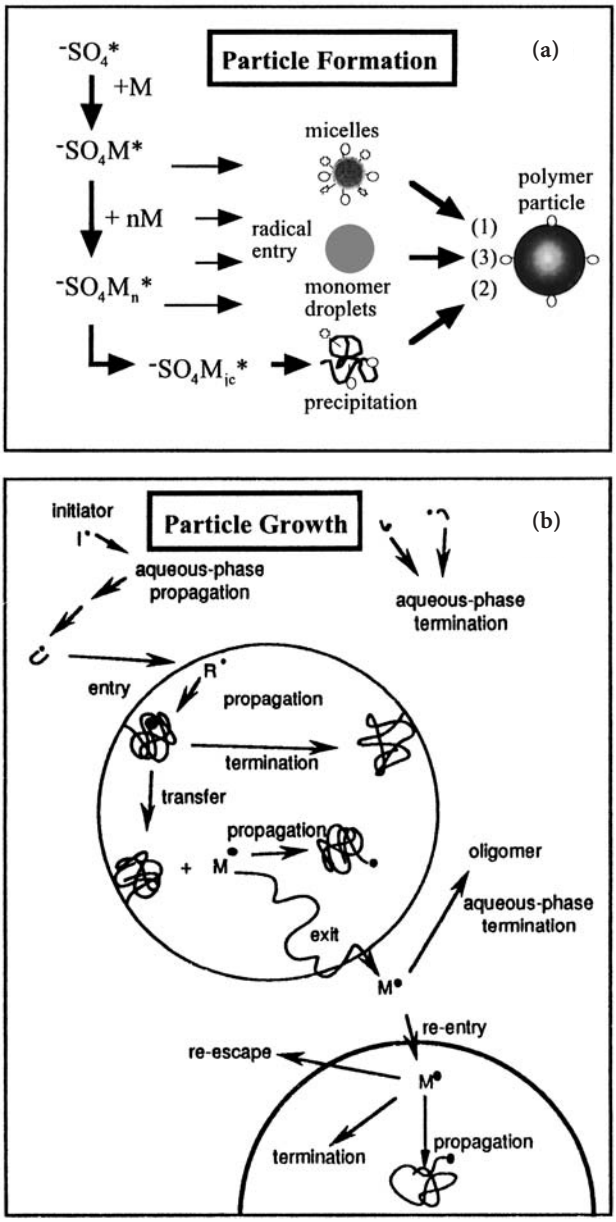

Fig. 1 (**a**) Three major mechanisms of particle formation, and (**b**) various chemical and physical events that occur during the process of particle growth in an emulsion polymerization

cle formation and growth in emulsion polymerization on the basis of the achievements made by Harkins et al. [5]. This is now called the Smith-Ewart theory. It is not an exaggeration to say that almost all of the theoretical developments in emulsion polymerization that have been made so far are based on the Smith-Ewart theory.

2.2 Summary of the Smith-Ewart Theory

The Smith and Ewart theory (the S-E theory) describes the basic concept of emulsion polymerization. Its main points are briefly reviewed here. Smith and Ewart showed that the rate of emulsion polymerization, which proceeds exclusively in the polymer particles, is given by

$$R_p = k_p[M_p]\bar{n}N_T \tag{1}$$

where k_p is the propagation rate constant, $[M]_p$ is the monomer concentration in the monomer-swollen polymer particles, N_T is the number of monomer-swollen polymer particles per unit volume of water and $\bar{n}$ is the average number of radicals per particle, defined as

$$\bar{n} = \sum_{n=1}^{\infty} nN_n \Big/ \sum_{0}^{\infty} N_n = \sum_{n=1}^{\infty} nN_n \Big/ N_T \tag{2}$$

where N_n is the number of polymer particles containing n free radicals. N_n is described by the following balance equation that takes into account three rate processes: (1) radical entry into, (2) radical desorption (exit) from, and (3) bimolecular radical termination inside the polymer particle

$$\begin{aligned} dN_n/dt = {} & (\rho_e/N_T)N_{n-1} + k_f(n+1)N_{n+1} + k_{tp}[(n+2)(n+1)/v_p] \\ & - N_n\{\rho_e/N_T + k_f n + k_{tp}[(n(n-1)/v_p]\} = 0 \end{aligned} \tag{3}$$

where k_f is the rate coefficient for radical desorption per particle, v_p is the volume of a polymer particle, k_{tp} is the rate coefficient for bimolecular radical termination inside the polymer particles, and ρ_e is the overall rate of radical entry into polymer particles, defined by

$$\rho_e = \rho_w + k_f\bar{n}N_T - 2k_{tw}[R_w^*]^2 \tag{4}$$

where ρ_w is the rate of radical production per unit volume of water, k_{tw} is the rate coefficient for bimolecular radical termination in the aqueous phase, and $[R_w^*]$ is the radical concentration in the aqueous phase.

On the other hand, they derived an expression that predicts the number of polymer particles produced, N_T, assuming that (i) a monomer-swollen emulsifier micelle is transformed into a polymer particle by capturing a free radical from the aqueous phase, (ii) the volumetric growth rate per particle μ is constant, at least during particle formation, and (iii) free radical activity does not transfer out of a growing particle

$$N_T = k(\rho_w/\mu)^{0.4}(a_s S_0)^{0.6} \quad (5)$$

where k is a constant between 0.37 and 0.53, a_s is the surface area occupied by a unit amount of emulsifier, S_0 is the initial emulsifier concentration (the concentration of emulsifier forming micelles), and ρ_w is the rate of radical generation per unit volume of water, given by

$$\rho_w = 2k_d f[I_0] \quad (6)$$

where k_d is the rate constant for initiator decomposition, f is the initiator efficiency, and $[I_0]$ is the initial initiator concentration. Since the appearance of the S-E theory, much effort has been directed into investigating the physical meanings of various parameters such as ρ_e, k_f and k_{tp}, and the effects of these parameters on the three key factors of emulsion polymerization, $[M]_p$, $\bar{n}$ and N_T.

3
Kinetics and Mechanisms of Emulsion Polymerization

3.1
Radical Entry

One of the most important parameters in the S-E theory is the rate coefficient for radical entry. When a water-soluble initiator such as potassium persulfate (KPS) is used in emulsion polymerization, the initiating free radicals are generated entirely in the aqueous phase. Since the polymerization proceeds exclusively inside the polymer particles, the free radical activity must be transferred from the aqueous phase into the interiors of the polymer particles, which are the major loci of polymerization. Radical entry is defined as the transfer of free radical activity from the aqueous phase into the interiors of the polymer particles, whatever the mechanism is. It is believed that the radical entry event consists of several chemical and physical steps. In order for an initiator-derived radical to enter a particle, it must first become hydrophobic by the addition of several monomer units in the aqueous phase. The hydrophobic oligomer radical produced in this way arrives at the surface of a polymer particle by molecular diffusion. It can then diffuse (enter) into the polymer particle, or its radical activity can be transferred into the polymer particle via a propagation reaction at its penetrated active site with monomer in the particle surface layer, while it stays adsorbed on the particle surface. A number of entry models have been proposed: (1) the surfactant displacement model; (2) the collisional model; (3) the diffusion-controlled model; (4) the colloidal entry model, and; (5) the propagation-controlled model. The dependence of each entry model on particle diameter is shown in Table 1 [12].

However, some of these models have been refuted, and two major entry models are currently widely accepted. One is the diffusion-controlled model, which assumes that the diffusion of radicals from the bulk phase to the surface

Table 1 Dependence of entry rate coefficient on particle diameter, as predicted by different models [12]

Entry model	Dependence on d_p
Surfactant displacement [7]	none
Collisional [8]	d_p^2
Diffusional [9]	d_p
Colloidal [10]	d_p
Propagational [6, 11]	no dependence

of a polymer particle is the rate-controlling step. The other is the propagation-controlled model, which assumes that since only z-mer radicals can enter the polymer particles very rapidly, the generation of z-mer radicals from (z–1)-mer radicals by a propagation reaction in the aqueous phase is the rate-controlling step.

3.1.1 Diffusion-Controlled Entry

Smith and Ewart [4] first proposed that the transfer of free radical activity into the interior of a polymer particle takes place by the direct entry of a free radical into a polymer particle. They pointed out that the rate of radical entry into a polymer particle is given by the rate of diffusion of free radicals from an infinite medium of concentration $[R_w^*]$ into a particle of diameter d_p with zero radical concentration,

$$\rho_e/N_T = 2\pi D_w d_p [R_w^*] = k_{ep}[R_w^*] \tag{7}$$

where D_w is the diffusion coefficient for the radicals in the water phase and k_{ep} the mass transfer coefficient for radical entry into a particle. However, for simplicity, they actually used a rate coefficient that is proportional to the square of the diameter (the surface area). Since then, most researchers have treated the problem of particle formation by assuming that the rate of radical entry into a micelle and a polymer particle is proportional to the surface area (*the collisional entry model*) [8, 13].

On the other hand, Nomura and Harada [14] proposed a kinetic model for the emulsion polymerization of styrene (St), where they used Eq. 7 to predict the rate of radical entry into both polymer particles and monomer-swollen micelles. In their kinetic model, the ratio of the mass-transfer coefficient for radical entry into a polymer particle k_{ep} to that into a micelle k_{em}, k_{ep}/k_{em}, was the only one unknown parameter (Eq. 37). They determined the value of k_{ep}/k_{em} to be about 10^3 by comparing the model's predictions with experimental results. However, the observed value of k_{ep}/k_{em} was at least two orders of magnitude greater than that predicted by Eq. 7, because $k_{ep}/k_{em}=d_p/d_m$ (d_m is the

diameter of a micelle) according to Eq. 7 and the value of d_p/d_m would be 10 at the most during particle formation. This was considered to indicate that the radical capture efficiency of a micelle is a factor of about 100 less than that of a particle. Taking this into consideration, they implicitly introduced a concept called the "radical capture efficiency of a micelle relative to a polymer particle" to adjust for this disagreement and pointed out two possible reasons for the lower radical capture efficiency of a micelle. One is that the energy barrier against the entry of charged radicals into micelles may be higher than that into polymer particles. The other is that an oligomeric radical, having entered a micelle, may pass through the micelle without adding at least one extra monomer unit because the volume of the micelle is so small that the mean residence time of the radical in the micelle is too short for the radical to add another unit.

The concept of "radical capture efficiency" was further elaborated on by Hansen et al. [15–17]. By applying the theory of mass transfer with simultaneous chemical reactions, they proposed the following expression to represent the *net rate* of radical absorption by a particle, introducing an "*absorption efficiency factor*" *F* into Eq. 8

$$\rho_e/N_T = 2\pi D_w d_p [R_w^*] F = k_{ep}[R_w^*]. \tag{8}$$

Therefore, *F* represents a factor that describes the degree to which absorption is lowered compared to irreversible diffusion, and is given by

$$\frac{1}{F} = \left(\frac{D_w}{\lambda D_p}\right)(X \coth X - 1)^{-1} + W' \tag{9}$$

where $X=(d_p/2)\{(k_p[M]_p+nk_{tp}/v_p)/D_p\}^{1/2}$ and λ is the equilibrium partition coefficient between particles and water for radicals, W' is the potential energy

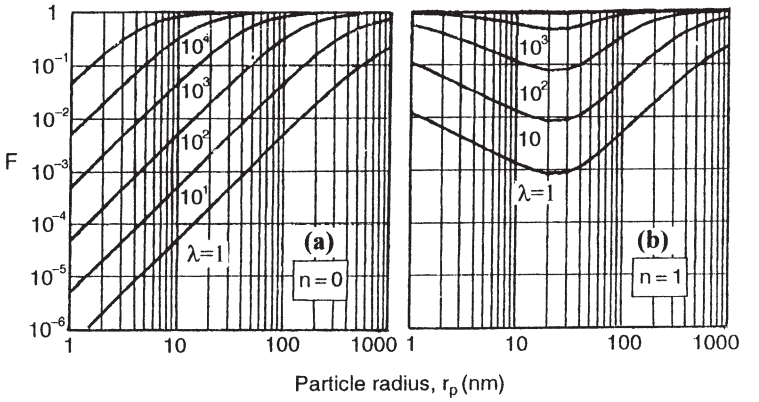

Fig. 2 Capture efficiency *F* as a function of particle size r_p for different values of the partition coefficient, λ, and the number of radicals in a polymer particle for St polymerization; (**a**) n=0 and (**b**) n=1

barrier analogous to Fuchs' stability factor, D_p is the diffusion coefficient for the radicals inside a particle, k_p is the propagation rate constant, $[M]_p$ is the monomer concentration in particles, n is the number of radicals in a particle, N_A is Avogadro's number and v_p is the particle volume. It should be noted that radicals are captured inside the particles only if they react therein; otherwise they will eventually diffuse out and back to the water phase. Figure 2 shows an example of F versus particle radius r_p, calculated from Eq. 9. The important conclusion of Eq. 9 is, as is clear from Fig. 2, that the value of F for a particle containing radicals is higher than that for a particle containing no radicals. According to Fig. 2a, it approximately holds that $F \propto d_p^2$, and hence this model gives $k_{ep}/k_{em}=(d_p/d_m)(F_p/F_m)=(d_p/d_m)^3 \cong 10^3$, the value of which is in good agreement with the result obtained by Nomura et al. in the emulsion polymerization of St [14].

A much simpler model for the radical capture (absorption) efficiency F can be derived by introducing the concept of radical desorption from a polymer particle, developed in Section 3.2.1. The probability F for a radical to be captured inside a particle containing n radicals by any chemical reaction (propagation or termination) is given by

$$F = \frac{k_p[\mathrm{M}]_p + k_{tp}(n/v_p)}{K_o + k_p[\mathrm{M}]_p + k_{tp}(n/v_p)} \tag{10}$$

where K_o is the overall radical desorption rate constant for a particle, defined by Eq. 19 and shown later in Section 3.2.1. For simplicity, no distinction is made here between radicals with and without initiator fragments at their ends. In the case where $K_o \gg k_p[\mathrm{M}]_p$, $k_{tp}(n/v_p)$, substitution of Eq. 19 into Eq. 10 leads to

$$F = k_p[\mathrm{M}]_p/K_o = \left(\frac{k_p[\mathrm{M}]_p m_d}{12D_w}\right)\left(1 + \frac{\psi D_w}{m_d D_p}\right) d_p^2 \propto d_p^2 \tag{11}$$

The result of Eq. 11 agrees with $F \propto d_p^2$ obtained above by Ugelstad and Hansen [15]. Therefore, both Eq. 9 developed by Hansen and Ugelstad and Eq. 11 developed here can explain the value of $k_{ep}/k_{em} \cong 10^3$ found experimentally by Nomura et al. [14], although no direct experimental confirmation of the validity of these radical capture models have been reported yet.

Unzueta et al. [18] derived a kinetic model for the emulsion copolymerization of methyl methacrylate (MMA) and butyl acrylate (BA) employing both the micellar and homogeneous nucleation mechanisms and introducing the radical absorption efficiency factor for micelles, F_m, and that for particles, F_p. They compared experimental results with model predictions, where they employed the values of $F_p=10^{-4}$ and $F_m=10^{-5}$, respectively, as adjustable parameters. However, they did not explain the reason why the value of F_m is an order of magnitude smaller than the value of F_p. Sayer et al. [19] proposed a kinetic model for continuous vinyl acetate (VAc) emulsion polymerization in a pulsed

sieve plate column reactor, where they assumed that both micellar and homogeneous nucleation takes place, and introduced the radical absorption efficiency factor F_m for micelles and F_p for polymer particles, respectively. They could explain the experimental results by employing $F_m=1.0\times10^{-5}$ and $F_p=3.3\times10^{-3}$ in the model predictions, indicating that $k_{ep}/k_{em}=330$. This value agrees fairly well with the value of 100 found for the St system [14], but is 30 times less than $k_{ep}/k_{em}=10^4$ found for the VAc system [20]. Araújo et al. [21] developed a detailed dynamic mathematical model that describes the evolution of particle size distributions (PSDs) during the emulsion copolymerization of VAc and Veova10 in a continuous loop-tubular reactor and compared results from it with their experimental data. They could describe the process of micellar particle formation by introducing radical absorption efficiency factors for micelles of $F_m=1.5\times10^{-4}$ and for particles of $F_p=1.5\times10^{-3}$, respectively, although they also did not provide a reason why the value of F_m is 1/10 of the value of F_p. This gives $k_{ep}/k_{em}=(d_p/d_m)(F_p/F_m)\cong10^2$ if one assumes that $d_p/d_m\cong10$. On the other hand, Herrera-Ordóñez et al. [22] also developed a mathematical model for St emulsion polymerization employing Eq. 8 as the radical capture rate coefficient, where the expression for the capture of monomeric radicals is that used by Hansen and Ugelstad [15, 17], while a more detailed modification was made for the entry of initiator-derived radicals.

3.1.2 Propagation-Controlled Entry

Maxwell et al. [11] proposed a radical entry model for the initiator-derived radicals on the basis of the following scheme and assumptions. The major assumptions made in this model are as follows: An aqueous-phase free radical will irreversibly enter a polymer particle only when it adds a critical number z of monomer units. The entrance rate is so rapid that the z-mer radicals can survive the termination reaction with any other free radicals in the aqueous phase, and so the generation of z-mer radicals from (z–1)-mer radicals by the propagation reaction is the rate-controlling step for radical entry. Therefore, based on the generation rate of z-mer radicals from (z–1)-mer radicals by propagation reaction in the aqueous phase, they considered that the radical entry rate per polymer particle, ρ ($\rho=\rho_e/N_T$) is given by

$$\rho = k_{pw}[\mathrm{IM}^{\star}_{z-1}][\mathrm{M}]_w N_T \tag{12}$$

where k_{pw} is the propagation rate constant in the aqueous phase and $[M]_w$ is the monomer concentration in the aqueous phase. By substituting the steady-state concentration of (z–1)-mer radicals $[\mathrm{IM}^{\star}_{z-1}]$ into Eq. 12, the approximate expressions for ρ and the initiator efficiency, f_{entry} are derived, respectively, as

$$\rho = \frac{2k_d[\mathrm{I}]}{N_p}\left\{\frac{\sqrt{k_d[\mathrm{I}]k_{t,w}}}{k_{p,w}[\mathrm{M}]_w}+1\right\}^{1-z} = \frac{2k_d[\mathrm{I}]}{N_p}f_{entry} \tag{13}$$

$$f_{\text{entry}} = \left\{ \frac{\sqrt{k_{\text{d}}[\text{I}]k_{\text{t,w}}}}{k_{\text{p,w}}[\text{M}]_{\text{w}}} + 1 \right\}^{1-z} \tag{14}$$

There has been discussion on the value of z. Maxwell et al. [11] proposed a semi-empirical thermodynamic model to predict the value of z for persulfate-derived oligomeric radicals, which is given by

$$z \cong 1 + \text{int}\left(-23\ \text{kJmol}^{-1}/\{RT \ln[\text{M}_{\text{sat}}]_{\text{w}}\}\right) \tag{15}$$

where the integer function (int) rounds down the quantity in parentheses to the nearest integer value and $[\text{M}_{\text{sat}}]_{\text{w}}$ is the saturation solubility of the monomer in mol dm^{-3}. On the other hand, Sundberg et al. [23] proposed a thermodynamic method for estimating the critical chain length z of entry radicals with a hydrophilic end group (such as SO_4^-) using a simple two-layer lattice model. The values of z calculated by both Sundberg et al. and by Maxwell et al. (Eq. 15) are listed in Table 2.

Several research articles have been published that deal with the methodology for determining the radical entry rate ρ, the initiator efficiency f_{entry} and the actual values of z. Hawkett et al. [24] developed a method for determining the value of ρ along with the desorption rate coefficient k_{fs}, termed the *slope-and-intercept* method. This method is experimentally simple, but has several drawbacks [25]. For example, it is only applicable to the so-called zero-one system ($\bar{n} \leq 0.5$) with negligible radical termination in the aqueous phase. It is usually very difficult to judge whether or not the radical termination in the aqueous phase is negligible. Moreover, it gives a large error if an induction period caused by any trace of impurity exists. Marestin et al. [26] proposed an experimental method for directly determining the entry rate of a critical size MMA oligomer into the polymer particle using the seeded emulsion polymerization of MMA

Table 2 Predicted Z values for persulfate-derived radicals

Monomer	Z value	
	Maxwell et al., at 50 °C [1]	Sundberg et al., at 25 °C [23]
2-EHA	–	1
Styrene (St)	2–3	2
Butyl methacrylate (BMA)	3	2
Butyl acrylate (BA)	2–3	2
Butadiene (Bu)	3	2
Ethyl acrylate (EA)	–	4
Methyl methacrylate (MMA)	4–5	4
Vinyl acetate (VAc)	–	5
Methyl acrylate (MA)	–	8
Acrylonitrile (AN)	–	>10 (estimate: 12)

initiated by KPS. The initial seed latex used was synthesized so as to have radical traps (TEMPO) covalently bound onto the particle surface. When an aqueous phase-propagating radical entered a seed particle, the nitroxide moiety led to the formation of a stable alkoxyamine. Therefore, the kinetics of radical entry into the seed particles was followed by monitoring the decay of the ESR signal from the nitroxide in the samples withdrawn from the reactor. They obtained f_{entry}=0.36 for KPS at 70 °C and f_{entry}=0.33 for V-50 at 70 °C, respectively. Maxwell et al. [11] obtained the value of $z \cong 2$ by comparing the model predictions with the experimental results in the emulsion polymerization of St. Schoonbrood et al. [27] reported $z \cong 18$ for a 80:20/St:MA emulsion copolymerization system. However, there is an example where it is difficult to explain the kinetic behavior of the emulsion copolymerization of St and AAm without assuming z=(one St monomer unit), as shown later in Section 3.2.3.

3.1.3 Miscellaneous Kinetic Problems in Radical Entry

Two major entry models – the diffusion-controlled and propagation-controlled models – are widely used at present. However, Liotta et al. [28] claim that the collision entry is more probable. They developed a dynamic competitive growth model to understand the particle growth process and used it to simulate the growth of two monodisperse polystyrene populations (bidisperse system) at 50 °C. Validation of the model with on-line density and on-line particle diameter measurements demonstrated that radical entry into polymer particles is more likely to occur by a collision mechanism than by either a propagation or diffusion mechanism.

One of the most basic and important problems to be clarified in emulsion polymerization is what kind of radicals can enter the polymer particles. A proposal now widely accepted is that in the emulsion polymerization of St initiated by, for example, potassium persulfate (KPS), an entering radical must be surface active, so it must be a charged oligomer such as $\cdot M_z SO_4^-$ [11]. Tauer et al. [29] carried out MALDI-TOF-MS investigations of the polymer inside the particles at the end of a persulfate-initiated emulsifier-free emulsion polymerization of St, and showed that besides sulfate end groups, a variety of different end groups for the polymer molecules exist almost independently of the buffer concentration employed during the polymerization. These results support the existence of the following end group combinations: H–H, H–OH, K^{+-}OO–OH, K^{+-}OO–K^{+-}OO, OH–OH, $K^{+-}OSO_3$–H, $K^{+-}OSO_3$–OH, $K^{+-}OSO_3$–$K^{+-}OSO_3$. They concluded from these experimental results that the entering radicals can be either corresponding primary radicals (H, OH, or O_3SO radicals) or oligomer radicals, and therefore surface activity is not a prerequisite condition for the entering radicals.

Another important problem that has been debated for a long time is whether or not the electric charges and the emulsifier layers on the surfaces of the polymer particles affect the radical entry rate of a charged radical (ρ). It is now con-

firmed that for conventional emulsifiers such as sodium lauryl sulfate (NaLS, electrostatic stabilizer), the extent of the surface coverage on a particle and the ionic strength have no effect on radical entry, within experimental error margins [10, 30]. Adams et al. [30] found that the radical entry rate is independent not only of the surface coverage and the ionic strength, but also of differences in the kind of charges between the particle surface and the entering free radical. Furthermore, they refuted, on the basis of experimental data, the proposals that the rate of radical entry is controlled by surfactant displacement [7] and by collision of free radicals with the polymer particles [31]. Penbos et al. [10] carried out the seeded emulsion polymerization of St using a PSt seed latex with negative surface charge in combination with three different initiators: persulfate anions (negatively charged radicals), hydrogen peroxide/iron (II) (neutral radicals) and 2,2′-azobis(2-amidinopropane) (V-50, cationic free radicals). They found that the rate of radical entry showed no significant dependence on the kind of charges of these initiating radicals. El-Aasser et al. [25] examined the effect of an adsorbed layer of the nonionic emulsifier (steric stabilizer) TritonX-405 (octylphenoxypolyethoxy ethanol with an average number of 40 ethylene oxide units) on the rate of radical entry by changing the ratio of anionic (NaLS) and nonionic emulsifiers in the seeded emulsion polymerization of St initiated by KPS. They concluded that any variation in surface coverage by the nonionic emulsifier did not significantly affect the value of ρ within experimental error, suggesting that the adsorbed layer of the nonionic emulsifier on the particle surface would not act as a barrier to radical entry. Contrary to the observations of El-Aasser et al. [25], Kuster et al. [32] observed a large decrease in the desorption rate coefficient for monomeric radicals in the emulsion polymerization of St conducted using poly(ethylene oxide) nonylphenol surfactant with an average number of 30 ethylene oxide units as the steric stabilizer. They concluded from this observation that a "hairy" layer near the particle surface would also act as a barrier for the entry of such uncharged radicals because re-entry of desorbed radicals is the reverse process of desorption. Wang et al. [33] conducted the seeded emulsion polymerization of St using the reactive surfactant sodium dodecyl allyl sulfosuccinate (TREM LF-40) and its polymeric counterpart, poy(TREM), and only observed an increase in the PSt molecular weight when poly(TREM) was used. This was considered to be a consequence of the decrease in the rate of bimolecular radical termination resulting from the decrease in the rate of radical entry into the polymer particles due to the diffusion barrier of the hairy layer near the particle surface to the diffusing radicals.

On the other hand, several reports have been published that point out that when a polymeric surfactant acting as an electrosteric stabilizer is used, the rate of radical entry into a polymer particle should decrease due to a diffusion barrier of the hairy layer built up by the polymeric surfactant adsorbed on the surface of the polymer particles [34–36]. Coen et al. [34] found that in the seeded emulsion polymerization of St using a PSt seed latex stabilized electrosterically by a copolymer of acrylic acid (AA) and St, the electrosteric stabilizer greatly reduced the radical entry rate ρ compared to the same seed latex

with a conventional electrostatic stabilizer. The explanation was that the "hairy" layer on the surface of the polymer particle acted as a diffusion barrier to the entering radicals. Kim et al. [35] also observed the decrease in the value of ρ in the seeded emulsifier-free emulsion polymerization of MMA conducted using KPS as the initiator and a PSt seed latex electrosterically coated by a copolymer of St and styrenesulfonate (NaSS), which constitutes a thick hairly layer on the particle surface. Vorwerg et al. [36] observed a decrease in the value of ρ, although it was dependent on the pH, in the seeded emulsion polymerization of St using seed latexes electrosterically stabilized with poly(acrylic acid). Leeman et al. [37], on the other hand, synthesized amphiphilic water-soluble polyelectrolytes, a poly(methyl methacrylate-*block*-sulfonated glycidyl methacrylate) block copolymer (PMMA-*b*-SPGMA; polyanionic block copolymer) and a poly(methyl methacrylate-*block*-quaternized *N*,*N*′-dimethylaminoethyl methacrylate) block copolymer (PMMA-*b*-QPDMAEMA; polycationic block copolymer). They carried out the emulsion polymerization of MMA at 60 °C in the presence of these two copolymers as surfactants and with the following four types of initiators: KPS producing anionic radicals, H_2O_2 and AIBN both producing neutral radicals and AAP (2,2′-azobis(2-amidinopropane)) which generates cationic radicals in acid medium and neutral radicals in basic medium. There was no major difference in the rate of polymerization R_p when the initiators producing neutral radicals were combined with either of these two oppositely charged copolymer surfactants. But a large decrease in R_p was observed when the charge of the entering radical was different to the charge of the block polyelectrolyte surfactant. Considering the experimental results of El-Aasser et al. [25], the former finding is acceptable, but the latter one is contrary to our expectations and the conclusions given in the articles [34–36]. Therefore, clarifying whether or not the adsorbed layer of polymeric surfactants on the particle surface act as a diffusion barrier to the entering radicals is still an important problem that needs to be solved in the future.

In the emulsion copolymerization of the water-soluble monomer acrylamide (AAm) and the sparingly water-soluble monomer St using KPS as initiator, Kawaguchi et al. [38] observed odd kinetic behavior. Regardless of the fraction of AAm in the monomer feed, the polymerization of both monomers started from the beginning of the reaction, but soon the AAm polymerization slowed down and finally stopped, while the polymerization of St continued very smoothly to the end. Nomura et al. [39] examined the reason for this abnormal kinetic behavior and ascribed the reason to unusual radical entry behavior. They studied the seeded emulsion copolymerization of St and AAm at 50 °C using PSt particles as the seed and KPS as the initiator, and found that the change in the number of PSt seed particles N_s caused a drastic change in the kinetic behavior of this emulsion copolymerization system. When the number of seed particles was less than a certain critical value N_c (~2.5×10^{12} particles/cm^3-water), both St and AAm started polymerizing as soon as the initiator was added. However, when the number of seed particles was higher than N_c, an apparent induction period suddenly appeared for AAm polymerization; in other words,

although more than 99% of the initially charged AAm existed in the aqueous phase, the AAm polymerization did not start until the St conversion exceeded around 75%. Therefore, the apparent induction period was the time necessary for the St conversion to reach 75%. On the other hand, the St polymerization started and continued very smoothly from the beginning to the end of the reaction, independently of the AAm polymerization. We have not yet succeeded in explaining this interesting phenomenon quantitatively, but the reason may be explained qualitatively as follows [40]. Using values for the monomer reactivity ratio and the concentrations of St and AAm in the aqueous phase, it is clear that the addition rate of St radicals to AAm is about 100 times faster than to St and the addition rate of AAm radicals to AAm is about 5 times faster than to St in the aqueous phase. Therefore, once an AAm radical is formed in the aqueous phase, this AAm radical preferentially adds AAm monomer in the aqueous phase without entering the polymer particles due to its hydrophilicity. When the number of initially charged PSt seed particles is higher than N_c, no AAm polymerization occurs in the aqueous phase although all free radicals are produced in the aqueous phase and almost all AAm monomer units exist in the aqueous phase. This implies that KPS radicals preferentially add St monomer units as soon as they are generated in the aqueous phase and enter the seed particles before the resultant St radicals add one AAm monomer unit. This is because the mean residence time of the St radicals in the aqueous phase before they enter the seed particles is shorter than the average time necessary for these radicals to add one AAm monomer unit. On the other hand, when the number of seed particles is less than N_c, the mean residence time of most of the St radicals would become longer than the average time necessary for a St radical to add one AAm monomer unit, and so these St radicals are mostly transformed into AAm radicals, although some of these radicals can enter the seed particles and continue St polymerization inside the particles. Therefore, the St radicals produced continue AAm polymerization in the aqueous phase. The mechanism of radical entry proposed in this copolymerization system contradicts the conclusions of Maxwell et al. [11], who claimed that KPS radicals need to add at least 2–3 St monomer units before entering the monomer-swollen polymer particles.

3.2 Radical Desorption

3.2.1 Desorption in Homopolymer Systems

The desorption (exit) of free radicals from polymer particles into the aqueous phase is an important kinetic process in emulsion polymerization. Smith and Ewart [4] included the desorption rate terms into the balance equation for N_n particles, defining the rate of radical desorption from the polymer particles containing n free radicals in Eq. 3 as $k_f n N_n$. However, they did not give any

detailed discussion on radical desorption. Ugelstad et al. [41] pointed out that the rate coefficient for radical desorption (the desorption rate coefficient) could be a function of particle size, the rate of chain transfer to monomer, the rate of polymerization and the diffusion coefficients involved in the transport processes leading to desorption of radicals, and suggested that, in the emulsion polymerization of VCl, the desorption rate coefficient, k_f might be expressed in the form

$$k_f = kv_p^{-2/3} = k'd_p^{-2} \tag{16}$$

On the other hand, Nomura and Harada [14, 42–45] pointed out that radical desorption from the polymer particles and micelles plays a decisive role in particle formation and growth, and further that there are many examples of kinetic deviations from the S-E theory that are attributable to radical desorption. First, they theoretically derived the desorption rate coefficient from both stochastic [42] and deterministic approaches, [14, 42, 43] based on a scheme consisting of the following three consecutive steps: (1) chain-transfer of a polymeric radical to a monomer molecule or a species like CTA in a polymer particle, followed by (2) diffusional transportation of the resulting low molecular weight radical to the particle-water interface, and (3) successive diffusion into the bulk water phase through a stagnant film adjacent to the surface of the particle. In modeling the rate coefficient for radical desorption, the following assumptions were made:

A1. Polymer particles contain at most one radical (zero-one system).
A2. An oligomeric radical with no more than *s* monomer units can desorb from and re-enter into a polymer particle with the same rate, irrespective of its chain length.
A3. Instantaneous termination takes place when another radical enters a particle already containing a radical.
A4. No distinction is made between radicals with or without an initiator fragment on its end.
A5. Water-phase reactions such as propagation, termination, and chain-transfer to a monomer are negligible for the desorbed radicals. This means that all of the desorbed radicals would re-enter particles and the loss of these radicals occurs only through the event given by the assumption A3).
A6. The physical and chemical properties of chain transfer agent (CTA) radicals are approximately equal to those of monomer radicals.

Based on these assumptions, they derived the desorption rate coefficient k_f as

$$k_f = K_{oI}\left[\frac{\rho_w(1-\bar{n})}{K_{oI}\bar{n} + k_i[M]_p\bar{n}N_p}\right] + K_o\left[\frac{k_{mf}}{k_p} + \frac{k_{Tf}[T]_p}{k_p[M]_p} + \frac{\rho_w(1-\bar{n})k_i}{K_{oI}\bar{n} + k_i[M]_p k_p\bar{n}N_p}\right] \cdot \sum_{j=1}^{S}\left(\frac{k_p[M]_p}{K_o\bar{n} + k_p[M]_p}\right)^j \tag{17}$$

When it is assumed that initiator-derived radicals do not exit and only monomeric and CTA radicals produced by chain transfer to a monomer and/or a CTA can desorb (s=1), Eq. 17 can be simplified as

$$k_f = K_o\left(\frac{k_p[M]_p}{K_o\bar{n} + k_p[M]_p}\right)\left(\frac{k_{mf}}{k_p} + \frac{k_{Tf}[T]_p}{k_p[M]_p}\right) \tag{18}$$

where k_{mf} and k_{Tf} are the chain transfer rate constants to monomer and to CTA, respectively, and K_o is the overall desorption rate constant per particle for monomeric (or CTA) radicals, which is approximately given by [42–44]

$$K_o = \left(\frac{2\pi D_w d_p}{m_d v_p}\right)\left[1 + \frac{\psi D_w}{m_d D_p}\right]^{-1} = \left(\frac{12 D_w \delta}{m_d d_p^2}\right) \tag{19}$$

where δ=$(1+\psi D_w/m_d D_p)^{-1}$ denotes the ratio of the aqueous-side to overall diffusion resistance, ψ is a numerical constant between 1 and 6 that depends on the mass-transfer coefficient employed (ψ=1 if Eq. 7 is assumed to be applicable to the mass-transfer process inside the polymer particles) [42–45], m_d is the partition coefficient for monomer radicals between the polymer particle and aqueous phases, defined by m_d=$[M]_p/[M]_w$, and the term, $\psi D_w/m_d D_p$ is the ratio of the particle-side to water-side diffusion resistance. Ugelstad et al. [9] obtained the same expression as Eq. 19 with ψ=1. On the other hand, Casey et al. [1, 46] also derived the same expression as Eq. 19 with δ=1. However, it must be noted that when the diffusion resistance inside the particle is far greater than that in the aqueous-side effective diffusion film, that is, $D_w/m_d D_p \gg 1$, one gets

$$K_o = \left(\frac{2\pi D_w d_p}{m_d v_p}\right)\left[1 + \frac{\psi D_w}{m_d D_p}\right]^{-1} = \left(\frac{12 D_p}{d_p^2}\right) \tag{19a}$$

For the St emulsion polymerization, for example, in the absence of CTA, it usually holds that $K_o\bar{n} \ll k_p[M]_p$, at least in the range where monomer droplets exist. Then, Eq. 18 is reduced to

$$k_f = K_o\left(\frac{k_{mf}}{k_p}\right) = \left(\frac{12 D_w \delta}{m_d d_p^2}\right)\left(\frac{k_{mf}}{k_p}\right) = \left(\frac{12 D_w C_m \delta}{m_d}\right) d_p^{-2} \tag{20}$$

where C_m is the monomer chain transfer constant. The validity of Eq. 20 has been demonstrated by Nomura et al. [20, 42, 44, 47] and Adams et al. [48]. Equation 18 was derived under the assumption that the physical and chemical properties of a CTA radical are approximately equal to those of a monomeric radical. However, if it is necessary to take into account the differences in the physical and chemical properties between monomeric and CTA radicals, Eq. 18 can be modified approximately as

$$k_f = K_{om}\left(\frac{k_{mf}[M]_p}{K_{om}\bar{n} + k_p[M]_p}\right) + K_{oT}\left(\frac{k_{Tf}[T]_p}{K_{oT}\bar{n} + k_{iT}[M]_p}\right) \tag{18a}$$

where K_{om} and K_{oT} are the overall desorption rate constants per particle for monomeric and CTA radicals, respectively.

Ugelstad et al. [9] later derived almost the same desorption rate coefficient as Eq. 19 given by

$$k_f = \left(\frac{12D_w}{m_d d_p^2}\right)\left(\frac{k_{mf}}{k'_p}\right)\left(1 + \frac{D_w}{m_d D_p}\right)^{-1} = \left(\frac{12D_w\delta}{m_d d_p^2}\right)\left(\frac{k_{mf}}{k'_p}\right) \tag{21}$$

where k'_p is the rate constant for the reaction between a monomeric radical formed by chain transfer and a monomer, the value of which may be different from the value of k_p, the propagation rate constant.

Asua et al. [49–51] modified Eq. 18 in the absence of a CTA to include more general cases, taking into account the fate of the desorbed radicals (both chemical reactions in the water phase and re-entry) as

$$k_f = k_{mf}[M]_p\left(\frac{K_o}{K_o\beta + k_p[M]_p}\right) \tag{22}$$

where β stands for the fraction of desorbed radicals that cannot re-enter because of the aqueous phase termination or propagation, and is given by

$$\beta = \frac{k_p[M]_w + k_{tw}[T^*]_w}{k_p[M]_w + k_{tw}[T^*]_w + k_a N_T} \tag{23}$$

where $[T^*]_w$ is the total radical concentration in the water phase and k_a is the mass-transfer coefficient for radical entry, and $[M]_w$ is the monomer concentration in the water phase.

On the other hand, Casey and Morrison et al. [52, 96] derived the desorption rate coefficient for several limiting cases in combination with their radical entry model, which assumes that the aqueous phase propagation is the rate-controlling step for entry of initiator-derived free radicals. Kim et al. [53] also discussed the desorption and re-entry processes after Asua et al. [49] and Maxwell et al. [11] and proposed some modifications. Fang et al. [54] discussed the behavior of free-radical transfer between the aqueous and particle phases (entry and desorption) in the seeded emulsion polymerization of St using KPS as initiator.

3.2.2 Desorption in Copolymer Systems

As we discuss later in Section 3.3.3, Nomura et al. [45, 47] first derived the rate coefficient for radical desorption in an emulsion copolymerization system by

extending the approach developed for emulsion homopolymerization under the same assumptions as A1–A6 given in Section 3.2.1. This methodology is now termed the "*pseudo-homopolymerization approach*". According to this approach, the average rate coefficient for radical desorption, defined, for example, in a binary emulsion copolymerization system with monomers A and B, $\bar{k}_f$, is given by

$$\bar{k}_f = k_{fA}(\bar{n}_A/\bar{n}_t) + k_{fB}(\bar{n}_B/\bar{n}_t) = k_{fA}f_A + k_{fB}f_B \tag{24}$$

where k_{fA} is the desorption rate coefficient for A-monomeric radicals, $\bar{n}_t$ is the average number of total radicals per particle, $\bar{n}_A$ the average number of A-radicals per particle ($\bar{n}_t = \bar{n}_A + \bar{n}_B$), and f_A is the fraction of A-radicals in the particle phase and is expressed, at steady-state, as a function of the propagation rate constant k_p, the monomer reactivity ratio r', and the monomer concentration in the polymer particles $[M]_p$, in the following form.

$$\bar{n}_t = \bar{n}_A + \bar{n}_B \tag{25}$$

In the case where all the desorbed A-monomeric radicals reenter the polymer particles, the desorption rate coefficient for A-monomeric radicals k_{fA} is given by

$$k_{fA} = K_{oA}\left[\frac{C_{mAA}r_A[M_A]_p + C_{mBA}[M_B]_p}{r_B\{(K_{oA}\bar{n}_t/k_{pAA}) + [M_B]_p\} + [M_A]_p}\right] \tag{26}$$

where K_{oA} is the overall desorption rate constant per particle for A-monomeric radicals given by Eq. 19 in Section 3.2.1 and C_{mBA} is the chain transfer constant for a B-radical to A-monomer.

López et al. [55] investigated the kinetics of the seeded emulsion copolymerization of St and BA in experiments where the diameter and number of seed particles, and the concentration of initiator were widely varied. The experimental data were fitted with a mathematical model in which they used the desorption rate coefficient developed by Forcada et al. [56] for a copolymerization system. The desorption rate coefficient for the A-monomeric radical that they used was a modification of Eq. 22 and Eq. 23, and is given by

$$k_{fA}f_A = (k_{mf,AA}f_A + k_{mf,BA}f_B)[M_A]_p\left(\frac{K_{0A}}{\beta_A K_{0A} + k'_{pAA}[M_A]_p + k'_{pAB}[M_B]_p}\right) \tag{27}$$

where $k_{mf,AB}$ denotes the chain transfer constant of the A-radical to the B-monomer and β_A is the fraction of the desorbed A-monomeric radicals that cannot reenter the polymer particles because of the aqueous phase termination or propagation. Barudio et al. [57], on the other hand, developed a simulation model for emulsion copolymerization based on the pseudo-homopolymerization approach, where they used the average rate coefficient for radical desorption given by $\bar{k}_{de} = (12D_w z/m_d d_p^2)(\bar{k}_{mf}/\bar{k}_p)$. Saldivar et al. have presented a survey of

emulsion copolymerization models that have been published in the literature, and a comprehensive mathematical model for emulsion copolymerization [58], along with its experimental verification [59, 60]. In Appendix A of the former paper, they present a detailed discussion on the average rate coefficient for radical desorption, which is applicable to a multimonomer system.

Only a few experimental studies have been published that aim to demonstrate the validity of the average rate coefficient for radical desorption given by Eqs. 24 to 27 [45, 47] directly. Vega et al. [61] modeled the batch emulsion copolymerization of AN and Bu in order to simulate an industrial process and improve the final polymer quality. The mathematical model they used was an extended version of that developed by Guliotta et al. [62] for the continuous emulsion polymerization of St and Bu. Due to the high solubility of AN in water, the effect of the desorption of AN radicals was taken into consideration in the model. The average rate coefficient for radical desorption used was given by Eqs. 24 and 27. Barandiaran et al. [63] proposed a method to estimate the rate coefficient for radical desorption in emulsion copolymerization and gave the values of this parameter for the MA-VAc and MMA-BA emulsion copolymerization systems.

3.2.3 Miscellaneous Kinetics Problems in Radical Desorption

The rate coefficient for radical desorption was derived by assuming that the adsorbed layer of conventional or polymeric surfactant on the surface of the polymer particle does not act as an interfacial diffusion barrier to the desorbing neutral monomeric radicals. However, Kusters et al. [32] studied the kinetics of particle growth in emulsion polymerization systems with a surface-active initiator (an "inisurf"). The inisurf employed was the diester of 4,4′-azobis(4-cyanopentanoic acid), the initiator moiety, with poly(ethylene oxide) nonylphenol, the surfactant moiety. They observed a large decrease (one order of magnitude) in the desorption rate coefficient for monomeric radicals in the emulsion polymerization of St. They ascribed the reason for the decrease in the rate of radical desorption to a "hairy" layer of the polymeric surfactant, which would play the role of a diffusion barrier. Coen et al. [34] also reported that in the seeded emulsion polymerization of St using a PSt seed latex stabilized electrosterically by a copolymer of AA and St, the electrosteric stabilizer greatly reduced the rate of radical desorption compared to the same seed latex with an electrostatic stabilizer. They interpreted the reason for the decrease in the rate of radical desorption by assuming that the aqueous-phase diffusion of monomeric radicals is slower in the hairy layer. Recently, Vorwerg et al. [36] carried out a kinetic study of the seeded emulsion polymerization of St using PSt seed lattices electrosterically stabilized with poly(acrylic acid) (pAA). They found that seed lattices with a high-coverage of pAA (above 50 μC cm^{-2}) exhibited a significant reduction in radical desorption (by a factor of ~3 compared to the ionically stabilized seed) at low pH.

3.3 Particle Formation and Growth

3.3.1 Particle Formation

As we mentioned in Section 2.1 (Fig. 1a), there are three major models for particle formation in emulsion polymerization. According to these models, polymer particles are formed:

1. When a free radical in the aqueous phase enters a monomer-swollen emulsifier micelle and polymerization proceeds therein (*micellar nucleation*).
2. When the chain length of a free radical growing in the aqueous phase exceeds its solubility limit and precipitates to form a particle nucleus (*homogeneous nucleation*).
3. When a free radical growing in the aqueous phase enters a monomer droplet and polymerization proceeds therein (*droplet nucleation*).

However, when the resultant polymer particles become unstable and coagulate, then whatever the mechanism of particle formation is, the final number of polymer particles produced is determined by a limited coagulation between existing polymer particles (*coagulative nucleation*).

Smith and Ewart [4] derived an expression that can predict the number of polymer particles produced, by assuming that:

1. A monomer-swollen emulsifier micelle is transformed into a polymer particle by capturing a free radical from the aqueous phase [4, 5].
2. The volumetric growth rate per particle μ is constant, at least during particle formation ($\mu = dv_p/dt$=constant).
3. Free radical activity does not transfer out of a growing particle ($k_f \cong 0$).
4. The amount of emulsifier that dissolves in the water phase without forming micelles and adsorbs on the surface of emulsified monomer droplets may be neglected.

Based on these assumptions, two limiting cases were discussed.

Case A: The rate of radical entry into micelles that results in the formation of new particles is approximately equal to the rate of radical generation in the water phase (ρ_w), as long as emulsifier micelles are present; in other words,

$$\frac{dN_T}{dt} = \rho_w \tag{28}$$

Particle formation stops at the time t_c, when the emulsifier micelles have just disappeared because all of the emulsifier molecules comprising the emulsifier micelles have been transferred to the surfaces of growing polymer particles for adsorption. The volume $v_{p,c}$ at time t_c of a particle formed at time τ is $v_{p,c} = \mu(t_c - \tau)$, and so the surface area $a_{p,c}$ of this particle at time t_c is given by

$a_{p,c}=\sigma(t_c-\tau)^{2/3}$ where $\sigma=[(4\pi)^{1/2}3\mu]^{2/3}$. Therefore, the total surface area $A_{p,c}$ of all the polymer particles present at time t_c is given by the integral $A_{p,c}=\int_0^{t_c}\sigma(t_c-\tau)^{2/3}\rho_w d\tau = 3/5\ \sigma\rho_w t_c^{5/3}$. No micelles exist ($A_m=0$) at time t_c, and so all of the charged emulsifier molecules are adsorbed onto the surfaces of polymer particles present. Therefore, it holds that $A_{p,c}=(3/5)\sigma\rho_w t_c^{5/3}=a_s S_0$. In this case, the number of polymer particles produced (N_T) can be obtained by substituting t_c into $N_T=\rho_w t_c$ as

$$N_T = 0.53(\rho_w/\mu)^{0.4}(a_s S_0)^{0.6} \tag{29}$$

where A_m and A_p are the total surface area of the micelles and the total surface area of the polymer particles per unit volume of water, respectively, a_s is the surface area occupied by a unit amount of emulsifier, and S_0 is the amount of initially charged emulsifier per unit volume of water (the initial emulsifier concentration).

Case B: Radicals enter both micelles and polymer particles at rates that are proportional to their surface areas (collision theory), so that the rate of new particle formation is given by

$$dN_T/dt = \rho_w\left(\frac{A_m}{A_m + A_p}\right) = \frac{\rho_w}{1 + A_p/A_m} \tag{30}$$

Then, it follows that

$$N_T = 0.37(\rho_w/\mu)^{0.4}(a_s S_0)^{0.6} \tag{31}$$

On the other hand, Nomura et al. [14] proposed a different approach for predicting the number of polymer particles produced, where the new concept of "radical capture efficiency" of a micelle relative to a polymer particle was proposed. The assumptions employed were almost the same as those of Smith and Ewart, except that the volumetric growth rate μ of a polymer particle was not considered to be constant. It was also assumed that all of the radicals formed in the aqueous phase enter either micelles or polymer particles with negligible termination in the aqueous phase. In this approach, the following elementary reactions and their respective rates were defined.

(1) Particle formation by radical entry into a micelle

$$R^* + m_s \rightarrow N^*,\ k_{em} m_s [R_w^*] \tag{32}$$

(2) Formation of a dead particle by radical entry into an active particle containing a radical

$$R^* + N^* \rightarrow N_0,\ k_{ep} N^* [R_w^*] \tag{33}$$

(3) Formation of an active particle by radical entry into a dead particle containing no radical

$$R^* + N_0 \rightarrow N^*,\ k_{ep} N_0 [R_w^*] \tag{34}$$

where m_s is the number of monomer-swollen micelles, $[R_w^*]$ the concentration of free radicals in the aqueous phase, N^* the number of active particles containing a radical, N_0 the number of dead particles containing no radical, k_{em} the rate constant for radical entry into micelles, and k_{ep} the rate constant for radical entry into particles. Using these rate expressions, the following equations, describing the balance of radicals in the aqueous phase and the rate of particle formation, were obtained:

$$\frac{d[R_w^*]}{dt} = \rho_w - k_{em} m_s [R_w^*] - k_{ep} N_T [R_w^*] \tag{35}$$

$$\frac{dN_T}{dt} = k_{em} m_s [R_w^*] \tag{36}$$

where N_T is the total number of polymer particles produced ($N_T = N^* + N_0$). Introducing the aqueous phase concentration $[R_w^*]$, obtained by applying the steady state assumption to Eq. 35 into Eq. 36, and rearranging leads to

$$\frac{dN_T}{dt} = k_{em} m_s [R_w^*] = \frac{\rho_w}{1 + (k_{ep} N_T / k_{em} m_s)} = \frac{\rho_w}{1 + (\varepsilon N_T / S_m)} \tag{37}$$

where $k_{ep} N_T / k_{em} m_s$ denotes the ratio of the rate of radical entry into polymer particles to that into micelles and is rewritten as $\varepsilon N_T / S_m$, where $\varepsilon = (k_{ep}/k_{em}) M_m$ and ε is the one unknown parameter, which affects the number of polymer particles produced. Here, S_m is the total number of emulsifier molecules forming micelles, and M_m is the aggregation number of emulsifier molecules per micelle, defined by $M_m = S_m / m_s$. By solving a set of simultaneous differential equations describing N_T, N^*, the monomer conversion X_M, and using the balance equation for the number of emulsifier micelles m_s, the number of polymer particles produced N_T can be predicted with respect to the initial emulsifier (S_0) and initiator concentrations (I_0) (or $\rho_w = 2 k_d f [I_0]$) as shown by $N_T \propto \rho_w^{0.3} S_0^{0.7}$. In the case of VAc emulsion polymerization [20], the authors took into account radical desorption from the polymer particles, yielding the following expression in place of Eq. 37.

$$\frac{dN_T}{dt} = k_{em} m_s [R_w^*] = \frac{\rho_w + k_{de} \bar{n} N_T}{1 + (k_{ep} N_T / k_{em} m_s)} = \frac{\rho_w + k_{de} \bar{n} N_T}{1 + (\varepsilon N_T / S_m)} \tag{38}$$

In this derivation, it was assumed that only monomer-transferred radicals could desorb from the polymer particles, and that radical termination in the aqueous phase was negligible. The calculated result was correlated by $N_T \propto \rho_w^{0.04} S_0^{0.94}$, from which it was found that radical desorption from the polymer particles decreases the value of the exponent of the initiator dependence and increases the value of the exponent of the emulsifier dependence. To obtain agreement between the predicted and experimental values of N_T, however, it was necessary

to introduce a value of ε that is far greater than that predicted by using the diffusion theory given by Eq. 7 ($k_{ep}/k_{em}=d_p/d_m$). A value of $\varepsilon=1.28\times10^5$ was necessary for St emulsion polymerization [14], and a value of $\varepsilon=1.2\times10^7$ for VAc emulsion polymerization [20], while the value of ε predicted by diffusion theory (Eq. 7) was ~1000 in both systems because $M_m\approx100$ and $d_p/d_m\approx10$ hold (roughly) in Interval I of particle formation, as already discussed in Sect. 3.1.1. The authors, therefore, proposed the concept of the "radical capture efficiency" of a micelle relative to a polymer particle to correct for this disagreement. The same phenomenon has been encountered by several researchers [18, 19, 21] (Sect. 3.1.1). However, the reason for the disagreement between the predicted and experimental values of ε has not been found yet.

As we discussed in Sect. 3.1.1, Hansen et al. [15] made significant improvements to the concept of the radical capture efficiency proposed by Nomura et al. [14]. Taking this concept into consideration, they examined the effect of radical desorption on micellar particle formation in emulsion polymerization [65]. Assuming that radical entry is proportional to the x^{th} power of the micelle radius and the polymer particle radius, they proposed the following general expression for the rate of particle formation:

$$\frac{dN_T}{dt}=(\rho_w+k_f\bar{n}N_T)\left(\frac{\delta_{ce}m_s d_m^x}{\delta_{ce}m_s d_m^x+N_T d_p^x}\right)=\frac{\rho_w+k_f\bar{n}N_T}{\left[1+\frac{N_T}{\delta_{ce}m_s}\left(\frac{d_p}{d_m}\right)\right]} \tag{39}$$

where δ_{ce} is the radical capture efficiency of a micelle relative to a polymer particle, and is related to ε by $\delta_{ce}=(M_m/\varepsilon)(d_p/d_m)^x$. The condition $x=1$ corresponds to the diffusional entry model, while the condition $x=2$ corresponds to the collisional entry model. Using $x=1$, they calculated the effect of radical desorption in the emulsion polymerizations of St, MMA, VAC, and VCl on the number of polymer particles produced, and demonstrated that the following general rule for initiator and emulsifier exponents, which was first found by Nomura et al. [20, 43], could also be applied to the emulsion polymerizations of these monomers.

$$N_T \propto I_0^{1-z}S_0^z \tag{40}$$

where $0.6<z<1.0$. The value of z increases from 0.6 (a common value for St) to 1.0 (a common value for VAc) with increasing radical desorption.

Particle formation below the critical micellar concentration (CMC) in emulsion polymerization is now accepted to take place according to the homogeneous nucleation mechanism. Among several quantitative treatments of homogeneous particle formation in emulsion polymerization, the best-known model was that proposed by Fitch and co-workers [66]. Their model is based on the assumption that when the chain length of a free radical growing in the aqueous phase reaches its solubility limit (critical chain length), it precipitates to form a primary particle, and that particle formation will be hindered if these growing oligomers are absorbed in polymer particles formed earlier. Hansen

et al. [67] made significant improvements on the Fitch model [the HUFT (Hansen-Ugelstad-Fitch-Tsai) model]. According to Hansen et al, the rate of particle formation is given by

$$\frac{dN_T}{dt} = k_{pw} M_w (R_{Ij_{Icr}} + R_{Mj_{Mcr}}) \tag{41}$$

where k_{pw} and M_w are the propagation rate constant and the monomer concentration in the aqueous phase, respectively, and R_{Ijcr} and R_{Mjcr} are the aqueous phase concentrations of oligomer radicals with critical chain length derived from initiator and monomer radicals, respectively. This equation means that oligomers stemming from initiator and monomer radicals precipitate as particles when they propagate beyond their respective critical degree of polymerization, j_{Icr} and j_{Mcr}. The authors derived the steady-state expressions for R_{Ij} and R_{Mj} and obtained a general equation for homogeneous particle formation by nserting them into Eq. 41. Furthermore, in order to simplify it, they neglected particle formation from oligomers stemming from the desorbed monomeric radicals, along with several other assumptions, and obtained

$$\frac{dN_T}{dt} = \rho_w (1 + k_{tw} R_w / k_{pw} M_w + \bar{k}_c N_T / k_{pw} M_w)^{-j_{Icr}} \tag{42}$$

where $\bar{k}_c$ is the average rate coefficient for radical entry into polymer particles, and R_w is the total radical concentration in the aqueous phase. Assuming that, as an approximation, radical absorption by particles may be neglected in the calculation of R_w, one gets

$$N_T(t) = \{[k_1 \rho_w j_{cr} t + (k_2 + 1)^{j_{cr}}]^{1/j_{cr}} - k_2 - 1\}/k_1 \tag{43}$$

where $R_w = (\rho_w / k_{tw})^{1/2}$ in this case, and $k_1 = \bar{k}_c / k_{pw} M_w$ and $k_2 = (k_{tw} \rho_w)^{1/2} / k_{pw} M_w$.

On the other hand, Tauer et al. [68] developed a framework for modeling particle formation in emulsion polymerization on the basis of a combination of classical nucleation theory with radical polymerization kinetics and the Flory-Huggins theory of polymer solutions. The basic assumption adopted was that water-borne oligomers form stable nuclei under critical conditions. The only adjustable model parameter was the activation energy of nucleation. The model allows us to calculate the chain length of the nucleating oligomers, the number of chains forming one nucleus, the diameter of the nucleus, the total number of nuclei formed, and the rate of nucleation. Further, they experimentally studied particle formation in the very early stages of the emulsifier-free emulsion polymerization of St by monitoring the optical transmission and the conductivity of the reaction mixture on-line [69].

Usually particle formation by initiation in the monomer droplets (*droplet nucleation*) is not considered important in conventional emulsion polymerization. This is because of the low absorption rate of radicals into the monomer droplets, relative to the other particle formation rates. However, when the monomer

droplets are very small, they become an important source of particle formation because the monomer droplets can compete for aqueous phase free radicals with emulsifier micelles. This mode of heterogeneous polymerization is now called "miniemulsion polymerization" and is reviewed in another chapter.

It is accepted that particle formation below the CMC in emulsion polymerization takes place by homogeneous nucleation. However, there have been claims that homogeneous nucleation is the main particle formation mechanism, even above the CMC. Lichti et al. [70] investigated the mechanism of particle formation in the emulsion polymerization of St using sodium dodecyl sulfate (SDS) as an emulsifier, and proposed the concept of "*coagulative nucleation*". They measured the full PSDs by electron microscopy at consecutive times soon after the cessation of particle formation, and found that the PSDs obtained during particle formation (Interval I) were positively skewed, confirming the role of coagulation, even above the CMC. Based on this phenomenon, they concluded that the particle formation process does not occur by either simple micellar entry or homogeneous nucleation mechanisms. Therefore, they suggested a mechanism for particle formation where the homogeneous nucleation of oligomers in the aqueous phase creates small primary polymer particles, and these primary particles coagulate to produce polymer particles. On the basis of this experimental finding, Feeny et al. [71] proposed a detailed theory for coagulative nucleation and the PSDs in emulsion polymerization. The theory combined and extended Müller-Smoluchowski coagulation kinetics with the DLVO theory. Expressions were provided for the time evolutions of the nucleation rate, particle number, and PSD. They showed that with physically reasonable values for the parameters of the coagulation kinetics, agreement was obtained with experimental data for the St emulsion polymerization system. Richards et al. [72] developed a mathematical model for emulsion copolymerization. The model combined the theory of coagulative nucleation of homogeneously nucleated precursors with detailed species material and energy balances to calculate the time evolution of the concentration, size and colloidal characteristics of polymer particles, the monomer conversion, the copolymer composition, and the molecular weight in an emulsion copolymerization system.

Although it is now accepted that particle formation below the CMC in emulsion polymerization takes place according to the homogeneous nucleation mechanism, there has been debate as to whether homogeneous nucleation is still operative even above the CMC, especially when relatively water-soluble monomers are polymerized in emulsion in the presence of emulsifier micelles. To date, most investigators believe that in the emulsion polymerization of partially water-soluble monomers such as MMA and methyl acrylate (MA), polymer particles are generated not by a micellar mechanism, but by homogeneous nucleation even in the presence of emulsifier micelles. This is because the emulsion polymerization involving these monomers does not follow the Smith-Ewart theory, and moreover, because an inflection point cannot be seen around the CMC of the emulsifier on the particle number versus initial emulsifier concentration curve, where an abrupt and sharp decrease in the number

of polymer particles produced is usually observed if particle formation occurs by the micellar mechanism [73, 74]. Nomura et al. [75] carried out the emulsion polymerization of vinylidene chloride (VDC) at 50 °C using NaLS as the emulsifier and KPS as the initiator. They found that $N_T \propto S_m^{0.7} I_0^{0.3} M_0^0$, where S_m is the initial concentration of emulsifier forming micelles, I_0 is the initial initiator concentration and M_0 is the amount of monomer initially charged per unit volume of water. Although the solubility of VDC in water at 25 °C is 2.5×10^{-2} mol/dm^3-water (~0.25 wt%), which is about ten times more water-soluble than St, but is about 1/10 of the water-solubility of MMA, an inflection point was definitely observed around the CMC on the particle number versus initial emulsifier concentration curve. This seems to indicate that micellar nucleation occurred, although Gilbert et al. [70, 71, 76] refuted micellar nucleation even in the emulsion polymerization of sparingly water-soluble monomer St in the presence of SDS micelles. Sajjadi et al. [77] investigated the kinetic features of the batch emulsion polymerization of BA using SDS as the emulsifier and KPS as the initiator. They observed that the number of polymer particles produced was proportional to the 0.54th power of emulsifier concentration, to the 0.39th power of initiator concentration, and was practically independent of the monomer/water ratio. Particle formation was found to occur even during Interval III, when undissociated micelles existed.

Experimental investigations that deal in detail with particle formation in emulsion copolymerization are scarce. Nomura et al. [78] studied the kinetics of particle formation and growth in the emulsion copolymerization of VDC and MMA using NaLS as the emulsifier and KPS as the initiator. The number of polymer particles produced was determined using particle diameters measured by both electron microscopy (TEM) and dynamic light scattering (DLS) for comparison. They found that $N_T \propto S_0^{1.0} I_0^{0.3} \Phi^0$, where S_0 and I_0 are the initial emulsifier and initiator concentrations, respectively, and Φ is the weight fraction of MMA in the initial monomer feed. It was also found that the particle number determined via the DLS particle diameter was always about 1/2~1/3 of that determined by TEM. This is due to the difference between the average particle diameters determined from TEM and DLS. Yuan et al. [79] carried out the emulsion terpolymerization of St, butadiene (Bu) and AA, and found that the mechanism of water-soluble oligomer formation during the emulsion polymerization differed depending on whether the SDS emulsifier concentration was above or below the CMC. This may demonstrate that particle formation is also closely connected to the presence of emulsifier micelles.

Herrera-Ordóñez et al. [22, 80] discussed particle formation during the emulsion polymerization of St above the CMC of the emulsifier used (SDS), based on their detailed mathematical model for emulsion polymerization. By comparing the model predictions with experimental data, they concluded that micellar nucleation dominates over the homogeneous nucleation above the CMC, and that coagulation is not significant, even if it does take place. Furthermore, they [81] concluded that particle formation by micellar nucleation is at all times at least ten orders of magnitude greater than that by homoge-

neous nucleation, even in the emulsion polymerization of relatively water-soluble monomer MMA. Recently, however, Varela de la Rosa et al. [82–84] carried out detailed experimental studies on the emulsion polymerization of St at 50 °C, using SDS as the emulsifier and KPS as the initiator, and proposed the modified description shown by the following, which is very different from the widely accepted classical description of St emulsion polymerization.

1. In Interval I, the rate of polymerization and the number of polymer particles produced increase. Particle formation takes place predominantly by micellar nucleation. Micelles disappear between 5% and 10% conversion, marking the end of this interval.
2. In Stage II (referred to as Stage II to differentiate it from the classical Interval II), the rate of polymerization and the number of polymer particles continue to increase but at a slower rate. Polymer particles are formed by homogeneous nucleation as long as monomer droplets and enough emulsifier (>0.05 mM) are present in the system. The end of this stage is marked by the disappearance of monomer droplets, but particle nucleation may or may not end at this time.
3. The number of polymer particles produced is proportional to the 0.36^{th} power of the initial monomer concentration.

Therefore, the mechanism of particle formation is still anything but a settled question, even in the emulsion polymerization of St.

Only a few papers [85–88] have been published so far that discuss methodologies that could be used to discriminate experimentally between micellar and homogeneous nucleations. Nomura et al. [85, 86] proposed an experimental method to gauge to what extent the homogeneous and micellar nucleations are operative in a given emulsion polymerization system. The method involves the emulsion copolymerization of the sparingly water-soluble monomer St with partially water-soluble monomers such as MMA or MA, followed by measurement of the composition of the copolymers produced at the very beginning of the reaction, including the interval of particle formation. This method is based on the fact that the composition of the copolymer produced at the very beginning of the reaction reflects the comonomer composition at the locus of particle formation. In other words, the copolymer composition serves as a probe of the locus of particle formation. They carried out the emulsion copolymerizations of St-MMA and St-MA, where the weight ratio of two monomers was 1:1. The copolymer compositions observed at the very beginning of the reactions (far less than 1% monomer conversion) in the presence of emulsifier (NaLS) micelles were definitely very different from those observed when the emulsifier micelles were absent, reflecting the comonomer composition in the locus of particle nucleation. These experimental results revealed that the micellar nucleation is the main particle formation mechanism, even in the emulsion polymerization of moderately water-soluble MMA and MA in the presence of emulsifier micelles. Recently, Chern et al. [87, 88] proposed a novel method in which a water-insoluble dye was used as a probe to study the particle nucleation

mechanism. The rationale behind the method was that if particle formation took place by homogeneous nucleation, the resultant polymer particles would contain negligible amounts of dye because the transport of the dye species from the monomer droplet phase to the resultant polymer particles could be neglected due to the insolubility of the dye in the aqueous phase. If, on the other hand, particle formation took place by micellar nucleation, the resultant polymer particles would contain an amount of dye corresponding to that solubilized in the micelles. They carried out the semibatch emulsion polymerization of St and of MMA in the presence of the dye. In the semibatch emulsion polymerization of MMA, for example, the experimental results showed that when the emulsifier (SDS) concentration is above its CMC, mixed mode particle nucleation (micellar and homogeneous nucleation) was the predominant mechanism. However, a question raised for this study is that if the transport of the dye species from the monomer droplets to the resultant polymer particles can be neglected, how is the dye transported from the monomer droplet phase, where the dye is dissolved, to the monomer-swollen micelle phase where the dye is solubilized.

Semibatch seeded emulsion polymerizations are quite common in industrial operations. One of the most important problems in semibatch seeded emulsion polymerization is how to control secondary particle formation. It is well known that the amount of emulsifier must be carefully fed during starved-fed semibatch seeded emulsion polymerization. Too little emulsifier leads to emulsion instability and hence coagulation, while too much emulsifier leads to secondary particle formation by the micellar mechanism. Wang et al. [89] developed a method for controlling the emulsifier level in starved-fed emulsion polymerization. Morrison et al. [90] studied the conditions for secondary particle formation in emulsion polymerization systems where the amount of added emulsifier was below the CMC. They advanced their discussion based on the HUFT model (Eq. 41), incorporating their reaction-controlled entry model, and deduced a simple means for determining conditions for the onset and extent of secondary particle formation. Coen et al. [91] further extended the work of Morrison et al. [90] and proposed an extensive model for the PSD, particle number, particle size and amount of secondary particle nucleation in emulsion polymerization. Prescott et al. [92] proposed a simplified model for particle formation, which is particularly useful for exploring the conditions required for the growth of large particles, while avoiding secondary particle formation. Butucea et al. [93] studied the seeded emulsion polymerization of VCl to establish the conditions needed to avoid the formation of new polymer particles (secondary nucleation), and proposed new parameters: (1) MSA, the minimum surface area of seed particles necessary to capture all initiator-derived (ionic) radicals generated in the aqueous phase at a given initiator concentration; (2) MCCI, the maximum critical concentration of initiator per unit surface of seed particles under which the formation of new polymer particles is avoided; (3) PVR_1, the polymer volume per active growing radical necessary for the radical to be within the particle for one second.

It has been reported that both the surface charge density and the degree of surface coverage by emulsifier on the seed particles affect the behavior of secondary particle nucleation in seeded emulsion polymerization because these factors control the rate of radical entry into seed particles. Vorwerg et al. [36] carried out a kinetic study of seeded emulsion polymerization using PSt seed particles electrosterically stabilized with poly(acrylic acid), and studied the effect of the degree of surface coverage by poly(acrylic acid) on both radical entry (ρ) and desorption (k_f), through which secondary particle nucleation is influenced under the condition of a fixed number of seed particles. The behavior of ρ and k_f for the low-coverage particles was the same as that of the PSt seed stabilized by initiator fragments and adsorbed emulsifier. The high-coverage particles, on the other hand, exhibited strongly reduced k_f values (by a factor of three) at low pH, but ρ was only slightly lower than for the ionically stabilized seed, while at high and neutral pH, secondary particle nucleation and a decreased polymerization rate was observed with increasing pH (despite an increase in particle number), indicating a reduced ρ value. Therefore, an extensive electrosteric stabilizer reduced the rate coefficient for radical entry (and for radical desorption), inducing secondary particle nucleation. Cheong et al. [35, 94] investigated the effects of surface charge density on the kinetics of secondary particle formation. They carried out three emulsifier-free seeded emulsion polymerizations of MMA using monodispersed seed particles with different surface charge densities, prepared from the St and NaSS comonomers using the two-stage shot-growth process. In the case of the highest surface charge density (72.7 μC/cm^2), secondary particle nucleation was observed. They ascribed the reason for this to the reduced rate of radical entry into the seed particles resulting from electrical repulsion between seed particles and entering oligmeric radicals [35]. They [94] proposed a mathematical model to explain the effects of seed particle surface charge density on secondary particle nucleation by introducing a modified Smolchowski equation and the DLVO theory.

Sajjadi [95] examined the conditions for secondary particle formation and coagulation in the seeded semibatch emulsion polymerization of BA under monomer-starved conditions. They arrived at very interesting conclusions: (1) particle coagulation occurred if the particle surface coverage (θ_{cr1}) dropped below θ_{cr1}=0.25±0.05; (2) secondary particle formation occurred above a critical surface coverage of θ_{cr2}=0.55±0.05, indicating that the presence of micelles in the reaction vessel is not the only prerequisite for micellar nucleation to occur; (3) the number of polymer particles remained approximately constant if the critical surface coverage was within (θ_{cr1}=0.25)<θ<(θ_{cr2}=0.55), and; (4) this surface coverage band is equivalent to the surface tension band of 42.50±5.0 dyne/cm that is required to avoid particle formation and coagulation in the course of polymerization. Sajjadi [96] also carried out an experimental investigation on particle formation under monomer-starved conditions in the semibatch emulsion polymerization of St. They observed that the number of polymer particles formed increased with a decreasing monomer feed rate, and

that a much larger number of particles (1–2 orders of magnitude greater) than that generally expected from a conventional batch emulsion polymerization was obtained. It is clear from Eq. 29 that any variation in the formulation or process variables that results in a reduction in the volumetric growth rate per particle μ will enhance particle formation as long as polymer particles are generated from emulsifier micelles. A depressed rate of particle growth can be achieved either by the starvation of polymer particles or by a reduction in the capability of polymer particles to swell monomer, with the exception of impurities (see Sect. 3.5) and radical desorption (see Sect. 3.2). In this case, the former was the reason for an increase in particle formation. The latter could be achieved, for example, if a small amount of crosslinking agent was used in the formulation. It is well known that crosslinking will decrease the extent of particle swelling by a monomer and thereby reduce the rate of particle growth [97]. Sajjadi [98] also investigated particle nucleation in the seeded emulsion polymerization of St in the presence of Aerosol-MA emulsifier micelles and in the absence of monomer droplets (Interval III). A larger number of polymer particles were found to form in Interval III than in the corresponding seeded batch operation in the presence of monomer droplets. The increase in the number of polymer particles could be attributed to the reduced rate of growth of new particles, which retarded the depletion of the emulsifier micelles.

There are an enormous variety of commercial emulsifiers that are employed in emulsion polymerization. Emulsifiers are generally categorized into four major classes: anionic, cationic, nonionic and zwitterionic (amphoteric). The anionic and nonionic emulsifiers are the most widely used. In addition, mixtures of emulsifiers are also often used. Since the effects of the molecular structure and chemical and physical properties of an emulsifier on particle formation are still far from being well understood, numerous experimental investigations on particle formation have been carried out to date with various nonionic emulsifiers [99–102], mixed emulsifiers (ionic and nonionic emulsifiers) [18, 103–106] and reactive surfactants [33, 107–110]. Recently, polymeric surfactants have become widely used and studied in emulsion polymerizations [111–116]. A general review of polymeric surfactants was published in 1992 by Piirma [117]. Recently, emulsion polymerization stabilized by nonionic and mixed (ionic and nonionic) emulsifiers was reviewed by Capek [118].

Özdeğer et al. studied the role of the nonionic emulsifier Triton X-405 (octylphenoxy polyethoxy ethanol) in the emulsion homopolymerization of St [99] and *n*-butyl acrylate (*n*-BA) [100], and in the emulsion copolymerization of St and *n*-BA [101]. In the emulsion homopolymerization of St, they noted two separate nucleation periods, resulting in bimodal PSDs. Although the total concentration of the emulsifier was maintained at a level above its CMC based on the water phase in the recipe, the portion of the emulsifier initially present in the aqueous phase was below the CMC due to partitioning between the oil and aqueous phases. Due to the nature of this emulsifier, the first of the two nucleation periods was attributed to homogeneous nucleation, while the second was

attributed to micellar nucleation. In the case of *n*-BA, contrary to the case of St, the emulsifier was found to partition primarily into the aqueous phase, leading to nucleation in the presence of micelles and unimodal PSDs. Particle formation was accompanied by limited aggregation in the early stages of the reaction with particles being formed past 50% monomer conversion in some cases. In the emulsion copolymerization of St and *n*-BA, unimodal PSDs were observed at the lowest (4.2 mM) and the highest (12.5 mM, 16.2 mM) levels of the emulsifier, while bimodal PSDs were produced at intermediate levels. These results were also attributed to emulsifier partitioning between the oil and aqueous phases. Lin et al. [102] also studied the kinetics of the emulsion polymerization of St in the presence of the nonionic emulsifier NP40 (nonylphenol polyethoxylate with an average of 40 oxyethelene units per molecule). The initially charged emulsifier concentration was well above its CMC. The number of polymer particles produced was proportional to the 2.4^{th} power of the total emulsifier concentration. This deviation of particle formation kinetics from the S-E theory (the 0.6^{th} power) was attributed to the low water solubility of the emulsifier (higher solubility in the monomer droplets), the increased agglomeration of polymer particles for the system with the lower amount of emulsifier, and the increased contribution of miniemulsion polymerization kinetics to the system with a higher emulsifier level.

Anionic emulsifiers provide electrostatic stability to the resultant polymer particles. The efficiency of anionic emulsifiers is dependent on various parameters, such as ionic strength and pH, but this can be a major drawback in terms of the stability of the resultant polymer particles. On the other hand, nonionic polymeric emulsifiers provide the steric stabilization provided by the thermodynamically-favored steric repulsion between particles. It is therefore practical to use mixtures of anionic and nonionic emulsifiers in emulsion polymerization to take advantage of these two different stabilization mechanisms. Chern et al. [104, 105] studied the CMC of the mixed emulsifier SDS/NP40 for various compositions at 25 °C and at 80 °C by performing surface tension measurements. They examined the effect of the mixed emulsifier SDS/NP40 on particle formation in the emulsion polymerization of St at 80 °C. They found that adding only a small amount of SDS to NP40 dramatically increased the number of polymer particles produced, and that the emulsion polymerization of St with the mixed emulsifier SDS/NP40 did not follow the conventional S-E theory. The number of polymer particles produced, N_T, was described by the expression $N_T \propto S_0^{\alpha}$, where S_0 is the concentration of mixed emulsifier, and the values of α were 0.60, 0.76, 1.3 and 1.1 for experiments with molar concentrations of NP40 of 0%, 40%, 70% and 100%, respectively. Colombié et al. [106] investigated the role of mixed anionic-nonionic emulsifier systems in particle formation in the emulsion polymerization of St. They carried out the emulsion polymerization of St using a mixture of SDS and Triton X-405 at 70 °C. They found that adding just 1 mM SDS to 6.4 mM Triton X-405 produced a dramatic increase in the rate of polymerization and the number of polymer particles produced. The increase in the number of polymer particles was 17 times that without SDS. When in-

creased amounts of SDS (3 and 5 mM) were used in combination with 6.4 mM Triton X-405, the number of polymer particles produced increased. No secondary particle nucleation was noted upon the disappearance of the droplets, and the resulting latexes were stable. They attributed this behavior to the change in the partitioning of the Triton X-405 between the oil and aqueous phases by changing the amount of SDS added. When no SDS was used, 95% of the Triton X-405 was associated with the oil phase as opposed to 78% when 5 mM SDS was used. Therefore, increasing the amounts of Triton X-405 in the water phase by increasing the amount of SDS added allowed the formation of mixed emulsifier micelles, resulting in an increase in the number of polymer particles produced and the rate of polymerization. Unzueta et al. [103] carried out the semicontinuous emulsion copolymerization of MMA and *n*-BA using mixed emulsifier systems (anionic sodium lauryl sulfate and nonionic polyethylene oxide lauryl ether (Brij35)) and found that narrower PSDs with larger average particle sizes were obtained with mixed emulsifier systems than those obtained with single anionic systems. Furthermore, they developed a mathematical model for the emulsion copolymerization of MMA and *n*-BA with mixed anionic/nonionic emulsifier systems, where the CMC and micelle composition of mixed emulsifiers was predicted using the thermodynamics of nonideal mixtures [18].

Reactive surfactants have also been used in emulsion polymerization [33, 107–110, 114]. This is because the disadvantages of the surfactants that are typically used in emulsion polymerization, such as instability of the latex and surfactant migration during film formation, can be overcome in theory by using a reactive surfactant. Studies of the use of reactive surfactants in heterophase polymerizations (up to 1997) have already been extensively reviewed [107]. Amalvy et al. [108] investigated the particle formation process in the emulsion polymerizations of St, MMA and VAc stabilized by sodium dodecyl sulfopropyl maleate, a polymerizable surfactant (surfmer), focusing their attention on whether the reactivity of the surfmer with the main monomer(s) and the polymerization locus play critical roles in the particle formation in emulsion polymerization systems. The results obtained suggested that the presence of the surfmer did not affect the particle formation mechanism. They concluded from the shape of the $\log N_T$ vs $\log S_0$ (surfmer concentration) plot that the polymer particles were formed by micellar nucleation in the case of St and by homogeneous nucleation in the case of MMA and VAc. Wang et al. [33, 109, 110, 114] studied the emulsion polymerization of St using the reactive surfactant sodium dodecyl allyl sulfosuccinate (TREM LF-40) and its polymeric counterpart (poly(TREM)) as anionic polymeric emulsifiers in terms of the polymerization kinetics. The use of TREM LF-40 gave $N_T \propto S_0^{0.5-0.6}$ and $R_p \propto N_T^{0.7}$ at constant initiator concentration. The reasons for the unusual kinetics compared to those with SDS ($R_p \propto N_T^{1.0}$) were ascribed to chain transfer to TREM LF-40, copolymerization of St with TREM LF-40, and the influence of the homopolymer TREM LF-40 (poly(TREM)) and/or the copolymer (poly(TREM-*co*-St)) on the entry and the exit rates of the free radicals. In contrast, by

varying the initiator concentration, the kinetics were found to have the same dependencies as the conventional emulsifier ($R_p \propto N_T^{1.0} \propto I_0^{0.4}$). In the case of poly-(TREM), the dependencies of R_p and N_T on S_0 and I_0 varied depending on experimental conditions ($R_p \propto N_T^{1.0} \propto S_0^{0.2-0.4}$, and $R_p \propto N_T^{1.0} \propto I_0^{0.6-0.8}$). It was inferred that homogeneous nucleation was dominant when using poly(TREM), even at concentrations exceeding its CMC. This was different from the monomeric TREM LF-40 emulsifier.

Recently, polymeric surfactants have received considerable attention in industry. They provide the steric repulsion between interacting particles, which gives the latex excellent stability against high electrolyte concentration, freeze-thaw cycling and high shear rates. Cochin et al. [111] carried out a comparative study of the emulsion polymerization of St using conventional, polymerizable and polymeric emulsifiers. Ayoub et al. [112] investigated the emulsion polymerization of St with amphiphatic copolymers [of VAc and methoxy polyoxyethlene (PVAc-b-MPOE)(35:65, 27:73, 19:81 wt/wt) prepared with a macroradical initiator in the presence of benzoyl peroxide] as the emulsifier. The experimental results for the number of polymer particles produced (N_T) versus emulsifier concentration (S_0) were as follows: $N_T \propto S_0^{1.82}$ (65%), $N_T \propto S_0^{2.1}$ (73%) $N_T \propto S_0^{1.66}$ (81%). They [113] also studied the emulsion polymerizations of VAc and St using the polymeric emulsifier prepared from polyoxyethylene methylether (POE, 66%) and St (34%). They did not measure the number of polymer particles produced, but the rate of polymerization was found to be proportional to the 0.9th and 0.76th powers of the initiator (KPS) concentrations, and to the 0.77th and 0.66th powers of the emulsifier concentrations for VAc and St monomers, respectively. Kato et al. [115] investigated the emulsion polymerization of St using poly(methyl methacrylate (MMA)-*co*-methacrylic acid (MAA)) with different copolymer compositions as polymeric emulsifiers. They examined the effect of the copolymer compositions, molecular weights and MAA contents of the polymeric emulsifiers on the number of polymer particles produced. They found that the number of polymer particles produced showed a slight dependence on the copolymer molecular weight, having a maximum when the molecular weight was in the range 5,000–10,000, and decreasing monotonously with the content of MMA in the copolymer. Cheong et al. [116] studied the kinetics of particle nucleation and growth in the emulsion polymerization of St using water-soluble polyurethane resins (PUR) as the emulsifier. They found that the number of polymer particles produced became constant in the early stage of polymerization when the concentration of the initially charged PUR was lower. However, the monomer conversion where the particle number became constant increased with increasing the initial PUR concentration. The constant particle number observed (N_T) was correlated as $N_T \propto [PUR]_0^{0.6-0.7}[KPS]_0^{0.4}$ (where $[PUR]_0$ and $[KPS]_0$ are the PUR and KPS concentrations, respectively). These dependencies are almost the same as those predicted by the S-E theory.

3.3.2 Particle Growth in Homopolymer Systems

As is clear from Eq. 1, the rate of particle growth (R_p/N_T) is proportional to the monomer concentration, $[M]_p$ and the average number of radicals per particle, $\bar{n}$, respectively. Thus, $\bar{n}$ is one of the basic parameters that characterize the kinetic behavior of particle growth in an emulsion polymerization system. Early researchers devoted their efforts to deriving a quantitative description of $\bar{n}$ by solving Eq. 3 for $\bar{n}$ defined by Eq. 2 [4, 119, 120].

Smith and Ewart [4] did not obtain a general solution to Eq. 3, but rather solved it for three limiting cases at steady-state conditions, that is, $dN_n/dt=0$.

Case 1. The number of radicals per particle is smaller than unity.

In this case, it holds that, $\rho_e/N_T \ll k_f$, $(\rho_e/N_T)N_0 \cong k_f N_1$, and $N_0 \cong N_T$. Furthermore,

a. When radical termination in the water phase is dominant; in other words, $\rho_w \cong 2k_{tw}[R_w^*]^2$, then

$$\bar{n} = (\rho_w/2k_{tw})^{1/2} m_d \nu_p \ll 0.5 \tag{44}$$

where k_{tw} is the termination rate constant in the water phase, ρ_w is the rate of radical generation per unit volume of water, $[R_w^*]$ is the concentration of radicals in the water phase, and m_d is the partition coefficient of radicals between the water and the polymer particle phases. However,

b. When termination in the polymer particles is dominant,

$$\bar{n} = (\rho_w/2k_f N_T)^{1/2} \ll 0.5 \tag{45}$$

The requirement for this condition is obtained as $(4\pi^2 D_w^2 d_p^2 N_T/k_f) \gg k_{tw}$ from additional assumptions that $\rho_e = 2\pi D_w d_p [R_w^*] N_T$ and $2k_{tw}[R_w^*]^2 \ll 2(\rho_e/N_T)N_1$, where D_w is the diffusion coefficient for the radicals in the water phase and d_p the diameter of the particles.

Case 2. The number of radicals per particle is approximately equal to 0.5.

The requirements for this case are given as $k_f \ll \rho_e/N_T < k_{tp}/\nu_p$. Then we have

$$\bar{n} = 0.5 \tag{46}$$

Equation 46 usually holds in St emulsion polymerization under normal conditions and is generally well known as the S-E theory.

Case 3. The number of radicals per particle is larger than unity.

This situation will prevail when the average time interval between successive entries of radicals into a polymer particle is much smaller than the average time for two radicals in the same particle to coexist without mutual termination; in other words, $\rho_e/N_T \gg k_{tp}/\nu_p$.

$$\bar{n} = (\rho_e \nu_p/2k_{tp})^{1/2} \gg 0.5 \tag{47}$$

Moreover, when both radical termination in the water phase and radical desorption from the particles are negligible, Eq. 47 is reduced to

$$\bar{n} = (\rho_w \nu_p / 2k_{tp} N_T)^{1/2} \gg 0.5 \tag{48}$$

In this case, the kinetic behavior is quite similar to that of suspension polymerization, except that the polymer particles are supplied with free radicals from the external water phase. When the polymerization proceeds according to Eq. 48, the system is sometimes referred to as obeying "*pseudo-bulk*" kinetics.

A general solution to Eq. 3 was provided by Stockmayer [121] with minor corrections by O'Toole [119]. On the other hand, Ugelstad et al. [120] proposed the most useful and widely applicable expression for $\bar{n}$ given by

$$\bar{n} = (a/4)\frac{I_m(a)}{I_{m-1}(a)} = (1/2)\cfrac{2\alpha}{m+\cfrac{2\alpha}{m+1+\cfrac{2\alpha}{m+2+\ldots}}} \tag{49}$$

where $I_m(a)$ is the modified Bessel function of the first kind, $m=k_f\nu_p/k_{tp}$, and $\alpha=a^2/8=\rho_e\nu_p/k_{tp}N_T$. On the other hand, the radical balance in the water phase (Eq. 4) leads to the following relationship using the non-dimensional parameters, α, α_w, m and Y.

$$\alpha = \alpha_w + m\bar{n} - Y\alpha^2 \tag{50}$$

where $\alpha_w=\rho_w\nu_p/k_{tp}N_T$ and $Y=2k_{tw}k_{tp}/k_a^2N_T\nu_p$. They solved the simultaneous equations, Eq. 49 and Eq. 50 for $\bar{n}$, and plotted the calculated value of $\bar{n}$ against the value of α_w that consisted of variables of known values with m varied as a parameter for various fixed values of Y. Figure 3(a) shows an example of the plot of $\log\bar{n}$ versus $\log\alpha_w$ for varying m and Y=0 [120].

On the other hand, Nomura et al. [122a] provided a semi-theoretical expression for $\bar{n}$ corresponding to Y=0, and compared it with the experimental data shown in Fig. 3(b) [122b].

$$\bar{n} = \frac{1}{2}\left[\left\{\left(\alpha_w + \frac{\alpha_w}{m}\right)^2 + 2\left(\alpha_w + \frac{\alpha_w}{m}\right)\right\}^{1/2} - \left(\alpha_w + \frac{\alpha_w}{m}\right)\right] + \left(\frac{1}{4} + \frac{\alpha_w}{2}\right)^{1/2} - \frac{1}{2} \tag{51}$$

The values predicted by Eq. 51 agree well with those predicted by Eq. 49 within less than 4%. This type of plot is called a "*Ugelstad plot*" and has been applied as a criterion to determine whether a system under consideration obeys either zero-one kinetics ($\bar{n}\leq 0.5$) or pseudo-bulk kinetics ($\bar{n}>0.5$).

Nomura et al. [42, 43, 64] showed that when the value of the term k_{tp}/ν_p is very large (the rate of bimolecular termination in the polymer particles is very rapid), $\bar{n}$ is expressed by

$$\bar{n} = (-C + \sqrt{C^2 + 2C})/2 \tag{52}$$

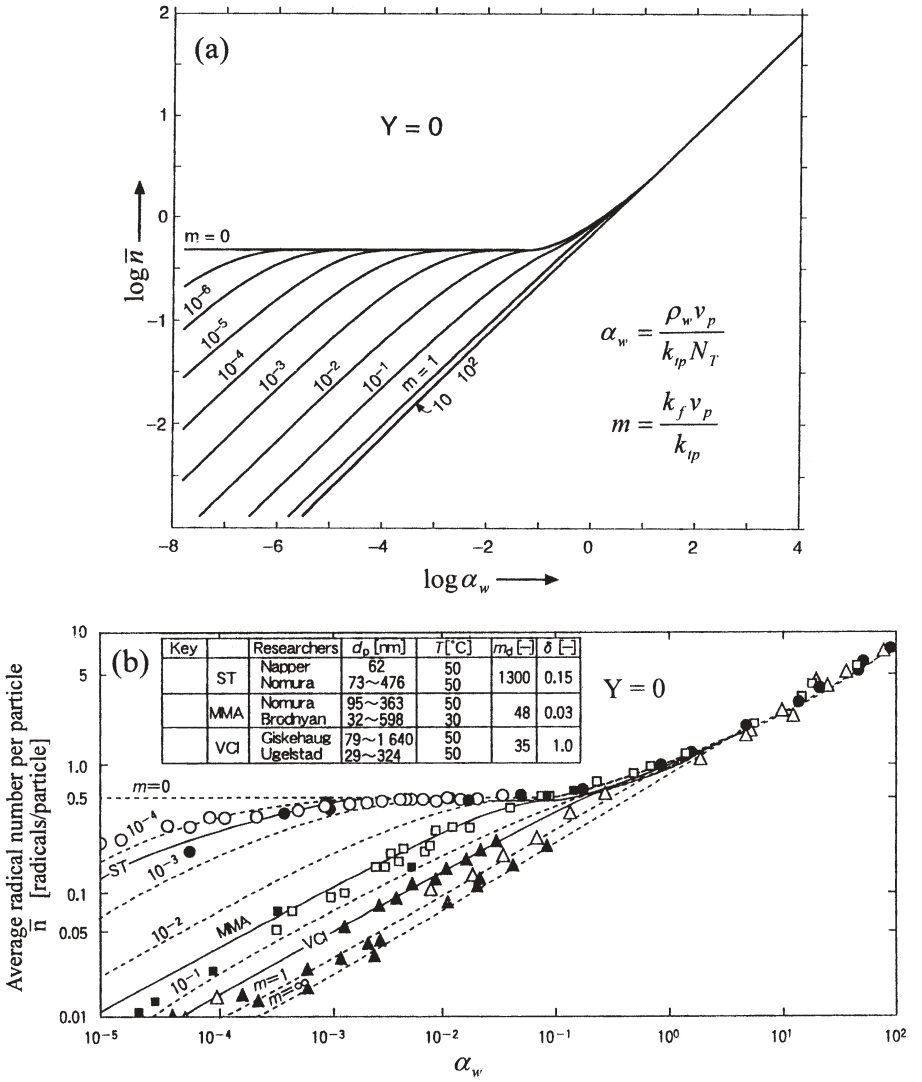

Fig. 3 (**a**) Average number of radicals per particle $\bar{n}$ as predicted by Eqs. 49 and 50, and presented as a function of the parameters α_w and m for Y=0, (**b**) comparison between predicted and observed values of $\bar{n}$.

where $C=\rho_w/k_fN_T$. In Fig. 4, they plotted the value of $\bar{n}$ against the value of C for the monomers of VCl, VAc, MMA, *n*-BMA and St obtained from the literature. It was found that the experimental values of $\bar{n}$ are in fairly good agreement with those predicted by Eq. 52, although the values of the parameters used in this comparison may not necessarily be exact.

An example of a successful application of the Ugelstad plot to determine some of the rate coefficients involved in emulsion polymerization was pre-

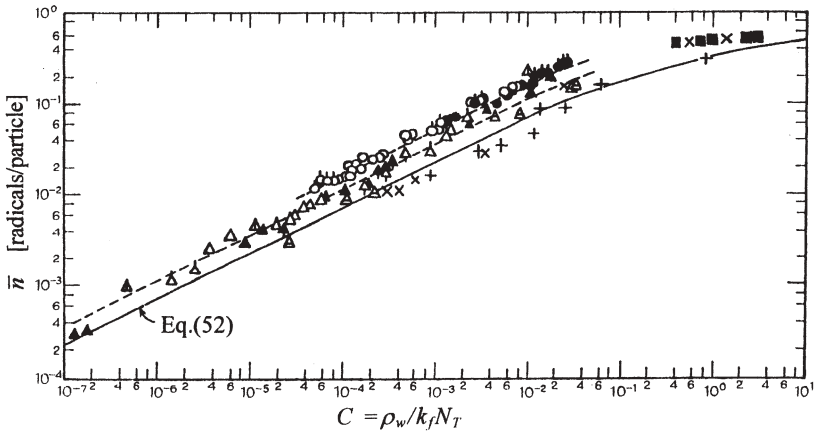

Table 3 Properties of several monomers and reaction conditions

Monomer	Temp. [°C]	k_p [l/mol·sec]	k_{fm}/k_p [–]	m [—]	Key in Fig. 4	$N_T \times 10^{-14}$ [particle/cc]	$\rho_w \times 10^{-12}$ [molecule/cc·sec]	Researcher
Vinyl chloride	50	10000	1.2×10^{-3}	35	△	12	0.73–7.3	
					↑	4.0	0.73–7.3	
					↑	2.2	1.82–3.65	Peggion
					▲	0.43–380	7.4	
					△	1.8–8.5	74	
					▲	66–32400	4.5	Giskehang
					△	0.30–6.4	3.6–28.5	Ugelstad
Vinyl acetate	50	3340	2.0×10^{-4}	28	↓	1.0–1.3	2.8–16.8	
					●	2.2	2.8–16.8	Authors
					○	5.0–6.0	0.7–11.2	
					○	10–15	5.6	
Methyl methacrylate	30	251	1.0×10^{-5}	48	×	0.018–121	0.032–0.95	Brodnyan
n-Butyl methacrylate	30	362	3.2×10^{-5}	830	+	1.5–113	0.19–0.95	
Styrene	50	227	1.2×10^{-5}	1300	■	1.6–10	3.7	Authors

Fig. 4 Comparison of experimental values of $\bar{n}$ with those predicted by Eq. 52

sented by Nomura et al. [123]. Although this approach is rather laborious and time-consuming, they could successfully determine the propagation rate constant k_p and the value of m, from which the desorption rate coefficient k_f could then be deduced, in seeded and unseeded emulsion polymerization of VDC at 50 °C. On the other hand, Hawkett et al. [24] developed a method for determining ρ and k_f termed the *slope-and-intercept* method. This method is simple and straightforward, but has several drawbacks (as stated in Sect. 3.1.2), so care must be taken when this method is used. Asua et al. [12, 124] proposed a new approach for the estimation of kinetic parameters such as the entry and desorption rate coefficients, the termination rate constant in the aqueous phase, the rate coefficient for initiator decomposition and the propagation rate constant in emulsion homopolymerization systems under zero-one conditions.

They claim that accurate values for the parameters are obtainable with this approach provided that a sufficient number of experiments with a minimum range of variation are available.

Recently, several modeling papers have been published which are useful for the design and operation of emulsion homopolymerization processes [22, 80, 81, 125–127]. Mendoza et al. [125] developed a mathematical model that could predict the monomer conversion, particle diameter, number of polymer particles produced, and the number-average and weight-average molecular weights in the unseeded emulsion polymerization of St using *n*-dodecyl mercaptan as CTA. This model was validated by fitting the experimental data to the model's predictions. Kiparissides et al. [126] proposed a comprehensive mathematical model to quantify the effect of the oxygen concentration on the polymerization rate and PSD in the unseeded emulsion polymerization of VCl. Particle formation was assumed to proceed by both the homogeneous and micellar nucleation mechanisms. Asua et al. [127] developed a mathematical model for seeded emulsion polymerization stabilized with polymerizable surfactants (surfmers). The model included the most distinctive features of surfmer polymerization, including partitioning of the unreacted surfmer between the surface of the polymer particles and the aqueous phase, and the surfmer burying itself inside the polymer particles. The model also included the possibility of having radical concentration profiles in the polymer particles. Herrera-Ordóñez et al. [22, 80, 81] proposed a detailed mathematical model of the kinetics of St emulsion polymerization, which was a modification and adaptation of previous works reported in the literature. By comparing model predictions with experimental results, they arrived at the conclusion that initiator-derived radicals with only one monomeric unit also make a significant contribution to the rate of radical capture by polymer particles, which contradicts the conclusion obtained by the Sydney Group [11, 91]. They applied the model to the emulsion polymerization of MMA above the CMC of the emulsifier to discuss the mechanism of particle formation and growth in this system, and concluded that particle formation by micellar nucleation is at all times at least ten orders of magnitude greater than the homogeneous one, although MMA is moderately water-soluble [81].

Although the emulsion polymerization of VAc is already one of the most studied systems, research articles on this topic are still being published [128–132]. Gilmore et al. [128, 129] presented a mathematical model for particle formation and growth in the isothermal semibatch emulsion polymerization of VAc stabilized with poly(vinyl alcohol) (PVA). The model accommodated grafting onto the PVA backbone during particle formation, and polymeric stabilization. When the emulsion recipe, process conditions and kinetic parameters are supplied, the model can predict the various species concentrations along with the monomer conversion and particle size and number profiles. In Part II of a series of papers [129], model predictions were compared with semibatch and batch experimental results. Budhiall et al. [130] investigated the role of grafting in particle formation and growth during the emulsion polymerization of VAc with partially hydrolyzed PVA as the emulsifier and KPS as the initiator.

They found that: (1) the number of polymer particles produced was dependent on the PVA blockiness; (2) the PVA with the higher degree of blockiness led to the formation and stabilization of more polymer particles; (3) particle formation continued to high conversions for the more random PVA (Poval 217), whereas it appeared to stop at intermediate conversions for the blockier PVA (PVA217EE); (4) all systems exhibited limited aggregation of the polymer particles during the polymerization process, and; (5) the greatest amount of grafting of the PVA stabilizer onto the polymer particles occurred early in the reactions (X_M<25%), presumably contributing primarily to the stabilization of the particles. Shaffie et al. [131] studied the kinetics of the emulsion polymerization of VAc initiated by redox initiation systems of different persulfate cations such as KPS, sodium persulfate (NaPS), and ammonium persulfate (APS); each of them was coupled with a developed acetone sodium bisulfate adduct as the reducing agent. In emulsion polymerization, the exhaustion of the separate monomer droplet phase (the onset of Interval III) is usually followed by a decrease in the rate of polymerization due to the decrease in monomer concentration in the polymer particles. This is not the case for the emulsion polymerization of VAc, where the rate of polymerization remains constant throughout most of Interval III (ca. 20~90% conversion). In the case of VAc, Interval III starts from around 20% conversion [20, 64]. In order to explain the reason for the independence of the polymerization rate from the monomer concentration, Nomura et al. [20] developed a model that takes into account the particles containing at most two free radicals, where no instantaneous termination inside the particles is assumed. Based on this model, they ascribed the reason to an increase in the value of $\bar{n}$ due to the gel effect, which compensates for the decrease in monomer concentration with conversion. The decrease in the termination rate constant inside the polymer particles due to an increase in viscosity with conversion (the gel effect) prolongs the coexisting time of two free radicals in the same particle, thereby increasing the value of $\bar{n}$. Chern et al. [133] also developed a model that includes particles containing at most two free radicals. However, they attributed the reason to a decrease in the rate coefficient for radical desorption due to an increase in viscosity with conversion, which results in an increase in the value of $\bar{n}$. On the other hand, Bruyn et al. [132] proposed a kinetic model that considers a zero-one system with instantaneous radical termination inside the particles. The model assumes that radical loss is by transfer to a monomeric species which is very slow to propagate and whose radical activity is lost by desorption and termination, either in the aqueous phase or when it enters a particle containing a radical. Since the transfer step is rate determining, the rate of this process is proportional to monomer concentration, which then cancels the dependence on the monomer concentration in the overall polymerization rate expression. This model also predicts that the radical loss rate coefficient should be either $k_{tr}C_p$ (Limit 2a [1]) or $2k_{tr}C_p$ (Limit 2b [1]), where k_{tr} is the rate coefficient for transfer to monomer and C_p is the monomer concentration in the particles. They [134] also studied the kinetics and mechanisms of the emulsion polymerization of vinyl *neo*-decanete

(VnD), a practically water-insoluble monomer (its water solubility≅4×10^{-5} M at 50 °C) at 50 °C using sodium persulfate (NaPS) as the initiator and SDS as the emulsifier. They found that the polymerization rate was nearly independent of particle number for a given initiator concentration (approximately independent of particle size). They regarded this as consistent with the Limit 2b zero-one kinetics of emulsion polymerization, whereby a monomeric radical resulting from transfer to a monomer goes from particle to particle by desorption and reentry until it eventually enters a particle containing a growing radical, whereupon it undergoes very rapid bimolecular termination. Therefore, they explained the kinetic behavior of this system with the same mechanisms and model applied to the VAc system [132]. The most important claim raised in these articles is that, contrary to the conclusion of Nomura et al. [43, 64], the rate coefficient of radical desorption is independent of the water solubility of a desorbing monomeric radical. Therefore, the validity of their claim is still open for discussion and further studies are needed for its final solution.

Matsumoto et al. [135] studied the kinetics of the emulsion crosslinking polymerization and copolymerization of allyl methacrylate (AMA) with MMA, BMA and ethylene dimethacryllate (EDMA).

3.3.3 Particle Growth in Copolymer Systems

Ballard et al. [136] presented an extended S-E theory that provides a description of the emulsion copolymerization system during Interval II and III and suggested the possibility of using an "*average*" rate coefficient to treat the copolymerization system. On the other hand, Nomura et al. [45, 47, 137] first developed an approach to generalize the S-E theory for emulsion homopolymerization to emulsion copolymerization by introducing "*average (or mean) rate coefficients*" for propagation, termination and radical desorption. This methodology was termed the "*pseudo-homopolymerization approach*" [138] or the "*pseudo-kinetic rate constant method*" [139] and is now widely applied, not only to emulsion copolymerization systems, but also to other homogeneous free radical copolymerization systems. Nomura et al. [47, 122a, 140] demonstrated that the equations derived so far for emulsion homopolymerization can also be applied without any modification to a binary emulsion copolymerization system with monomers A and B by substituting the following "*average rate coefficients*" for the corresponding rate constants for emulsion homopolymerization.

The polymerization rate for the A-monomer is expressed as

$$r_{pA} = \bar{k}_{pA}[M_A]_p \bar{n}_t N_T \tag{53}$$

where $[M_A]_p$ is the concentration of A-monomer in the polymer particles and $\bar{n}_t$ is the average number of total radicals per particle ($\bar{n}_t = \bar{n}_A + \bar{n}_B$). The overall rate of copolymerization is defined by

$$R_p = \overline{k_p}[M]_p \bar{n}_t N_T = r_{pA} + r_{pB} = (\bar{k}_{pA}[M_A]_p + k_{pB}[M_B]_p)\bar{n}_t N_T \tag{54}$$

where $\bar{k}_p$ is the overall propagation rate coefficient defined by Eq. 54 and is a function of the propagation rate constant, monomer reactivity ratio and mole fraction of each monomer in the polymer particles. In the case of a binary emulsion copolymerization system, for example, the average rate coefficients are defined as follows:

1. The average rate coefficient for the propagation of the A-monomer, $\bar{k}_{pA}$, is given by

$$\bar{k}_{pA} = k_{pAA} f_A + (k_{pBB}/r_B) f_B \tag{55}$$

Here

$$f_A = \frac{\bar{n}_A}{\bar{n}_t} = \frac{k_{pBB} r_A [M_A]_p}{k_{pAA} r_B [M_B]_p + k_{pBB} r_A [M_A]_p} \tag{25}$$

where k_{pBA} denotes the rate constant for the propagation of a B-radical to an A-monomer, f_A is the fraction of A-radicals in the particle phase ($f_A+f_B=1$), and r_B is the B-monomer reactivity ratio.

2. The average rate coefficient for radical desorption, $\bar{k}_f$, is defined using the equations

$$k_f = k_{fA}(\bar{n}_A/\bar{n}_t) + k_{fB}(\bar{n}_B/\bar{n}_t) = k_{fA} f_A + k_{fB} f_B \tag{24}$$

and

$$k_{fA} = K_{oA}\left[\frac{C_{mAA} r_A [M_A]_p + C_{mBA} [M_A]_p}{r_B\{(K_{oA}\bar{n}_t/k_{pAA}) + [M_B]_p\} + [M_A]}\right] \tag{26}$$

where k_{fA} is the desorption rate coefficient for the A-monomeric radicals, C_{mBA} is the chain transfer constant of a B-radical to an A-monomer, and K_{oA} is the desorption rate constant for A-monomeric radicals, given by Eq. 19 in Sect. 3.2.1.

3. The average rate coefficient for radical termination in the particle phase, $\bar{k}_{tp}$, is defined by

$$\bar{k}_{tp} = k_{tpAA} f_A^2 + 2k_{tpAB} f_A f_B + k_{tpBB} f_B^2 \tag{56}$$

where k_{tpAB} is the bimolecular radical termination rate constant between A- and B-radicals. Other average coefficients, such as the average chain transfer coefficient, can be defined, if necessary, using the same principle. This approach can be easily extended to multimonomer emulsion polymerization systems [138, 141]. Based on an exact mathematical treatment, Giannetti [142] concluded that the pseudo-homopolymerization approach represents a suitable approximation for most copolymerization systems of practical interest, except for very special cases.

Since the appearance of the pseudo-homopolymerization approach, a wide variety of mathematical models have been developed for emulsion copolymerization systems using this approach, in order to thoroughly understand the mechanisms involved in particle formation, growth processes, and to predict the copolymerization rate, the properties of the copolymer obtained (molecular weight and copolymer composition), and colloidal characteristics (the particle number and PDS) [18, 27, 55, 58–63, 122(a), 140, 143–147]. Nomura et al. [122(a)] first proposed a kinetic model that introduced the pseudo-homopolymerization approach. They showed that the model could fairly accurately predict the monomer conversion versus time histories observed in the emulsion copolymerization of St and MMA. Moreover, they showed that the model could be successfully applied to the MMA-VAc system to predict the propagation rate constant and monomer reactivity ratio for each monomer, respectively. Furthermore, they presented both experimental and modeling work for the unseeded emulsion copolymerization of St and MMA, including the particle formation process [140]. The model was an extension of that used for simulating the kinetic behavior of the emulsion homopolymerization of MMA [74]. This model describes both the number of polymer particles produced and the monomer conversion versus time histories observed in the emulsion copolymerization of St and MMA conducted at 50 °C using KPS as the initiator and NaLS as the emulsifier.

Barandiaran et al. [63] also developed a mathematical model based on the pseudo-homopolymerization approach. Furthermore, they proposed a method to predict the kinetic parameters ($k_d f$, k_{ep}, k_f) in emulsion copolymerization using only calorimetric measurements, and gave the values of these parameters for the MA-VAc, MMA-BA emulsion copolymerization systems. Schoonbrood et al. [27] carried out a kinetic study of the seeded emulsion copolymerization of St with the relatively water-soluble monomer MA to investigate the mechanisms of radical entry into particles, radical desorption from particles, and the fate of radical species in the aqueous phase. For this purpose, they extended their propagation-controlled entry model to an emulsion copolymerimerization system by applying the pseudo-homopolymerization approach. López et al. [55] used calorimetric measurements to study the kinetics of the seeded emulsion copolymerization of St and BA. They varied the diameters of the seed particles, the number of initially charged seed particles, and the initial initiator concentration. A mathematical model was used to fit the experimental data for conversion versus time using the entry and desorption coefficients as adjustable parameters. Martinet et al. [145] carried out the emulsion copolymerization of α-methyl styrene (αMSt) and MMA at various temperatures (60, 70, 85 °C) in order to study the kinetic behavior, investigating the conversion, particle size, and the average number of radicals per particle, as well as the copolymer composition, microstructure, molecular weight distributions (MWDs), and the glass transition temperature (T_g). Unzueta et al. [18] proposed a mathematical model for emulsion copolymerization with mixed emulsifier systems, and carried out the seeded and unseeded emulsion copolymerizations of MMA and BA. Good agreement was found between the experimental results in batch and semicon-

tinous reactors and the corrsponding model predictions. Vega et al. [61, 147] and Dubé et al. [144] both developed mathematical models for the emulsion copolymerization of AN and Bu initiated by a redox initiator system, with the aim of simulating an industrial process and of improving the final polymer quality. Due to the high solubility of AN in water, the following effects were included: (a) the homopolymerization of AN in the aqueous phase; (b) the desorption of AN radicals from the polymer particles, and; (c) homogeneous particle nucleation. Saldívar et al. [58–60, 143] carried out extensive investigations on emulsion copolymerization. In the first paper, they presented a detailed mathematical modeling of emulsion copolymerization reactors along with comprehensive reviews of earlier models [58]. Then, they validated their model with experimental results obtained in the emulsion copolymerization of St and MMA, and demonstrated the generality of the model by applying it to three illustrative problems [143]. Furthermore, they performed a systematic experimental study of ten binary and three ternary emulsion copolymerization systems involving St, MMA, BA, Bu, VAc, AA and E [59]. The predictions for the evolution of conversion and average particle diameter in batch emulsion copolymerizations from the model were compared with experimental data for four emulsion copolymerizations of St with the comonomers MMA, BA, Bu and AA. After data fitting for unknown or uncertain parameters, the model was capable of quantitatively explaining the experimental observations for conversion evolution, but could only qualitatively explain the particle size evolution [59].

In industrial emulsion polymerization processes, a small amount of water-soluble carboxylic monomer (such as AA) is often added to improve the colloidal stability and surface properties of the resulting latex particles. Therefore, numerous studies have been carried out to date to clarify the influence of the AA monomer on the kinetic behavior of the emulsion copolymerization of St and AA [148–152] and of emulsion terpolymerizations including AA [79, 153, 154]. Shoaf et al. [148] presented a kinetic model that describes the reaction behavior of emulsion copolymerization systems where significant polymerization occurs in both the particle and aqueous phases. The model was applied to two seeded carboxylated emulsion copolymerization systems, AA-St and methacrylic acid (MAA)-St. They observed that the reaction behavior is greatly affected by the type of acid monomer used, the partitioning of the monomer between the various phases, and the locus of polymerization, and furthermore that the mechanism for the AA-St system is more complicated than that for the MAA-St system. They suggested that the primary reaction locus in the AA-St system shifts from the particles to the aqueous phase after the hydrophobic monomer, St, has been consumed. Yang et al. [149, 150] studied the effects of the initial comonomer (AA) concentration on the monomer conversion and particle number (N_T) in the emulsifier-free emulsion copolymerization of St and AA. They proposed an end-chain extension model to explain the experimental results where the monomer conversion to the power of 2/3 is proportional to the reaction time and $\log(N_T)=36.00+9.44[AA]_w$. Slawinski et al. [151] investigated the influence of AA on the particle growth process, with pH as the main

parameter in the seeded emulsion copolymerization of St and AA. To avoid the effect of pH on the decomposition of KPS [153, 155], they carried out the copolymerization at pH 2.5 (complete protonation) or pH 7 (neutralization). It was found that pH was the dominating factor in the incorporation of AA onto the particle surface. Wang et al. [152] examined the effect of AA and MAA separately on the total monomer conversion and the distributions of the carboxylic groups at different positions (the surfaces and cores of particles, and in the aqueous phase) in the emulsifier-free emulsion copolymerization of St with AA or MAA. On the other hand, Santos et al. [153] carried out a batch emulsion terpolymerization of St, BA and AA or MAA to study the effect of pH on the polymerization rate, monomer conversion, and glass transition temperature of the polymers produced, as well as the distributions of the carboxylic groups at different positions (the surfaces and cores of particles, and in the aqueous phase). Yan et al. [154] studied the kinetics and mechanisms of an emulsifier-free emulsion terpolymerization of St, MMA and AA. They found that the rates of particle formation and copolymerization increased with increasing concentrations of AA and APS and polymerization temperature. Yuan et al .[79] carried out the emulsion terpolymerization of St, Bu and AA in order to understand the roles of the water-soluble oligomers produced. It was found that increasing the AA concentration in the recipe increased the water-soluble oligomer concentration and the number of polymer particles, thereby increasing the rate of polymerization.

On the other hand, Xu et al. [156] studied the emulsifier-free emulsion terpolymerization of St, BA and the cationic monomer *N*-dimethyl, *N*-butyl, *N*-ethyl metacrylate ammonium bromide (DBMA) using oil-soluble azobis (isobutyl-amidine hydrochloride) (AIBA) as the initiator. They found that with increasing DBMA and AIBA concentrations, the number of oligomeric radicals increased, resulting in an increased polymerization rate, as shown by $R_p \propto [\mathrm{DBMA}]^{0.64}[\mathrm{AIBA}]^{0.67}$. Fang et al. [157] investigated the kinetics and the colloidal properties of the resulting polymer latexes in the emulsifier-free emulsion copolymerization of St and the nonionic water-soluble comonomer AAm, using an amphoteric water-soluble initiator, 2,2′-azobis[*N*-(2-carboxyethyl)-2–2-methylpropionamidine]-hydrate (VA057). They found that the rate of polymerization at 20% conversion was proportional to the initiator concentration to the power of 0.52.

Kostov et al. [158, 159] carried out a kinetic and mechanistic investigation of tetrafluoroethylene and propylene with a redox system containing tert-butylperbenzoate (TBPB). They found that $R_p \propto I_0^{0.54} S_0^{0.42}$, where R_p is the rate of polymerization, I_0 is the initial TBPB concentration, and S_0 is the initial emulsifier ($C_7F_{15}\,COONH_4$) concentration. Noël et al. [160] studied the effect of water solubility of the monomers on the copolymer composition drift in the emulsion copolymerization of MA and vinyl ester combinations. Urretabizkaia et al. [161] investigated the kinetics of the high solids content semicontinuous emulsion terpolymerization of VAc, MMA and BA. The effects of operating variables (feed flow rate, total amount of emulsifier, concentration of initiator and so on)

on the time evolution of the conversion, terpolymer composition, and the total number of polymer particles were investigated. The experimental results were analyzed by means of a mathematical model that incorporated the main features of the system. Ge et al. [162] studied the inverse emulsion copolymerization of (2-methacryloyloxyethyl) trimethyl ammonium chloride and AAm initiated with KPS. Aqueous monomer solutions were emulsified in kerosene with a blend of two emulsifers (Span80 and OP10). Particle formation was supposed to take place by monomer droplet nucleation. The observed rate of polymerization is represented by $R_p \propto I_0^{0.52} S_0^{0.38} M_0^{1.50}$, where M_0 is the monomer concentration.

3.3.4 Monomer Concentration in Polymer Particles

It is clear from Eq. 1 that the monomer concentration in a polymer particle is one of the three key factors that control the particle growth rate, and accordingly, the rate of polymerization. In emulsion polymerization, the course of emulsion polymerization is usually divided into three stages, namely, Intervals I, II and III. In Intervals I and II of emulsion homopolymerization, the monomer concentration in the polymer particles is assumed to be approximately constant. In Interval III, it decreases with reaction time. Two methods are now used to predict the monomer concentration in the polymer particles in emulsion homopolymerization: empirical and thermodynamic methods.

According to the empirical method [14, 20, 163], the monomer concentration in Intervals I and II can be expressed as

$$[\mathrm{M}]_p = [\mathrm{M}]_{pc} \tag{57}$$

Interval III begins when the monomer droplets disappear from the system at the monomer conversion X_{Mc}. The monomer concentration in this interval ($X_M > X_{Mc}$) is approximately given by

$$[\mathrm{M}]_p = [\mathrm{M}]_{pc} \left(\frac{1 - X_M}{1 - X_{Mc}} \right) \tag{58}$$

where $[\mathrm{M}]_{pc}$ is the constant monomer concentration at saturation swelling.

On the other hand, several researchers [164–167] have tried to thermodynamically describe the swelling behavior of polymer particles by one monomer. The thermodynamic approach now used is based on the so-called Morton equation given by

$$\frac{\Delta F_{ip}}{RT} = \ln(1 - \varphi_p) + \varphi_p \left(1 - \frac{1}{\bar{P}_n} \right) + \chi \varphi_p^2 + \frac{2 V_m \gamma \varphi_p^{1/3}}{r_0 RT} = 0 \tag{59}$$

where ΔF_{ip} is the partial molar free energy of the monomer in the polymer particles, φ_p is the volume fraction of polymer in the polymer particles, $\bar{P}_n$ is

the number-average degree of polymerization, χ is the Flory-Huggins interaction parameter, r_0 is the unswollen radius of the particle, R is the gas constant, T is the temperature, V_m is the partial molar volume of the monomer, and γ is the interfacial tension between the particles and the aqueous phase. Since the value of $\bar{P}_n$ is usually very large, the term $1/\bar{P}_n$ can be neglected. Given values of χ and r_0, Eq. 59 can be solved iteratively to yield φ_p. Then, by introducing the value of φ_p into the following equation, one can get the saturation monomer concentration in the polymer particles.

$$[M]_{pc} = \frac{1 - \varphi_p}{V_m} \tag{60}$$

Maxwell et al. [166] discussed the effects of several factors on the saturation and partial swelling of polymer particles by monomers using Eq. 59 and the Vanzo equation [168] that deals with the partial swelling of polymer particles in Interval III. By comparing theory and experiments for the MA and poly(MA-*co*-St) system, the authors showed that the monomer partitioning was insensitive to temperature, particle radius, copolymer composition, polymer molecular weight, polymer cross-linking, the value of the Flory-Huggins interaction parameter, and the particle-water interfacial tension, and that the conformational entropy of mixing of monomer and polymer was the significant term in determining the degree of partial particle swelling by the monomer. Contrary to Maxwell et al. [166], Antonietti et al. [167] observed a pronounced dependence of the swelling ratio on particle size where absolute values of swelling were much lower than those described by the classical Morton equation. In order to explain this phenomenon, the authors presented a modified description that considered size-relevant effects (such as the Kelvin pressure and depletion) using an additional osmotic pressure term, which increases with the inverse of the particle size. They also studied the effect of different types of covalently bound surface stabilizing groups on the degree of swelling, and found that electrically-stabilized particles resulted in higher swelling ratios and significant lower values for the interfacial energy as compared to sterically stabilized particles.

In an emulsion copolymerization, monomer partitioning between the monomer droplet, polymer particle and aqueous phases plays a key role in determining the rate of copolymerization and the copolymer composition. Two approaches (empirical and thermodynamic) have been proposed to predict the monomer concentrations in the polymer particles in an emulsion copolymerization system. In the emulsion copolymerization of St and MMA, Nomura et al. [45, 122, 140] first proposed an empirical approach for predicting the saturated concentration of each monomer in the polymer particles as a function of the monomer composition in the monomer droplets, as shown by

$$[M_i]_p = \frac{1}{a_i + b_i / W_{i,m}} \tag{61}$$

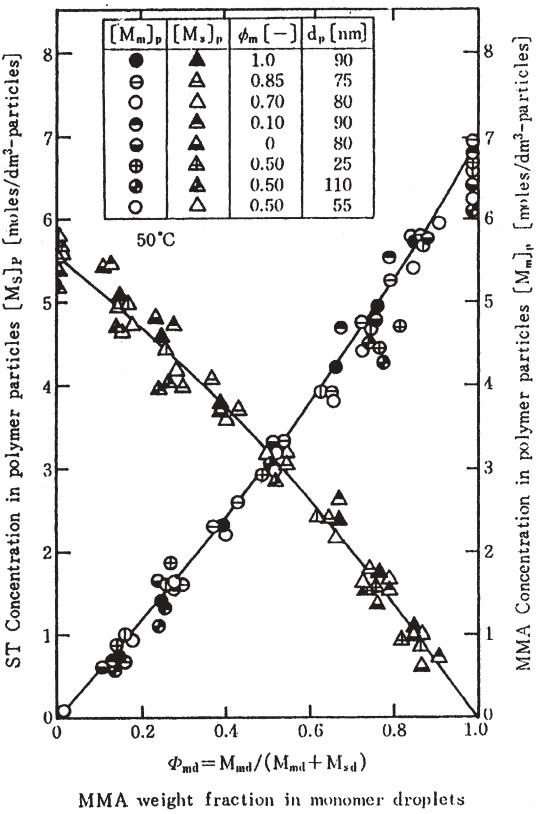

Fig. 5 Comparison of the observed saturation concentrations of St and MMA monomers in polymer particles with those predicted by Eq. 61 [45]

where the subscript i denotes monomer i, a_i and b_i are the numerical constants particular to monomer i, and $W_{i,\mathrm{m}}$ is the weight fraction of monomer i in the monomer droplets. Figure 5 is an example that shows good agreement between the predictions from Eq. 61 and experimental results.

The authors demonstrated experimentally that the saturation monomer concentration in the polymer particles was insensitive to particle radius and copolymer composition, and also that the weight fraction of the monomer i in the polymer particles ($W_{i,\mathrm{m}}$) was approximately equal to that in the monomer droplets ($W_{i,\mathrm{p}}$); in other words,

$$W_{i,\mathrm{m}} = W_{i,\mathrm{p}} \tag{62}$$

Thermodynamic methods were developed based on the extended equation by Ugelstad et al. [169], and have been further dealt with by various researchers [170–181]. Maxwell et al. [170] worked on the partitioning of two monomers between the polymer particle, monomer droplet and aqueous phases in an

emulsion copolymerization system, and proposed a thermodynamic approach that could be easily extended to deal with systems of three or more solvents and/or monomers. They derived the following equations for *i* and *j* monomers by taking into account the partial molar free energy of mixing of the monomer with polymer, the contribution of monomer to the interfacial free energy, the partial molar free energy of the monomer in the monomer droplets and the partial molar free energy of the monomer in the aqueous phase, respectively.

$$\ln\varphi_{pi} + (1 - m_{ij})\varphi_{pj} + \varphi_p + \chi_{ij}\varphi_{pj}^2 + \chi_{ip}\varphi_p^2 + \varphi_{pj} + \varphi_p(\chi_{ij} + \chi_{ip} - \chi_{jp}m_{ij}) + \frac{2V_{mi}\gamma\varphi_p^{1/3}}{r_0RT} = \ln\varphi_{di} + (1 - m_{ij})\varphi_{dj} + \chi_{ij}\varphi_{dj}^2 = \ln\left(\frac{[M_i]_w}{[M_i]_{w,sat}}\right) \quad (63a)$$

$$\ln\varphi_{pj} + (1 - m_{ji})\varphi_{pi} + \varphi_p + \chi_{ij}\varphi_{pi}^2 + \chi_{jp}\varphi_p^2 + \varphi_{pi} + \varphi_p(\chi_{ij} + \chi_{jp} - \chi_{ip}m_{ji}) + \frac{2V_{mj}\gamma\varphi_p^{1/3}}{r_0RT} = \ln\varphi_{dj} + (1 - m_{ji})\varphi_{di} + \chi_{ij}\varphi_{di}^2 = \ln\left(\frac{[M_j]_w}{[M_j]_{w,sat}}\right) \quad (63b)$$

where φ_p is the volume fraction of polymer in the latex particles, φ_{pi}, φ_{di}, φ_{pj} and φ_{dj} respectively represent the volume fractions of monomers *i* and *j* in the polymer particles and monomer droplet phases, χ_{ij}, χ_{ip} and χ_{jp} are the Flory-Huggins interaction parameters between each of the respective monomers *i* and *j* and the polymer, m_{ij} is the ratio of the molar volumes of monomers *i* and *j* (so $m_{ij}=V_{mi}/V_{mj}$, where V_{mi} and V_{mj} are the molar volumes of monomers *i* and *j*, respectively), $[M_i]_w$ is the concentration of monomer *i* in the aqueous phase, and $[M_i]_{w,sat}$ is its saturation concentration value if there are no other monomers present. The derivations of Eq. 63a and Eq. 63b involve the reasonable assumption that m_{ip} and m_{jp}, the ratios of the respective molar volumes of monomers *i* and *j* and the molar volume of polymer are negligible compared to all other terms. Furthermore, they made the following three assumptions to simplify Eqs. 63a and 63b.

1. For many pairs of monomers, the differences between the molar volumes of the monomers is slight. If this is the case, the ratio of the molar volumes of monomer *i* and *j* is well approximated by unity, so $m_{ij}=m_{ji}=1$.
2. The contribution to the partial molar free energy arising from the residual (enthalpic and non-conformational entropic) partial molar free energy of mixing of the two monomers is small relative to all other terms in the monomer droplet phase.
3. The interaction parameters for each monomer with the same polymer are equal ($\chi_{ip}=\chi_{jp}$).

They finally obtained the following simple expressions for saturation swelling.

$$\frac{\varphi_{pi}}{\varphi_{pj}} = \frac{\varphi_{di}}{\varphi_{dj}} \quad (64)$$

$$f_{pi} = f_{di} \tag{65a}$$

$$f_{pj} = f_{dj} \tag{65b}$$

where f_{pi}, f_{di}, f_{pj} and f_{dj} represent the volume fractions of monomers *i* and *j* in the polymer particle and monomer droplet phases, respectively. This equation relates the ratios of the volume fractions (or concentrations) of monomers *i* and *j* in the monomer droplet and particle phases. Eq. 65 is basically the same as Eq. 62 derived empirically by Nomura et al. [122(a)]. The validity of Eq. 65 was experimentally demonstrated in the St-MA, St-BA and MA-BA systems using seed polymer particles with different copolymer compositions and diameters. Based on Eq. 65 and experimental results, they finally proposed the following simple empirical expressions that could predict the concentration of monomers *i* and *j* in the polymer particles.

$$C_i = f_{di}[(C_{i,m} - C_{j,m})f_{d,i} + C_{j,m}] \tag{66a}$$

$$C_j = f_{dj}[(C_{j,m} - C_{i,m})f_{d,j} + C_{i,m}] \tag{66b}$$

where C_i and C_j are the concentrations of monomers *i* and *j* in the polymer particles, and $C_{i,m}$ and $C_{j,m}$ the maximum saturations of monomers *i* and *j* in the polymer particles (the homo-monomer swelling concentrations in the particles). By comparing the predictions from Eqs. 64 and 65 with experimental data from the St-MA, St-BA, MA-BA systems, they demonstrated that Eqs. 64 and 65 could provide adequate predictions for the monomer concentrations in the polymer particles. In these discussions, the ratio of the molar volumes of monomers *i* and *j* (m_{ij}) was assumed to be unity. On the other hand, Schoonbrood et al. [171] examined the validity of the assumption m_{ij}=1, made by Maxwell et al. [170], and demonstrated that this assumption could be used with systems where m_{ij} deviated from 1, at least up to a value of 2.

Noël et al. [172] experimentally determined both the saturation and partial swelling of MA-VAc copolymer latex particles by MA-VAc monomer mixtures. Monomer partitioning at saturation swelling could be predicted using the simplified relationships developed by Maxwell et al. [170]. On the basis of the work by Maxwell et al. [166, 170], Noël et al. developed an extended thermodynamic model for monomer partitioning at the partial swelling of latex particles by two monomers with limited water solubility in order to predict the monomer concentrations and fractions within the different phases, and confirmed the validity of this model by showing that the model's predictions were in good agreement with the observed monomer partitioning.

On the other hand, Schoonbrood et al. [173] investigated multimonomer partitioning in latex particles and derived simple equations describing monomer partitioning among the latex particle, monomer droplet and aqueous phases during Intervals II and III in emulsion copolymerization with any number of low to moderately water-soluble monomers, by extending the approaches developed by Maxwell et al. [170] and Noël et al. [172]. They showed that it is mainly the conformational entropy from mixing the monomer and polymer

that governs the partitioning behavior, and that other contributions to the free energies of the monomers in the polymer particles are marginal. They confirmed that all of the assumptions made in this study were valid using experimental results for St, MMA and MA, and confirmed that the simple equations proposed describe the monomer partitioning with these three monomers in Intervals II and III very well. In this approach, the only parameters needed to calculate the monomer concentrations in all of the phases were the saturation concentrations of each monomer in the polymer particles, and the saturation concentrations of each monomer in the aqueous phase.

By combining thermodynamically-based monomer partitioning relationships for saturation [170] and partial swelling [172] with mass balance equations, Noël et al. [174] proposed a model for saturation and a model for partial swelling that could predict the mole fraction of a specific monomer *i* in the polymer particles. They showed that the batch emulsion copolymerization behavior predicted by the models presented in this article agreed adequately with experimental results for MA-VAc and MA-Inden (Ind) systems. Karlsson et al. [176] studied the monomer swelling kinetics at 80 °C in Interval III of the seeded emulsion polymerization of isoprene with carboxylated PSt latex particles as the seeds. The authors measured the variation of the isoprene sorption rate into the seed polymer particles with the volume fraction of polymer in the latex particles, and discussed the sorption process of isoprene into the seed polymer particles in Interval III in detail from a thermodynamic point of view.

These thermodynamic equations provide the most complete description of the swelling of polymer particles by monomers, but include a rather large number of parameters whose accurate estimation requires extensive work. Considering this, Gugliotta et al. [175] presented a criterion for choosing which monomer partitioning models developed so far in the mathematical modeling of emulsion copolymerization should be applied to a given system. In the mathematical simulations, the seeded emulsion copolymerization of four monomer systems with a wide variety of reactivity ratios and water-solubilities were considered: BA-St, VAc-MA, VAc-BA and St-MAA. They investigated the effect of the complexity of the monomer partitioning equations, the type of process, the solid contents, and the amount of seed on the time evolution of the conversion and copolymer composition, and tabulated a summary of recommended monomer partitioning models.

In the industrial production of structured AN-Bu-St (ABS) latex particles, the grafting copolymerization of AN and St on crosslinked polybutadiene (PB) seed latex is carried out in emulsion polymerization. Therefore, information on the effect of PB crosslinking density on the swelling of PB latex particles by a St-AN monomer mixture is very important for the production of ABS copolymers with desired properties. Mathew et al. [177] studied the effect of several thermodynamic parameters, such as the crosslinking density, particle size and monomer mixture composition on the swelling behavior of PB latex particles by pure St and AN, and St-AN mixtures of various compositions. They reported

that, in the case of mixtures, the higher the AN concentration in the mixture, the lower the maximum swelling by St, and the opposite effect was observed for AN swelling. The parameters describing the interaction between the two monomers were found to be functions of the composition in the initial mixture.

Liu and Nomura et al. [178–180] carried out a series of investigations on the swelling behaviors of St-AN (SAN) and ABS latex particles by St-AN monomer mixtures. In the first article, Nomura et al. [178] examined the effects of copolymer composition and its compositional inhomogeneity in SAN latex particles on their swelling behavior, and found that both the copolymer composition and the compositional inhomogeneity in SAN latex particles had little or no influence on the swellability of SAN latex particles with a St-AN monomer mixture, as long as the weight fraction of AN monomer units in SAN latex particles was less than a certain value (between 0.6 and 0.8). Based on the experimental data, they proposed semiempirical equations that could predict the saturation concentration of each monomer in the SAN latex particles as a function of the comonomer composition in the monomer droplets and the overall copolymer composition in the SAN latex particles. In the follow-on article, Liu et al. [179] investigated the possibility of a thermodynamic correlation between both the partial and saturation swelling of SAN latex particles by St-AN monomer mixtures. First, they determined the three unknown Flory-Huggins interaction parameters between each monomer and homopolymer, $\chi_{A,PA}$, $\chi_{A,PS}$, and $\chi_{S,PS}$ (S: styrene, PA: polyacrylonitrile, PS: polystyrene) by fitting the thermodynamic swelling equations to the experimentally observed monomer concentrations in SAN latex particles. Then, they showed that the AN concentrations predicted by using these interaction parameters agreed fairly well with those observed. However, agreement between the predicted and observed St concentrations was somewhat worse than that for the AN concentrations. On the basis of the preceding studies, Liu et al. [180] further studied the saturation swelling of ABS latex particles by a St-AN monomer mixture. In order to describe the observed saturation swelling behavior, they proposed a two-phase swelling model based on the assumptions that in ABS latex particles, St-AN (SAN) copolymer domains were randomly dispersed in a continuous PB matrix, and further that thermodynamic equilibrium was attained among the SAN copolymer domain, PB matrix and monomer droplet phases. By using the proposed model, the effects of various factors on the saturation concentrations of each monomer in the ABS latex particles were experimentally and theoretically discussed. The factors examined were the polymer crosslinking density $\overline{M}_C$, the interfacial tension between the PB latex particle and aqueous phases γ, the ratio of the molar volumes of the St and AN monomers m_{ab}, the weight fraction of AN units in the SAN copolymer domains H_A, and the weight fraction of PB in the ABS latex particles H_{PB}. It was found that the saturation concentration of each monomer in the SAN latex particles was insensitive to $\overline{M}_C$, γ, m_{AB} and H_A, but that H_{PB} had a large influence on the saturation concentration of the AN monomer but almost no influence on the saturation concentration of the St monomer. They finally concluded that the two-phase swelling model developed

in this study could predict the saturation concentrations of St and AN monomers in the ABS latex particles quite well.

On the other hand, Aerdts et al. [181] carried out partial and saturation swelling experiments in latex particles of St-MMA (SMMA) copolymers, polybutadiene (PB) and composite particles containing PB with St and MMA grafted on, and compared the results from them to predicted results from the semiempirical equations developed by Maxwell et al. [166, 170]. They showed that the partitioning of MMA was independent of the type of polymer/SMMA copolymers of different compositions and PB. Moreover, the partitioning of MMA in PB was independent of particle size, polymer crosslinking density and the presence of SMMA copolymer grafted onto PB. It was further shown that the swelling of latex particles by St and MMA monomer mixtures was also independent of the polymer type of the latex particles and that the saturation partitioning of monomers between the latex particle and monomer droplet phases could be predicted by the simplified equations of Maxwell et al. (Eq. 66).

Said et al. [182] studied the effects of adding inorganic electrolytes on the emulsion polymerization of St using three different ionic emulsifiers and potassium and sodium chlorides as the inorganic electrolytes. They observed a significant increase in the rate of polymerization in all cases as the concentration level of the added electrolyte was increased. At the same time, they carried out saturation swelling measurements and found a slight increase in the monomer concentration inside the polymer particles as the level of added electrolyte concentration was increased. They thought that one reason for an increase in the rate of polymerization was the increase in the monomer concentration inside the polymer particles as the level of added electrolyte concentration was increased.

Tognacci et al. [183] discussed various methods for measuring the monomer concentration in the polymer particles. The method proposed by the authors is a direct estimation of the solvent activity by the GC (gas chromatography) measurement of its partial pressure in the gas phase at equilibrium with the polymer particle, monomer droplet (if any) and aqueous phase in the latex. They proposed an original measuring technique and carried out measurements for different monomers (St, MMA, and VAc) and polymeric matrices (PSt and MMA-VAc copolymer), both above and below saturation conditions (corresponding to Intervals II and III). They compared the experimental data with that predicted by the monomer partitioning relationships derived by Maxwell et al. [166, 170] and Noël et al. [172].

3.3.5 Reaction Calorimetry

Reaction calorimetry has been widely explored in studies of the kinetics of heterophase polymerization in recent years [63, 82–84, 147, 184–191]. There are several advantages of using a reaction calorimeter: (1) the rate of polymerization is obtained directly, using the monomer conversion calculated from the

integral of the heat of reaction curve, and (2) nearly continuous information is obtained. Using this information, a more detailed examination of the polymerization kinetics can be made, allowing the observation of important features which cannot be seen using any other technique (such as gravimetry and gas chromatography). Therefore, reaction calorimetry provides a powerful tool for investigating heterophase polymerization [82]. Recently, many papers have been published on reaction calorimetry studies into the kinetics of emulsion polymerization. The kinetics of the emulsion polymerization of St was reinvestigated in detail [82–84, 184]. The effect of surface charge density on the kinetics of the seeded emulsion polymerization of St was studied [185]. The dependence of the reaction rate profiles on the water solubility of the monomers, on the presence of CTA, on the types and concentrations of the stabilizer and the initiator, and on the polymerization temperature was investigated [187]. The influence of oxygen on the kinetics of chemically initiated seeded emulsion homopolymerization of St and the seeded emulsion copolymerization of St and BA was investigated [188]. Reaction calorimetry has been used to estimate the parameters in emulsion copolymerization systems [63], to control monomer conversion and copolymer composition in semi-batch unseeded emulsion copolymerization on-line [186, 189–191], and to monitor the copolymer composition, the average molecular weight, and the average degree of branching in the semi-batch unseeded emulsion copolymerization of AN and Bu [147].

Most reaction calorimeters work according to heat-flow calorimetry principles. The heat of reaction Q_r evolved from a reaction mixture running at T_r under isothermal conditions is transferred to the fluid in the cooling jacket according to the equation

$$Q_r = R_p(-\Delta H_p) = UA_{const}(T_r - T_j) \tag{67}$$

where R_p is the reaction rate, ΔH_p is the heat of reaction per unit amount of reactant, U is the overall heat transfer coefficient, A_{const} is the constant heat transfer area, and T_j is the fluid temperature in the cooling jacket. The flow rate of the cooling fluid is so high that the cooling fluid temperature at any position in the jacket is considered to be, to a good approximation, equal to T_j. The temperature of the cooling fluid T_j is adjusted to keep the reaction temperature constant at T_r, and the heat of reaction Q_r is found by calculating the value of $UA_{const}(T_r - T_j)$. Here, the heat transfer area A_{const} and the value of U (determined by calibration before and after the reaction) are treated as constant during the reaction. However, the value of U is likely to change during the reaction wherever the viscosity of the reaction mixture varies and/or the deposition of scale on the heat transfer surface occurs during the reaction.

To avoid the drawbacks mentioned above, a novel calorimeter was developed [192], as shown in Fig. 6, which can accurately measure the heat of reaction independently of the variation of U during a reaction.

The working principle is as follows. A cooling fluid at temperature T_i at the inlet is fed into the cooling jacket at a constant mass flow rate F_{in}, and the wetted heat transfer area A_{var} in the jacket (which can be varied in this calorime-

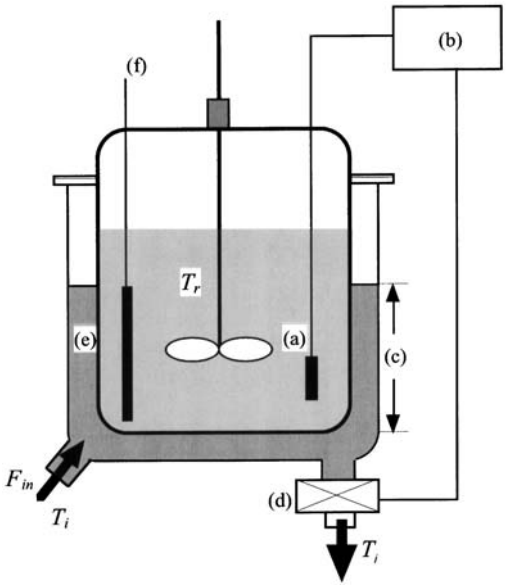

Fig. 6 Schematic diagram of a novel calorimeter with variable heat-transfer area

ter) is controlled to keep the temperature of the reaction mixture at the desired reaction temperature T_r by adjusting the fluid level (c) in the jacket, which is achieved by regulating the flow rate of the cooling fluid at the outlet with a computer-controlled throttle valve positioned there. The fluid temperature in the cooling jacket is considered to be T_j throughout the jacket because of satisfactory mixing due to the kinetic energy of the cooling fluid entering through a nozzle. Therefore, the temperature of the cooling fluid flowing through the outlet of the jacket is also T_j. To offset the heat loss from the reaction calorimeter Q_{loss}, a constant heat flux $Q_h (> Q_{loss})$ is passed into the reaction mixture through an immersed electrical heater (f) in order to maintain the reaction mixture at a constant temperature T_r even in the absence of the reaction. A reference run is carried out with no reaction before measuring the heat of reaction. Then, the steady-state heat balance for the reaction mixture in the calorimeter at temperature T_r is given by

$$Q_h = Q_{m0} + Q_{loss} \tag{68}$$

$$Q_{m0} = F_{in} C_p (T_i - T_j) = UA_{var} (T_r - T_j) \tag{69}$$

where Q_{m0} is the heat flux transferred to the cooling fluid across the reactor wall and T_j is the cooling fluid temperature at the outlet of the jacket. Since the values of F_{in}, T_i and T_j are measurable, the heat flux Q_{m0} is obtained by calculating the value of $F_{in} C_p (T_i - T_j)$, where C_p is the specific heat of the cooling fluid. Therefore, this calculated value of Q_{m0} gives a base-line reading and is constant

as long as Q_{loss} remains constant. On the other hand, when the reaction is allowed to take place at the constant temperature T_r, one gets the steady-state heat balances given by

$$Q_h + Q_r = Q_m + Q_{loss} \tag{70}$$

$$Q_m = F_{in}C_{pi}(T_i - T_j) = UA_{var}(T_r - T_j) \tag{71}$$

where Q_m is the heat flux corresponding to the new reading when the reaction is taking place. As long as the value of Q_{loss} is kept constant by maintaining the temperature around the region of the calorimeter constant, one gets the following expression from Eqs. 68 to 71.

$$Q_r = Q_m - Q_{m0} \tag{72}$$

Therefore, one can derive the heat of reaction Q_r independently of the value of U from the difference between the new and base-line readings.

3.4 Effect of Initiator Type

There are two types of chemical initiator that can be used to initiate emulsion polymerization. They are water-soluble initiators (such as KPS, hydrogen peroxide-iron (II) redox system) and oil-soluble initiators (like azobis-isobutyronitrile (AIBN), benzoil peroxide (BPO), benzoil peroxide-*N*,*N*-dialkylaniline redox system). Water-soluble initiators are more commonly used in emulsion polymerization than oil-soluble initiators. However, oil-soluble initiators are sometimes used when the fragments derived from ionic water-soluble initiators are not desirable either in the latex serum or on the surface of the polymer particles. Water-soluble initiators produce almost all of the free radicals in the water phase, because the amount of initiator partitioned into the organic phases is usually negligible. Contrary to water-soluble initiators, oil-soluble initiators distribute among the four phases: monomer-swollen micelles, monomer-swollen polymer particles, monomer droplets (if any), and the water phase. In the case of oil-soluble initiators, only a small fraction of radicals are produced in the water phase because the amount of initiator partitioned into the water is usally very small. Therefore, it is useful to find out whether the different principal initiator loci of polymerization systems with water-soluble and oil-soluble initiators brings about any differences in the kinetics and mechanisms of polymerization between both initiator systems.

Several researchers have carried out experimental and/or theoretical investigations on emulsion polymerizations initiated with oil-soluble initiators and reported that the kinetics of the emulsion polymerizations is basically similar to that initiated with water-soluble initiators [193–202]. Breitenbach et al. [193] carried out the emulsion polymerization of St initiated by BPO at 50 and 60 °C. The authors interpreted the experimental results by assuming a relatively rapid exchange of low molecular weight radicals between the micelle-polymer

particle and water phases. Van der Hoff [194] conducted the emulsion polymerization of St initiated by cumen hydroperoxide (CHP) and suggested three possible mechanisms. One possibility is the entry of single radicals generated from the fraction of the initiator dissolved in the water phase. A second possibility is that single radicals are formed by desorption of one of a pair radicals (that form within the particles or by a side reaction) into the water phase. Another possible mechanism is that pairs of radicals are produced in the emulsifier layer, and only the organic radical ($C_9H_{11}O\cdot$) enters the particle, while the inorganic initiator fragment ($OH\cdot$) remains in the water phase where it can undergo further reaction. The author stated that there was no direct evidence that any of these three mechanisms in fact came into play. Dunn et al. [195] carried out the emulsion polymerization of St at 60 °C using octadecyl sulfate as the emulsifier and AIBN as the initiator. They found that the number of polymer particles produced varied approximately with the 0.4^{th} power of the initially charged initiator concentration. This behavior is quite similar to that usually found in the emulsion polymerization of St initiated with KPS. They ascribed this kinetic similarity to desorption of either of the primary radicals that formed as a pair into the water phase, leaving a single radical inside the polymer particle for initiation. It was also found that only 4% of the whole initially charged initiator was effective in the emulsion polymerization in contrast with an efficiency of ~50% found in bulk or solution polymerizations. Barton et al. [196] investigated the effect of an oil-soluble initiator (AIBN) on the kinetics and mechanism of the emulsion polymerization of BMA at 60 °C in the presence of the anionic emulsifier disodium dodecylphenoxybenzene disulfonate. They compared the results obtained with the course of the emulsion polymerization of BMA initiated by KPS, and proposed that the radicals produced by decomposition in the aqueous phase determine the kinetics of the polymerization.

On the other hand, Il'menev et al. [197] carried out the emulsion polymerization of St at 50 °C using oil-soluble initiators such as AIBN, BPO and lauryl peroxide (LPO). The water-solubilities of AIBN, BPO and LPO at 20 °C are 3.6, 0.1 and 0.01 mol/dm^3-water, respectively. The rate of polymerization conducted at 50 °C with 0.025 mol/dm^3-St of each initiator was found to be (fastest to slowest): AIBN, BPO and LPO; in other words, in the order of decreasing water-solubility. They estimated the average times for a primary radical to terminate, propagate, and desorb into the aqueous phase, respectively, when a pair of radicals are generated in a micelle and a polymer particle. They concluded that the contribution to the polymerization (particle formation and growth) from the free radicals that are produced in pairs in the micelles and polymer particles is almost negligible, because they are very likely to cause rapid geminate termination, and that the free-radicals generated in the monomer droplets also play only a small part in the polymerization, because their desorption into the water phase can be ignored. This view was strongly supported later by the theoretical and experimental work of Nomura et al. [198–202]. Nomura et al. [198] proposed a theoretical approach by which the effects of various factors

on the average number of radicals per particle $\bar{n}$ could be predicted in seeded emulsion polymerizations initiated by oil-soluble initiators. In their approach, the following six kinetic events were considered, (i) the generation of a pair of radicals inside the particles, (ii) radical entry into the particles from the aqueous phase, (iii) overall radical desorption including both primary initiator radicals and single-unit monomeric radicals produced by chain transfer to monomer molecules, (iv) bimolecular termination of radicals in the particles, (v) bimolecular termination of radicals in the aqueous phase, and (vi) generation of radicals in the aqueous phase by decomposition of the initiator dissolved in the phase. Based on these events, they formulated a set of six differential equations describing the system in which particles containing more than six radicals per particle could be neglected. The authors introduced a new parameter $K=\rho_w/\rho_p$, where ρ_w is the rate of radical production per unit volume of water, and ρ_p is the rate of radical production inside the particles per unit volume of water. They solved a set of differential equations numerically and plotted the calculated values of $\bar{n}$ against $\alpha_p=(\rho_p \nu_p/k_{tp}N_T)$ for the range $0\leq K\leq\infty$. Here, the bimolecular termination of radicals in the water phase was assumed to be negligible ($Y=0$). An advantage of this approach is that the time evolution of the average number of radicals per particle can be evaluated. These plots were found to be quite similar to those obtained for the case of KPS, except for $K=0$. On the other hand, when $K=0$ (so the oil-soluble initiator employed is completely insoluble in water) no region of $\bar{n}=0.5$ was found regardless of the values of α_p and m (the parameter relating to the rate of radical desorption), and the polymerization proceeded according to suspension polymerization kinetics. Therefore, it was concluded that, kinetically, the similar behavior of emulsion polymerization initiated by oil-soluble initiators to that initiated by water-soluble initiators originated from the water-soluble portion of the oil-soluble initiator rather than from the desorption of the initiator radicals produced in the particles.

In order to delve deeper into the similarities and differences between the kinetic behaviors of emulsion polymerization initiated by oil-soluble initiators or water-soluble initiators, Nomura et al. [199–202] carried out extensive investigations into the kinetics and mechanisms of the unseeded and seeded emulsion polymerizations of St at 50 °C using sodium lauryl sulfate (NaLS) as the emulsifier and AIBN as the initiator, and obtained the following conclusions:

1. The latex (polymer) particles are generated from the emulsifier micelles and the number of latex particles produced is proportional to the 0.70^{th} power of the initial concentration of the emulsifier forming micelles and to the 0.30^{th} power of the concentration of initially charged AIBN. This behavior is very similar to that observed when the water-soluble initiator KPS is used.
2. The polymerization takes place both in the monomer droplets and in the latex particles produced. The polymerization inside the monomer droplets proceeds according to the kinetics of suspension polymerization until the

monomer droplets have disappeared from the reaction mixture due to complete absorption by the resultant latex particles. On the other hand, the polymerization in the latex particles proceeds according to emulsion polymerization kinetics, independently of the polymerization in the monomer droplets. The total amount of polymer produced inside the monomer droplets is only several percent of the whole polymer produced. Moreover, the molar mass of the polymer produced in the monomer droplets is the same as that produced by bulk polymerization under comparable conditions and is only about one-hundredth of that produced in the latex particles.

3. The free radicals produced from the fraction of initiator dissolved in the water phase are responsible for particle formation and growth in the emulsion polymerization of St initiated by AIBN. The free radicals produced in pairs in the polymer particles play almost no role in the polymerization inside the polymer particles because pairs of radicals produced within a volume as small as a monomer-swollen latex particle or a monomer-swollen micelle are very likely to recombine.
4. A kinetic model developed for unseeded emulsion polymerization based on the knowledge and conclusions obtained above could explain the progress of polymerization inside both the monomer droplets and the latex particles in the seeded emulsion polymerization of St initiated by AIBN at 50 °C.

Therefore, they showed both theoretically and experimentally that the kinetic behavior of the emulsion polymerization of St initiated by AIBN is basically similar to that initiated by KPS, and concluded that this similarity is mainly due to the radicals produced from the water-soluble fraction of the initiator, because the radicals produced pair-wise inside the small volume of a monomer-swollen latex particle or a monomer-swollen micelle are very likely to recombine.

Several researchers have also experimentally and theoretically investigated the reasons for this kinetic similarity [203–208]. Asua et al. [203] proposed a mathematical model that can predict the average number of radicals per particle $\bar{n}$ in seeded emulsion polymerization initiated by oil-soluble initiators. Their model includes the parameter f_w that denotes the fraction of the initiator dissolved in the aqueous phase, and the following various kinetic events: (i) generation of radicals inside the particles, (ii) desorption of primary initiator radicals from the polymer particles before reacting with a monomer molecule, (iii) termination of radicals by bimolecular reaction in the particles, (iv) desorption of single-unit monomeric radicals produced by chain transfer to monomer molecules, (v) absorption of radicals from the aqueous phase into the particles, (vi) termination of radicals in the aqueous phase, and (vii) generation of radicals in the aqueous phase by decomposition of the initiator dissolved in that phase. They calculated the average number of radicals per particle in a typical example of the seeded emulsion polymerization of St, using their model that distinguishes between desorption of primary initiator radicals and single-unit monomeric radicals. The effect of increasing the water-soluble fraction f_w of the initiator from 0 to 0.1 was calculated for various particle diameters in the range

23–231 nm. For a fixed particle size, the value of $\bar{n}$ was found to be essentially independent of the fraction f_w of the initiator present in the aqueous phase, even for f_w=0. Moreover, the plot of $\bar{n}$ versus the seed particle diameter was quite similar to that found for the emulsion polymerization initiated by KPS. The authors therefore concluded that the kinetic similarity mainly originated from desorption of the initiator radicals produced in the particles rather than from decomposition of the initiator present in the aqueous phase. Mørk et al. [208], however, pointed out that the almost identical values of $\bar{n}$ found for a completely water-insoluble initiator (f_w=0) appeared to contradict calculations performed by Mørk et al. [208] and Nomura et al. [198], and that calculations by Asua et al. [203] could not be taken as evidence that a desorption mechanism is the reason for the similarity. Alduncin et al. [204] studied the seeded emulsion polymerization and the miniemulsion polymerization of St using an oil-soluble initiator (AIBN) in an attempt to elucidate the main locus of radical formation in emulsion polymerization initiated by an oil-soluble initiator. The monomer/water weight ratio (M/W) was varied while keeping the monomer/initiator ratio constant. They found that the average number of radicals per particle ($\bar{n}$) increased as the M/W ratio increased. This was taken as evidence that the overall rate of radical entry into a particle increased when the M/W ratio increased. They claimed that this phenomenon could only be explained by assuming that the radicals responsible for emulsion polymerization initiated by oil-soluble initiators are mainly those produced from the initiator partitioned into the polymer particles, followed by desorption into the water phase. Mørk et al. [208] concluded, on the basis of their calculations, that the argument provided by Alduncin et al. [204] was not strong enough to resolve the issue of the similarities between the kinetic behaviors of emulsion polymerization with oil-soluble and water-soluble initiators.

Mørk et al. [206–208] recently published a series of theoretical works. In the first article of this series [206], the authors aimed to develop expressions that would allow easy and rapid calculation of the average number of radicals per particle in emulsion polymerizations with a constant number of reaction loci containing an oil-soluble initiator. Taking into account pairwise formation of radicals in the particles, desorption and reabsorption, water phase termination, solubility of the initiator in the water phase, and the possible formation of a single radical species, they derived the recurrence relation that determined the stationary state distribution of radicals in a particle. The calculation was based on a probabilistic analysis leading to a third-order recurrence relation solved using confluent, hypergeometric Kummer functions. The calculated results confirmed the previous finding of Nomura et al. [198] that the kinetics of emulsion polymerizations carried out with oil-soluble initiators are quite similar to those with water-soluble initiators, provided that the oil-soluble initiator is not completely insoluble in the water phase. The main intention of the second article [207] was to develop equations that make it relatively easy to assess the effects of the most common experimental variables on the stationary state average number of radicals per particle in a bidispersed seeded emulsion poly-

merization, and on the competitive growth of differently-sized seeded particles in this system. In the third article [208], the authors extended the third-order recurrence relation derived in the first article to the general case by including single radical formation in the particles; for example, by a redox reaction along with the formation of pairs of radicals by thermal decomposition. They carried out calculations for the case where single radicals are generated inside the particles by an oil-soluble initiator, with or without the simultaneous formation of pairs of radicals. The calculations showed that:

1. From a kinetic point of view, single radicals generated in the particles behaved quite similarly to radicals produced in the water phase.
2. However, at high rates of radical desorption, the effect of water phase termination on the average number of radicals per particle is much more prominent when the radicals are produced in the water phase.
3. In the system where an oil-soluble initiator generates both single radicals and pairs of radicals, the contribution of the latter to the average number of radicals per particle is almost negligible.
4. When an oil-soluble initiator distributes between phases, the single radicals that are responsible for the similar kinetic behavior observed with water-soluble and oil-soluble initiators originate from the water-soluble fraction of the initiator rather than from a desorption/reabsorption mechanism as claimed by Asua et al. [203] and Alducin et al. [204].

Consequently, the authors supported the conclusion of Nomura et al. [198, 199] that the reason for the similar kinetic behaviors observed for water-soluble and oil-soluble initiators originates from the water-soluble fraction of the initiator.

Unlike in conventional emulsion polymerization, no monomer droplets exist in a microemulsion polymerization system, and hence, oil-soluble initiators partition into the monomer-swollen micelles, the resultant polymer particles and the water phase. Therefore, in microemulsion polymerization, the polymerization only proceeds in the monomer-swollen micelles and the resultant polymer particles over the entire course of polymerization. Pairs of radicals produced in volumes as small as monomer-swollen micelles and polymer particles may terminate as soon as they are generated. If so, it is expected that the radicals responsible for the polymerization in the monomer-swollen micelles and the resultant polymer particles would usually be those generated from the fraction of the initiator dissolved in the water phase. In order to examine whether this expectation is correct, oil-in-water (O/W) microemulsion polymerizations of St were carried out using four kinds of oil-soluble azo-type initiators with widely different water-solubilities [209]. It was found that the rates of polymerization with these oil-soluble initiators were almost the same irrespective of their water-solubilities, when the polymerizations were carried out with the same rate of radical production for the whole system for all of the oil-soluble initiators used. Moreoever, the rate of polymerization with any of these oil-soluble initiators was only about 1/3 of that with KPS at the same rate of radical production. Considering that the rate of polymerization was pro-

portional to the 0.5^{th} power of the initiator concentration regardless of whether the initiator used was oil-soluble or water-soluble [210], the authors concluded that the apparent efficiencies of these oil-soluble azo-type initiators were all only 1/9 of that of KPS. This might suggest that although radicals were generated in the monomer-swollen micelles and polymer particles as well as the water phase, only 1/9 of the radicals generated were active in the microemulsion polymerization of St, while the rest were lost somewhere (possibly in the water phase) by bimolecular termination. These experimental results seem to support the desorption/reabsorption mechanism proposed by Asua et al. [203], although Candau et al. [205] also suggested that, in the case of AIBN, the radicals that initiate the polymerization are not those from the initiator localized within the monomer-swollen micelles, but from the initiator dissolved in the water phase. Therefore, the role of oil-soluble initiators in the kinetics of heterogeneous polymerizations such as emulsion and microemulsion polymerizations is still unanswered, and further studies are needed for its final elucidation. A recent review article [211] refers to the role of oil-soluble initiators in heterogeneous polymerizations including emulsion polymerization.

Conventional emulsion polymerizations are usually initiated by chemical initiators. However, there are some disadvantages in the use of chemical initiators. For example, some of the products produced by termination in the aqueous phase may undergo subsequent reactions, resulting in discoloration of the final latex, or any residual initiator present after the polymerization may act as an undesirable contaminant. To avoid these problems, alternative techniques for radical initiation that are safe and inexpensive have been explored. Ultrasound has been increasingly used to realize novel chemical reactions and enhance the reaction rate; this emerging field is called "sonochemistry". Relatively recently, several researchers have investigated the possibilities of using ultrasonic irradiation as a way to initiate free radical species in emulsion polymerizations of various monomers [212–219]. Biggs et al. [212] conducted pioneering work on the ultrasonically-initiated emulsion polymerization of St at 30 °C (±5 °C) using NaLS as the emulsifier and a 20 kHz horn sonifier as a ultrasound generator. From experiments carried out at a fixed ultrasound intensity, they concluded that: (1) radicals produced as a consequence of the cavitation process were sufficient to cause polymerization; (2) the rate of polymerization increased to a maximum at about 30% conversion before decreasing, showing no constant region; (3) the rate of polymerization increased with increasing concentration of initially charged NaLS (negligible polymerization without NaLS); (4) the diameters of final latex particles were very small (around 50 nm), and the PSt molecular weights were high ($>10^6$); (5) there was continuous formation of polymer particles, and; (6) the small particle sizes, high polymerization rates, and continuous nucleation of polymer particles were postulated to be due to the continuous formation of very small monomer droplets in the ultrasonic field, which could efficiently scavenge the radicals formed during the cavitation process. The authors concluded from these experimental results that this polymerization system had many similarities with microemulsion polymerization

but at a considerably reduced emulsifier level. They extended this study, mainly to clarify the effects of varying the input ultrasound intensity [213], and found that: (1) a marked increase in the rate of polymerization was seen as the input power was increased; (2) despite the increase in the rate of polymerization, the increasing intensity did not affect the resultant polymer particle sizes, which were in all cases 40–50 nm, and; (3) increases in both the concentration of NaLS and the reaction temperature resulted in an increased rate of polymerization at a fixed input intensity, but the particle sizes were invariant.

Cooper et al. [214] carried out the emulsion homopolymerization of BA and of VAc, and also the emulsion copolymerization of BA and VAc at 30 °C (±5 °C) using 20-kHz ultrasound as the initiator with SDS and Aerosol AT as the emulsifiers, respectively. The homopolymerization rate of VAc (10 wt%) was much lower than that of BA (10 wt%), and interestingly, lower rates of BA emulsion homopolymerization were observed at higher temperatures. The reason for such a large difference in the rate of polymerization between the BA and VAc systems was explained by the greater evaporation of the more volatile VAc monomer into the cavity, suppressing cavitation and thereby reducing the rate of radical production. The average particle sizes produced in the BA system and the copolymerization system with 50:50 wt% BA and VAc were very small; around 15–20 nm, respectively. But the average particle sizes produced in the emulsion homopolymerization of VAc were much larger, showing a size of around 300 nm. The reason for producing smaller polymer particles in both the BA homopolymer and BA-VAc copolymer systems than in the VAc homopolymer system even at low emulsifier concentrations was attributed to a high rate of particle formation due to a large number of very small monomer-emulsion droplets that were to be transformed into polymer particles.

Grieser et al. [215] investigated the kinetics and mechanisms of the emulsion polymerization of MMA and of BA at 30 °C (±5 °C) using ultrasonic irradiation (20-kHz horn sonifier) and a cationic emulsifier, dodecyltrimetylammonium chloride (DTAC). They observed the formation of stable dispersions with particle diameters in the range of 40–150 nm and with polymer molecular weights greater than 10^6 g mol^{-1}. In the case of MMA, the average particle size was found to be constant throughout the reaction time (sonication time) and independent of the initial DTAC concentration. The final particle size decreased as the initial DTAC concentration was decreased, but the rate of polymerization was approximately the same over the concentration range of DTAC examined. In the case of BA, the kinetic behavior was basically the same as that of MMA, except that the average particle size was constant (~30 nm) up to 50 min of sonication, after which a dramatic increase in size (100–140 nm) was observed when the initial TDAC concentration was comparatively low. Based on their experimental data, the authors proposed the kinetics and mechanisms of the ultrasonic (sonochemical) initiation in this polymerization process. When ultrasound is applied in a liquid medium, the cavitation event that occurs as ultrasound travels through the liquid medium, producing microbubbles in the solution. When the microbubbles rapidly collapse, this leads to high local temperatures

of the order of 4000–5000 K within the bubble and at least 1250 K in the liquid immediately surrounding the interfacial region. In an aqueous medium, such high temperatures lead to the homolysis of water, creating hydroxyl (·OH) and hydrogen (·H) radicals. The authors assumed that primary organic radicals produced from MMA and BA were unlikely to play a major role at 20 kHz even though MMA and BA are volatile and could enter cavitation bubbles to produce a variety of primary organic radicals by thermal decomposition. The hydroxyl and hydrogen radicals generated in the aqueous phase add several monomer units and then enter the miniemulsion droplets produced by ultrasonication, initiating polymerization. Therefore, the results obtained strongly support a polymerization process involving a miniemulsion polymerization system, where continuous formation of polymer particles takes place throughout the polymerization.

Chou and Stoffer [216, 217] carried out the ultrasonically-initiated free radical emulsion polymerization of MMA at ambient temperature using NaLS as the emulsifier, and published two articles on this topic. In the first article [216], the authors studied: (1) the nature and source of the free radicals for the initiation process; (2) the effects of different types of cavitations, and; (3) the dependence of the polymerization rate, the number of polymer particles generated, and the polymer molecular weight on the acoustic intensity, argon gas flow rate, surfactant concentration, and the initial monomer concentration. They found that, in the absence of argon gas flow, no polymerization took place, and that, contrary to Grieser et al. [215], the source of the free radicals for the initiation process came from the degradation of the NaLS, presumably in the aqueous phase. The molecular weight of the poly(MMA) obtained varied from $(2.5–3.5)\times10^6$ g mol^{-1}, and the monomer conversion was up to 70%. The rate of polymerization was found to be proportional to the acoustic intensity to the power of 0.98, to the argon gas flow to the power of 0.086, and to the emulsifier concentration to the power of 0.08 in the emulsifier concentration range of 0.035–0.139 M. The number of polymer particles was found to be proportional to the acoustic intensity to the power of 1.23, to the argon gas flow to the power of 0.16, and to the emulsifier concentration to the power of 0.3 in the emulsifier concentration range of 0.035–0.139 M. In the second article [217], the radical generation process was studied. Based on this experimental study, the authors tried to explain the kinetic data obtained in the previous work. In this study, radical trapping experiments were used to investigate the effects of acoustic intensity, argon gas flow rate, and NaLS concentration on the extent of free radical generation in aqueous NaSL solutions. Aqueous solutions of NaLS were ultrasonically irradiated in the presence of a radical scavenger. The NaLS molecules then decomposed by ultrasound to form free radicals in the aqueous phase. It was found that the extent of free radical generation increased as: (1) the 0.6^{th} power of the acoustic intensity, (2) the 0.44^{th} power of the argon gas flow rate, (3) the 0.35^{th} power of the emulsifier concentration in the emulsifier concentration range of 0.035–0.139 M. These experimental results were found to explain the effects of acoustic intensity, argon gas flow rate, surfactant con-

centration on the rate of polymerization and the number of polymer particles generated.

Recently, Wang et al. [218, 219] carried out the ultrasonically-initiated emulsion polymerization of MMA using a 20 kHz ultrasonic generator and NaLS as the emulsifier, respectively, in order to find a way to reach a high monomer conversion. It was found that, with increasing NaLS concentration, the monomer conversion increased significantly, but in the absence of NaLS, monomer conversion remained nearly zero. Therefore, the NaLS emulsifier played a key role and appeared to serve as an initiator. They observed that (1) an increase in the reaction temperature resulted in an increase in the monomer conversion, (2) an appropriate increase in the N_2 purging rate also increased the monomer conversion, and (3) the polymer particles prepared were nanosized, even with a small amount of emulsifier. Optimized reaction conditions were obtained using these experimental results, and so a high monomer conversion of about 67% and high molecular weight polymers of several million could be obtained in a period of about 30 min. They [219] also studied the ultrasonically-initiated emulsion polymerization of *n*-BA in order to investigate the factors that affect the induction period and the rate of polymerization, and proposed a mechanism for ultrasonically-initiated emulsion polymerization. Increasing the N_2 flow rate, temperature, NaLS concentration and power input, and decreasing the monomer concentration resulted in further decreases in the induction period and increased the rate of polymerization. Under optimized reaction conditions, the conversion of BA reached 92% in 11 min. In addition, they carried out a feasibility study on semicontinuous and continuous ultrasonically-initiated emulsion polymerization.

3.5 Effect of Additives and Impurities

Most kinetic studies on emulsion polymerization carried out in universities and industrial research laboratories have been done under extremely clean conditions. The polymerization is conducted in a high-purity nitrogen atmosphere with any remaining oxygen in the reaction system removed by degassing. High purity initiators and emulsifiers are used, and the commercially-available monomers are purified (by, say, distillation) to remove any inhibitors used during storage as well as any other reactive organic impurities that may act as radical scavengers or CTAs. In industry, however, it is usually impractical to purify the monomers, initiators, emulsifiers, water, and so on to remove reactive impurities from them. Moreover, the polymerization is usually carried out in an industrial-grade low-purity nitrogen atmosphere containing a trace of oxygen. The presence of inhibitors in the reaction mixture will affect both particle formation and growth processes. Therefore, it is very important to understand the effects of any impurities present in the starting materials when attempting the optimum design and operation of emulsion polymerization processes.

It has been recognized that the presence of oxygen during emulsion polymerization can have detrimental effects on the course of a reaction, causing inhibition periods and retarding the reaction rate. Relatively few publications have addressed the issue of the effects of oxygen in emulsion polymerization [126, 188, 220–223]. With the intention of clarifying the effect of stirring on emulsion polymerization, Nomura et al. [220] carried out St emulsion polymerization under three nitrogen atmospheres with different purities (containing a trace of oxygen) and at different stirring speeds. They observed that the faster the stirring speed, the longer the retardation period. They attributed the result to the diffusion limited transfer of oxygen from the headspace into the water phase through the liquid surface, which was controlled by stirring. Furthermore, they found that the polymerization rate following a long retardation period was often greater than that after a shorter retardation period, indicating that the final number of polymer particles produced with a long retardation period was higher than that with a shorter retardation period. The reason for this is discussed later. The same trend was also observed by other researchers [188, 222]. Cunningham et al. [222] examined the effects of oxygen on the induction period, conversion kinetics, molecular weight and particle size during the emulsion polymerization of St, by varying the initial dissolved oxygen concentration in the aqueous phase. They found that the length of the induction period did not vary linearly with the initial oxygen level, suggesting diffusion from the reactor headspace to the aqueous phase could have a significant impact on rates of particle formation and growth. Furthermore, the higher the initial dissolved oxygen level, the longer the induction period and the smaller the average diameter of polymer particles in the final latex product, which indicates that the longer the induction period, the greater the number of polymer particles produced. Their experimental results suggested that, during the induction and retardation period, the oxygen molecules in the reactor headspace were continuously transferred into the aqueous phase, and some of them are consumed by the radicals in the aqueous phase, but most of them diffuse further into both the monomer-swollen micelles and polymer particles. Therefore, the oxygen molecules that have diffused into the monomer-swollen micelles and polymer particles inhibit the growth of radicals within them, thereby reducing the volumetric growth rate per particle, μ and resulting in an increase in the number of polymer particles produced according to Eq. 29.

Arbina et al. [188] investigated the influence of oxygen on the kinetics of the chemically-initiated seeded emulsion homopolymerization of St and the seeded emulsion copolymerization of St and BA using reaction calorimetry. They discussed whether oxygen behaved kinetically as an ideal inhibitor. In the experiments, they observed that oxygen not only caused an inhibition period, but also behaved like a retarder by reducing the polymerization rate. Their explanation for this seemingly contradictory behavior was the existence of mass-transfer limitations from the reactor headspace to the latex, resulting in a gradual and continuous flow of oxygen into the aqueous phase. Their own experiments showed that this induction period decreased with increasing initiator concen-

tration. When the headspace to aqueous phase ratio was decreased, the induction period was reduced and the polymerization rate increased. The length of the retardation period caused by oxygen in the seeded emulsion polymerization is known to depend on the kind of monomer. In seeded emulsion polymerizations, the inhibition period may be followed by a retardation period during which the polymerization rate increases to a steady state value. The retardation period observed in the seeded emulsion polymerization of VAc is unusually long compared to that of St or MMA. Bruyn et al. [223] tried to quantitatively explain the reason for this unusually long retardation in terms of the initiator efficiency, f_{entry}, proposed by Maxwell et al. [11]. They argue that this unusually long retardation is due to the high radical entry efficiency of the aqueous phase oligomeric radicals, which allows latex particles to compete with dissolved oxygen for these initiating radicals. In the case of VAc, this is due to the high value of the product of the propagation rate constant and the water solubility. As oxygen is consumed, the competition increasingly favors the entry of initiating radicals into polymer particles and the rate of polymerization gradually increases. In another case, Kiparissides et al. [126] considered the different effects of the presence of oxygen on the kinetics and PSD in the emulsifier-free emulsion polymerization of VCl. Oxygen is capable of reacting with primary initiator radicals and the resulting oligomeric radicals in the aqueous phase to produce vinyl polyperoxides. Taking this into account, they developed a mathematical model into which the combined role of oxygen as an inhibitor and a radical generator, through the formation and subsequent decomposition of vinyl polyperoxides, was incorporated.

CTAs are used not only to reduce the molecular weight of the polymer produced, but also to limit the extent of the branching and crosslinking of the polymer produced in diene-polymerization. It is well known that an ideal CTA is able to reduce the molecular weight of the polymer produced in a homogeneous bulk or solution free radical polymerization, without affecting the overall rate of polymerization. For a long time it has been known that even an ideal CTA such as mercaptan could affect not only the molecular weight of the polymer produced in emulsion polymerization, but also the rate of the polymerization [224], but details about the effects of CTAs (including mercaptans) on the kinetics of heterophase radical polymerizations, like emulsion polymerizations, have only been revealed recently [225–229].

Whang et al. [225] observed that the rate of polymerization decreased in the seeded emulsion polymerization of St in the presence of carbon tetrabromide, which functions as an ideal CTA in the homogeneous bulk or solution free radical polymerization of St. They pointed out that this appeared to result from the enhanced rate of radical desorption of the free radicals from the polymer particles. Also, a substance which behaves as an ideal CTA in homogeneous polymerizations might apparently function as a retarder in heterogeneous free radical polymerization. Lichti et al. [227] advanced the discussion by Whang et al. [225] and argued that the increase in the rate of radical desorption which brought about the decrease in the rate of polymerization paralleled the increase

in the chain transfer constant for the additives: CBr_4>CCl_4>St. The efficiency of desorption of free radicals formed by chain transfer from the latex particles followed the inverse order CBr_4<CCl_4<St, and this reflected the reactivities of the low-molecular weight free radicals (formed by atom abstraction) with the monomer.

At almost the same time, Nomura et al. [226] carried out an extensive experimental study of the effect of typical CTAs such as CCl_4, CBr_4b, and four primary mercaptans (C_2, *n*-C_4, *n*-C_7 and *n*-C_{12}) on particle formation and growth processes in the unseeded emulsion polymerization of St. They found that these CTAs, which had almost no effect on the rate of bulk polymerization of St, decreased the rate of polymerization per particle μ and so increased the number of polymer particles produced (see Eq. 29). From a theoretical point of view, they suggested that these effects could be enhanced by increasing the rate of radical desorption from the polymer particles by adding a CTA with a higher value of the chain transfer constant and/or with higher water-solubility. Nomura et al. [20, 43] pointed out that the number of polymer particles produced N_T could be expressed as $N_T \propto S_0^z I_0^{1-z}$ in an emulsion polymerization system following micellar particle formation. They also showed that, by increasing the rate of radical desorption from the polymer particles in the interval of particle formation with the help of CTA, the emulsifier dependence exponent, z, would increase from about 0.6 to 1.0, thereby decreasing the initiator dependence exponent from about 0.4 to 0. This was also confirmed experimentally. Therefore, they demonstrated that the effect of CTA on particle formation and growth in the emulsion polymerization of St could be explained in terms of desorptions of chain-transferred radicals from the polymer particles.

Maxwell et al. [228] discussed the effect of CTA, such as mercaptan, on initiator efficiency and extended their quantitative model for initiator efficiency to take into account the effect of adding CTA. They assumed the following model. The effect of the CTA on the entry rate occurs by facilitating the production of aqueous-phase free radical species (CTA radicals) via transfer between species such as $\cdot M_nSO_4^-$ (where M is a monomer entity and n<z) and the CTA in the aqueous phase. The CTA radicals will be formed at a reasonable rate provided that the CTA is not too water-insoluble (as in $C_{12}H_{25}SH$) and the resultant CTA radical is able to enter the latex particles rapidly because of this relative insolubility in water. If the monomer-derived $\cdot M_nSO_4^-$ tends to suffer aqueous-phase termination rather than entry, the overall rate of entry (and hence initiator efficiency) will increase. They claimed that this mechanism could explain the accelerating (promoting) effect of intermediate molecular weight CTAs (C_{10}–C_{12}) on the emulsion polymerization of monomers such as Bu, where the z value is large and so initiator efficiency is very low in the absence of CTA, because most of the $\cdot M_nSO_4^-$ undergoes termination rather than entry into the latex particles. However, Weerts et al. [229] studied the "promoting effect" in the emulsion polymerization of Bu using SDS, potassium stearate and potassium oleate as the emulsifiers and sodium or potassium peroxodisulfate, 4,4′-azobis-(4-cyanopentanoic acid and AIBN as the initiators, and

concluded that the promoting effect appears to be related to impurities present in the emulsifier, because it was found to be completely absent in emulsifier-free polymerizations. They also demonstrated that a simple redox reaction between a sulfate radical anion and thiol could not provide a satisfactory explanation for the promoting effect. Therefore, the promoting effect of thiol in the emulsion polymerization of diene-hydrocarbons is still poorly understood.

Commercially-available monomers usually contain an inhibitor such as 4-*tert*-butylcatechol (TBC) or hydroquinone (HDQ) to prevent undesired autopolymerization before their use in polymerizations. In industry, however, distillation of the monomer to remove inhibitor is rarely carried out. Therefore, a good understanding of the effect of inhibitor on the kinetics of emulsion polymerization is important when designing and operating an industrial emulsion polymerization process. Huo et al. [230] investigated the effects of HDQ and TBC on the kinetics of the emulsion polymerization of St, where HDQ is a water-soluble inhibitor and TBC is an oil-soluble inhibitor, respectively. They found that HDQ produced an induction period proportional to the amount of HDQ present, but did not produce any significant difference in the rate of polymerization regardless of the different HDQ levels in the systems. Moreover, the final particle number, average particle diameter, molecular weights, and latex viscosities were identical to within experimental error for all four runs conducted. In contrast to HDQ, the monomer-soluble inhibitor TBC showed more complex effects. They found that the higher the level of TBC, the larger the number of polymer particles produced, and a longer induction time and an increased retardation of the initial rate of polymerization with increasing TBC level was evident, but the rate of polymerization at intermediate conversion increased for smaller TBC level runs because of the increased number of polymer particles produced. However, at higher TBC levels (200 ppm), TBC was never fully depleted before the polymerization was completed, and so in spite of the much larger number of polymer particles generated, the overall rate of polymerization never exceeded that for the purified monomer. The viscosity of the latex produced increased with the TBC level in the system, which was a direct consequence of the decrease in particle diameter. The average molecular weight of polymer formed decreased somewhat, and the polydispersity of the polymer produced increased from 1.5 to 2.0 with the TBC level, indicating that the dead polymer was predominantly formed by reactions with the impurity (TBC), which acted as a CTA as well as a retarder. These results were well predicted by the modification of an existing model for Case II emulsion polymerization which incorporated the effects of impurities. Penlidis et al. [221] also made necessary modifications to their Case I model for batch and continuous emulsion polymerization to account for the effects of reactive monomer-soluble impurities (TBC). A detailed mechanism was proposed through which TBC affected the emulsion polymerization of St [231]. TBC would oxidize into 4-*tert*-butyl-1,2-benzochinon (TBBC) during the storage of St and also during the sulfate-initiated emulsion polymerization of St. TBBC is soluble in St and is therefore readily absorbed by the polymer particles produced. TBBC is known to act

as a radical accepter, so radical transfer from a growing radical to TBBC may occur in the polymer particle. Because the TBBC radicals are relatively stable due to conjugation, probably most of the TBBC can be converted into TBBC radicals. Because of this radical transfer to TBBC, the chain growth in the particles stagnates and so the rate of polymerization per particle (μ) decreases, thereby increasing the number of polymer particles produced. The TBBC radicals, which desorb from the particles because of their charge, can react in different ways. The desorbed TBBC radicals react with persulfate radicals in the aqueous phase, converting the TBBC radicals back to TBBC and consuming persulfate radicals (the inhibition mechanism). These TBBC molecules may be taken up by the particles once more and transformed into TBBC radicals again, and so on. Of course, the desorbed TBBC radicals can also contribute to the emulsion polymerization in the usual way by reacting with monomer as initiating radicals.

Barton et al. [232] conducted the emulsion polymerization of the sparingly water-soluble monomer St and of the fairly water-soluble monomer MMA in the presence and absence of the water-soluble inhibitor, potassium nitrosodisulfonate (Fremy's salt). By using oil-soluble dibenzoyl peroxide (DBP) and water-soluble ammonium peroxodisulfate (APS) as the free-radical initiators, they examined the effect of the location of the initiator on the kinetics of these emulsion polymerizations with SDS as the emulsifier. Figure 7 shows an example of the experimental results.

When the emulsion polymerization of St was carried out in the presence of Fremy's salt and ammonium peroxodisulfate in the aqueous phase, a distinct

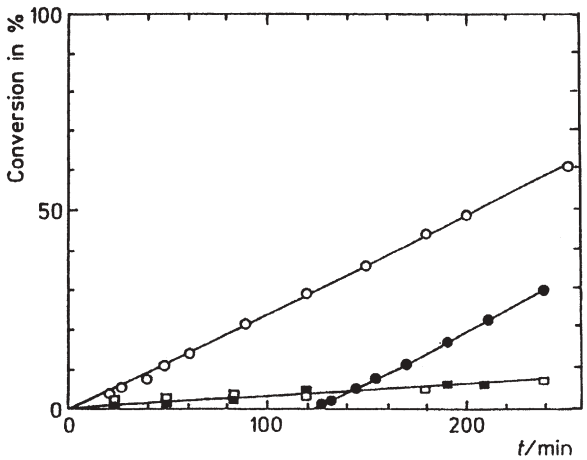

Fig. 7 A typical example of the effect of water-soluble (APS) and oil-soluble (DBP) initiators on the progress of the emulsion polymerization of St in the presence of a water-soluble radical inhibitor (Fremy's salt, FS); for [APS]=5×10^{-4} mol/dm^3, empty circles indicate [FS]=0, filled circles indicate [FS]=10^{-4} mol/dm^3; for [DBP]=5×10^{-4} mol/dm^3, empty squares indicate [FS]=0, filled squares indicate [FS]=10^{-4} mol/dm^3

inhibition period was observed, but after the end of the inhibition period the conversion versus time curve was almost the same as that encountered in the absence of Fremy's salt. On the other hand, when the emulsion polymerization of St was initiated by the oil soluble initiator DBP, the monomer conversion versus time curve observed in the presence of Fremy's salt was identical to that seen in the absence of Fremy's salt. In the case of MMA, the results were basically the same as those with St. Also, the rate of emulsion polymerization initiated by DBP was almost the same as the rate of bulk polymerization initiated by DBP. This indicated that in the emulsion polymerization initiated by DBP, the polymerization did not proceed in the monomer-swollen micelles and the resultant polymer particles according to emulsion polymerization kinetics, but in the monomer droplets according to bulk kinetics. This implies that neither member of a radical-pair generated in a monomer-swollen micelle initiates polymerization, either because geminate termination took place before either of the pair of radicals desorbs from the micelle into the aqueous phase, or because both of the radicals desorb as soon as they are generated and are scavenged in the aqueous phase. This finding is closely related to the claim [200] that in the emulsion polymerization of St initiated by oil-soluble initiators, the free radicals generated from the fraction of the initiator dissolved in the aqueous phase mainly participate in particle formation from the monomer-swollen micelles. Barton et al. claimed that, although many studies had been performed to clarify the effect of a variety of water-soluble and oil-soluble inhibitors on emulsion polymerization, no unequivocal results had been obtained for their effects on its kinetics, and specifically for their effect on particle formation, and that this problem is still open for discussion.

Ignoring their side effects, chain transfer agents (CTAs) were originally used in emulsion polymerization as additives to regulate the molecular weight distribution of the resultant polymers and to limit the extent of branching and crosslinking of the polymer produced in diene-polymerization. Recently, several investigations based on this point of view have been published [57, 125, 233–238]. Barudio et al. [57] studied the effect of CTAs (*tert*-butanethiol and *n*-dodecanethiol) on the microstructures of copolymers (the molecular weight distribution (MWD) and glass transition temperature (T_g)) and the diameters of polymer particles produced in the batch and semibatch emulsion copolymerizations of St and BA. The experimental results were interpreted in terms of enhanced radical desorption and diffusion limitations of CTA between the monomer droplet and particle phases. They proposed a kinetic model that was able to successfully compute the kinetic constants, the number of radicals per particle, the GPC/SEC diagram and the DSC thermogram related to the MWD and T_g, respectively. Salazar et al. [234] developed a mathematical model that included the effect of CTA (*tert*-nonyl mercaptan) on particle formation and the average molecular weights in the batch and monomer-starved emulsion polymerizations of St. Asua and co-workers [125, 233, 235–237] published several reports on the effects of CTAs on the kinetics and the microstructures of the resultant polymers in seeded and unseeded emulsion homo- and co-

polymerizations. Echevarria et al. [233] developed a closed-loop control strategy based on on-line gas chromatographic measurements of both monomer and CTA concentrations to obtain emulsion polymers of well-defined MWD. The control strategy was experimentally assessed, producing widely different MWDs in the emulsion polymerization of St using carbon tetrachloride (CCl_4) as CTA. Mendoza et al. [125] studied the effect of a CTA (*n*-dodecyl mercaptan) on the MWD in the emulsion polymerization of St. It was found that the CTA had no effect on the rate of polymerization but substantially affected the MWD of the resultant polymers, and that the efficiency of the CTA in reducing the MWD was lowered by mass-transfer limitations. The rate-controlling step for CTA mass-transfer was the diffusion of the CTA from the surface of monomer droplets to the aqueous phase, as already pointed out by Nomura et al. [239]. Mendoza et al. examined the process variables affecting CTA mass-transfer and developed a mathematical model that could predict monomer conversion, particle diameter, number of polymer particles, and number-average and weight-average molecular weights. Plessis et al. [237] investigated the effect of a CTA (dodecane-1-thiol) on the kinetics, gel fraction, level of branches and sol molecular weight distribution in the seeded semibatch emulsion polymerization of *n*-BA. They found that the gel fraction was strongly affected by the CTA concentration, and that the sol weight-average molecular weight decreased with increasing CTA concentration, whereas no effect on the kinetics and the level of branches was observed. Their proposed mathematical model was able to explain the effect of the process variables fairly well. Sayer et al. [235, 236] published two papers. One [236] discussed the effect of a CTA (dodecanethiol) on the kinetics and MWD of the semicontinuous emulsion copolymerization of MMA and BA. It was found that the CTA had only a slight effect on the reaction rate, but it significantly affected the secondary particle formation. Moreover, the effects of the CTA concentration on the gel formation and the mass-transfer limitations of the CTA were discussed. The other [235] dealt with the effects of different strategies for copolymer composition control on the MWD and gel fraction in the starved and semistarved seeded emulsion copolymerization of MMA and BA in the presence of dodecanethiol (CTA). It was shown that simultaneous control of the copolymer composition and the MWD was feasible. When the monomers were fed following the optimal semistarved strategy, the MWD was controlled by employing dodecanethiol as the CTA. Gugliotta et al. [238] studied the control of polymer molecular weight using *n*-nonyl mercaptan (*n*NM) as the CTA in the emulsion polymerization of St, with the aim of producing PSt latex particles of low molecular weight polydispersity at high conversion and in short reaction times. They claimed it was preferable to use *n*NM instead of other CTAs like *tert*-dodecyl mercaptan or CCl_4.

Okaya et al. [240] investigated the effect of additives such as alcohol (isopropyl alcohol) on the initial stage of the emulsion polymerization of MMA (1 wt%) initiated by APS in the presence of PVA (1%). They found that 90% of MMA and 60% PVA were grafted and that stable polymer particles with an

average diameter of 80 nm were produced. However, the addition of alcohols such as isopropyl alcohol to the system decreased the grafting to a great extent, resulting in an increase in particle size. This was attributed to decreased hydrogen abstraction from PVA by sulfate radicals, due to the competing hydrogen abstraction from the low molecular weight alcohol.

3.6 Effects of Other Important Factors

Batch, semi-batch and continuous emulsion polymerizations are usually carried out in stirred tank reactors, where agitation by a stirrer is necessary. The type of stirrer chosen and its stirring speed can often affect the rate of polymerization, the number of polymer particles and their size distribution (PSD), and the molecular weight of the polymer produced. However, the effect of stirring on emulsion polymerization has never been the main research parameter in research programs [241]. This is probably due to the conflicting results obtained so far by various researchers.

Shunmukham et al. [242] studied the effect of stirring on the emulsion polymerization of St, and concluded that violent agitation decreased the rate of polymerization, as shown in Fig. 8.

Schoot et al. [243], on the other hand, criticized Shunmukham's conclusion, stating that this strange effect of agitation observed by Shunmukham might have been due to the absorption of contaminant oxygen into the reaction mix-

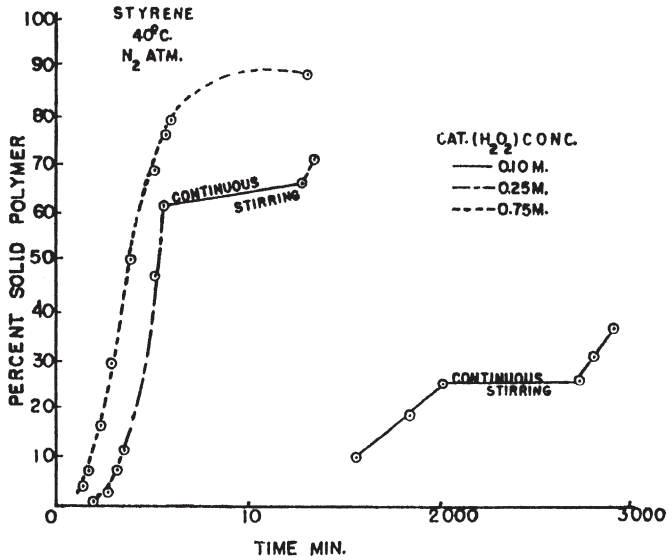

Fig. 8 A typical example of the effect of stirring on the progress of the emulsion polymerization of St in the presence of a typical inhibitor oxygen (40 °C, initiator: H_2O_2)

ture from nitrogen atmosphere in which the polymerization was carried out. Evans et al. [244] carried out the emulsion polymerization of VDC at 36±1 °C using NaLS as the emulsifier and APS as the initiator, and found that: (1) the first stage polymerization rate decreased with increasing stirring speed; (2) the second stage polymerization rate increased with increasing stirring speed, and; (3) the third stage polymerization rate was independent of stirring speed. To explain their results, they suggested two factors through which stirring affected the polymerization rate. The first factor was the reduced levels of effective emulsifier available for the formation of polymer particles, caused by the adsorption of emulsifier molecules onto monomer droplets finely dispersed by the stirring (in the first stage). The other factor was the effect of monomer-transport from the monomer droplets to the polymer particles where the polymerization proceeded (in the second stage) upon the rate. Omi et al. [245] came to the contrary conclusion that when the monomer used was St, stirring did not influence emulsion polymerization as long as initial emulsification conditions were not changed. They considered that stirring affected the polymerization only through the former of the two factors suggested by Evans et al. [244]. Later, Nomura et al. [75] carried out a kinetic study of the batch emulsion polymerization of VDC at 50 °C with KPS as the initiator and NaLS as the emulsifier, aiming to derive a quantitative explanation for the effect of stirring observed by Evans et al. [244]. Unfortunately, however, the polymerization proceeded very smoothly and the abnormal kinetic behavior caused by a change in the stirring speed was not observed. Therefore, they concluded that the effect of stirring observed by Evans et al. [244] in the VDC emulsion polymerization must be a very special case. Therefore, the reasons for such abnormal kinetic behavior remain a mystery.

These results illustrate that investigations into the effects of stirring on emulsion polymerization, have produced inconsistent results and conclusions. Further research was therefore needed to elucidate the effect of stirring in more detail. Nomura et al. [220] carried out an extensive investigation into the effect of stirring on the emulsion polymerization of St initiated by KPS at 50 °C with NaLS as the emulsifier, with the intention of explaining the effects of stirring quantitatively by showing how agitation affects emulsion polymerization, what steps of the polymerization are affected by stirring, and whether a suitable range of agitation exists in emulsion polymerization. The reactor used was a cylindrical glass vessel with a dished bottom, fitted with four baffle plates located at 90° intervals, and a four-bladed paddle type impeller. They concluded that the effect of stirring on emulsion polymerization appears through the following four factors:

1. When the polymerization is carried out in the presence of an imperfectly purified nitrogen atmosphere, the retardation period is prolonged with agitation due to an increase in the absorption rate of oxygen from the nitrogen atmosphere into the reaction mixture through the gas-liquid interface. It has often been observed that the polymerization rate after a longer

retardation period is higher than that after a shorter retardation period. The reason for this can be explained according to the S-E theory as follows. If the polymerization is retarded by oxygen during particle formation, the volumetric growth rate per particle (μ) decreases, and so the number of polymer particles produced (N_T) would increase according to Eq. 29. When the contaminant oxygen molecules in the nitrogen atmosphere are almost completely consumed and so the supply of them into the reaction mixture is not sufficient to restrain the polymerization appreciably, the polymerization rate increases in proportion to the increase in N_T.

2. In a pure nitrogen atmosphere, there is an optimum range of stirring speeds where emulsion polymerization is not affected by agitation. If the stirring speed is higher than the above-mentioned optimum range, the number of polymer particles decreases by coagulation during the course of polymerization, and so the polymerization rate also decreases.
3. At lower stirring speeds, on the other hand, stirring controls the rate of monomer transport from the monomer droplets to the polymer particles, thereby controlling the rate of polymerization. The rate-determining step is usually the monomer-transport step from the monomer droplets to the aqueous phase, because the monomer-transport step from the aqueous phase to the polymer particles is much faster than the former step due to the much greater total surface area of the polymer particles compared to that of the monomer droplets.
4. At low emulsifier concentrations near the CMC, an increase in the degree of agitation results in a reduction of the emulsifier used for the formation of polymer particles (like micelles). This is because the monomer droplets become smaller as the degree of agitation is increased, and so the amount of emulsifier adsorbed onto the surfaces of the monomer droplets increases in proportion to the increased surface area of the monomer droplets. This brings about a decrease in the number of polymer particles produced, and so a decrease in the rate of polymerization.

On the other hand, Weert et al. [246] investigated the effects of stirring on the kinetics of the emulsion polymerization of Bu at 60 °C using NaLS as the emulsifier. They carried out the polymerizations in a 2.3-liter reactor fitted with four baffle plates located at 90° intervals and a twelve-flat-bladed turbine impeller. In all of the experiments, the system was pre-emulsified by stirring for a few minutes at 400 rpm, before adjusting the stirring speed n to the desired level. The number of polymer particles produced, N_T, was found to remain constant within experimental error beyond a sufficiently high value of n, while a discontinuous increase in N_T became apparent towards lower values of n. The change in N_T was significant, especially at low n. They ascribed the reason for this change to the fact that the level of emulsifier available for particle formation and stabilization was influenced by the degree of agitation, as already pointed out by Nomura et al. [220]. They discussed the effect of stirring in connection with the flow conditions in the reactor, which are closely related to the stirring speed, and

finally arrived at the conclusions that the stirring speed influenced this polymerization system by reducing the effective emulsifier concentration available for particle formation and stabilization at higher n, and by limiting the diffusion of monomer to the polymer particles at low n. Arai et al. [247] studied the effect of agitation on the kinetics of the soapless emulsion polymerization of MMA in water at 65 °C. As expected, the stirring influenced the monomer conversion versus time history, the molecular weight of the polymer produced, and the number of polymer particles produced versus time. They found that agitation was an important factor that affected the rate of monomer-transport from the monomer droplets to the water phase. The authors proposed a quantitative kinetic model that could predict the effect of monomer transport on the rate of polymerization. Kostov et al. [158] also studied the effects of polymerization conditions, including stirring, on the emulsion copolymerization of tetrafluoroethlene (TFE) and propylene (P) with ammonium perfluorooctanoate, initiated by a redox initiator system containing *tert*-butylperbenzoate. They found that both the rate of copolymerization and the molecular weight of the copolymer produced increased as the stirring speed increased up to 450 rpm, but then became independent of the speed above 450 rpm. The explanation for this was that the stirring affected the rate of mass-transfer of TFE and P from the gaseous to aqueous phases, which was the rate-controlling step for speeds less than 450 rpm. Kim et al. [248] also reported the importance of agitation in the semi-batch emulsion polymerization of TFE carried out using a chemical initiator (APS) and a fluorinated surfactant (FC-143). The rate of polymerization was found to increase linearly with the stirring speed. Based on the experimental findings, they concluded that the diffusion or dissolution of TFE into the aqueous phase was the rate-determining step through which agitation affected the polymerization. Özdeğer et al. [249] investigated the effect of stirring speed and impeller type (axial and radial flow impellers) on the kinetics of the emulsion copolymerization of St and *n*-BA using Triton X-405 (octylphenoxy polyethoxy etanol) as the emulsifier. At low solids content (30%), the impeller type and speed did not have any significant effect on both the final number of polymer particles and the overall rate of polymerization. The PSDs were unimodal in all cases. For high solids content (50%), the rate of polymerization carried out with the axial flow impeller was slower, indicating that fewer polymer particles were produced. Bimodal PSDs were obtained for both cases. These differences were attributed to the partitioning of the emulsifier. The axial flow impeller created more shear than the radial flow impeller. This resulted in more monomer droplets being formed, leading to more of the emulsifier being associated with them. This also resulted in fewer emulsifier micelles being available for particle formation, thereby leading to the lower number of polymer particles produced.

In industrial emulsion polymerizations, CTAs like mercaptan are often used to regulate the molecular weight of the polymer produced. In some cases, other ingredients that directly participate in the polymerization reaction are used to modify the properties of the polymer latex produced. In these cases, these

reacting species must be transported from one phase, for example, the monomer droplets, via the aqueous phase, to the monomer-swollen polymer particles where the reaction takes place. Therefore, when designing a latex product to have particular properties, it is important to quantitatively elucidate the diffusional behavior of these reacting species when they move between the phases in an emulsion polymerization system. However, only a few researchers [125, 234, 239, 250–255] have presented quantitative discussions on the mass-transfer problem involved in emulsion polymerization. Brooks [250] discussed the monomer diffusion rate in an emulsion polymerization system. The author calculated the maximum diffusion rate from monomer droplets to a polymer particle via the water phase by using a simple diffusion equation and showed that this rate was usually far greater than the rate of polymerization per particle. He also suggested that an adsorbed emulsifier layer on the surface of the polymer particles would not impede monomer transfer to the particles. Finally, he concluded that in most systems the diffusional processes that occurred in the water phase would not affect the course of the polymerization. However, Nomura et al. [220] pointed out a possibility that the monomer-transport step from the monomer droplets to the water phase could control the polymerization rate when the intensity of agitation was comparatively low.

Nomura et al. [239] discussed the mass-transfer problem in more detail for the seeded emulsion polymerization of St initiated by KPS at 50 °C using NaLS as the emulsifier and CTAs as the diffusing species. They carried out the seeded emulsion polymerization of St using five normal aliphatic mercaptans with different molecular weights (*n*-C_7, *n*-C_8, *n*-C_9, *n*-C_{10}, and *n*-C_{12}) under the conditions of 400 rpm (stirring speed), N_T=1.4×10^{14} particles/cm^3-water (the number of seed polymer particles), d_{po}=48 nm (the average diameter of seed particles), and T_{mo}=8.44×10^{-6} mol/cm^3-water (the concentration of initially charged mercaptan per unit volume of water), and measured the consumption rate of each mercaptan. They found that the consumption rate decreased drastically with the molecular weight of mercaptan, although the consumption rate of *n*-C_8 was not so different from that of *n*-C_7. They analyzed these experimental data using a proposed diffusion model derived on the basis of the so-called two-films theory, and concluded that the concentration of the CTA in the polymer particles during the polymerization dropped to a value much lower than the one that would be attained if thermodynamic equilibrium for the CTA were reached between the monomer droplets and the polymer particles. This was due mainly to the CTA molecules' resistance to transfer across the diffusion film at the interface between the monomer droplet and water phases. The authors suggested that the proposed model can also be used to predict the rate of mass-transfer of any sparingly water-soluble reacting species from monomer droplets to the polymer particles where this species participate directly in the polymerization (this may include the monomer itself).

It is well known that emulsion polymerizations of highly water-insoluble monomers such as octadecyl methacrylate (OM), dodecyl methacrylate (DM), and stearyl acrylate (SA) are generally not feasible using traditional surfactant

systems. This is because monomer transport from the monomer droplets to the water phase is diffusion limited [239]. However, almost simultaneously, Rimmer et al. [256, 257], Leyer et al. [258] and Lau et al. [259] reported that these highly water-insoluble monomers could be emulsion polymerized in the presence of β-cyclodextrin (β-CD). These studies uncovered a very interesting phenomenon. Rimmer et al. [256, 257] successfully conducted the emulsion polymerization of OM and DM at 70 °C using KPS as the initiator and Dowfax 2A1 as the emulsifier. They claimed that the reason for this successful polymerization was that the use of β-CD appeared to aid monomer transport from the monomer droplets to the polymer particles across the aqueous phase by increasing the apparent water-solubility of these monomers, because the CDs apparently solubilize the hydrophobic compounds in aqueous media. On the other hand, Leyrer et al. [258] reported that they also succeeded in emulsion-polymerizing SA in the presence of methyl-β-CD, and claimed that in this case the CD served as a phase transfer agent, because the ability of the CD to form a water-soluble complex with hydrophobic molecules made it easier for the SA molecules to leave the monomer droplets and to be released from the complex after arriving at the surfaces of the growing polymer particles. The authors reported that only 5 wt% of CD was necessary to polymerize almost 100% of SA.

Recently, Soares and Hamielec [252] presented a review article on the study of transport phenomena in emulsion polymerization and introduced a case study on how to increase the amount of ethylene (E) content in the copolymer produced by the emulsion copolymerization of E and VAc under the conditions of a mass-transfer-controlled polymerization rate. Zubitur et al. [255] studied the effect of agitation on the batch and semicontinuous emulsion polymerizations of St in a reactor equipped with a four-paddle type stirrer and dodecyl mercaptan as the CTA. Here, the CTA mass-transfer from the monomer droplets to the aqueous phase was the rate-controlling step. They showed that the molecular weights of polymers decreased as the stirring speed was increased because of the improvement in the CTA mass transfer from the monomer droplets to the aqueous phase due to the improved emulsification of the monomer droplets. For semicontinuous polymerization, the instantaneous conversion increased as the stirring speed was increased for speeds less than 150 rpm because the system was monomer diffusion controlled, whereas at stirring speeds higher than 150 rpm, the agitation was strong enough for the polymerization rate to be kinetically controlled. They [251] further studied the effect of agitation on the monomer and CTA transport step from the monomer droplets to the polymer particles in the semicontinuous emulsion polymerization of St and BA with KPS as the initiator and NaLS as the emulsifier, respectively. Polymerizations were carried out in a 2 dm^3 glass reactor fitted with a stainless-steel anchor-type stirrer. It was found that when neat monomer addition was used, a mild degree of agitation (0.1 kW/m^3) was needed to overcome monomer mass transfer limitations. However, a moderate degree of agitation (0.3 kW/m^3) was not enough to avoid mass transfer limitations when dodecyl mercaptan (CTA) was present. Preemulsification of the feed was used to minimize the mass transfer

limitations of both the monomer and the CTA, even for a gentle degree of agitation (0.01 kW/m^3). The molecular weights of the polymers produced depended on the presence of the CTA. In the presence of the CTA, the molecular weights decreased with the stirring speed, whereas they increased in the absence of the CTA.

Salazar et al. [234] investigated how the molecular weight could be controlled in a starved emulsion polymerization of St using *tert*-dodecyl mercaptan and *tert*-nonyl mercaptan (more water-soluble) as the CTAs. The authors showed that in a starved polymerization with *tert*-dodecyl mercaptan, a mass-transfer resistance to the mercaptan was required to fit the observed PSt molecular weights to the model predictions, but this extra mass-transfer resistance could be neglected in the case of the more water-soluble *tert*-nonyl mercaptan. Cunningham et al. [253, 254] investigated the seeded emulsion polymerization of St in order to study the effects of *n*-dodecly mercaptan on the polymer molecular weight distribution. In the emulsion polymerization of St with *n*-dodecly mercaptan as the CTA, the transport of the CTA from the monomer droplets to the polymer particles is diffusion limited, meaning that it was difficult to calculate molecular weights, except perhaps by using empirical approaches. They developed a methodology that used the mass transfer model developed by Nomura et al. [239], which allowed the CTA concentration within the polymer particles to be determined, regardless of whether or not the CTA was at its equilibrium value, and validated the essential correctness of the approach by comparing experimental molecular weight distributions with the model's predictions. The authors further suggested that the methodology used might be amenable to online applications. Mendoza et al. [125] carried out a study of the kinetics of St emulsion polymerization using *n*-dodecly mercaptan as the CTA. In this study, it was found that the CTA had no effect on the polymerization rate, but had a substantial effect on the molecular weight distribution (MWD). The efficiency of the CTA in reducing the MWD was lowered by the mass transfer limitations. The process variables affecting the CTA mass-transfer were also investigated. For example, the average molecular weight of the polymers produced was found to decrease with increasing stirring speed. The authors developed a mathematical model to predict monomer conversion, the number of polymer particles, and the number-average molecular weights, and then validated the proposed model by fitting it to the experimental data.

During an emulsion polymerization, one often encounters the formation of coagulum, which is sometimes fatal for products such as paints. Moreover, it may prevent the scale-up of commercially-acceptable latex. Therefore, the formation of coagulum during an emulsion polymerization is an important industrial problem and may be closely related to agitation. Although some researchers [260–262] postulated that coagulum may form during emulsion polymerization due to tangential or shear stresses, which originate in the reaction mixture due to agitation, the literature has very little information on any quantitative experimental data in this field. Vanderhoff [260] discussed this problem and proposed two mechanisms for the formation of coagulum in

the emulsion polymerization process: (i) a failure of the stability of the latex, giving rise to flocculation and growth of the aggregates to macroscopic size (lumps), and (ii) a different mechanism of polymerization, for example polymerization in large monomer droplets or a separate monomer layer in the vapor space above the latex and on the reactor surfaces. Lowry et al. [261] studied the phenomenon of shear-induced coagulation in emulsion polymerization carried out in a stirred tank reactor. Here, the authors correlated the coagulum formation for different emulsion polymerizations to various agitation parameters. For a low Reynolds number, it was shown that the stirring speed is important, whereas, for a high Reynolds number, power consumption is the important parameter. Matejicek et al. [262] studied the influence of agitation on the creation of coagulum during the semicontinuous emulsion terpolymerization of St-BA-AA carried out in 25 dm^3 and 5 m^3 reactors, respectively, and gave the relationship between the amount of coagulum formed and the intensity of agitation. The authors found that the amount of coagulum formed (Y%) was correlated to the specific impeller power input ε_i introduced by agitation, showing that the dependence of the coagulum content in the dispersion on impeller speed passes through a minimum.

4
Kinetic Aspects in Polymer Structure Development

4.1
Molecular Weight Distribution (MWD)

4.1.1
Monte Carlo (MC) Simulation Method

Polymerization rate represents the instantaneous status of reaction locus, but the whole history of polymerization is engraved within the molecular weight distribution (MWD). Recently, a new simulation tool that uses the Monte Carlo (MC) method to estimate the whole reaction history, for both linear [263–265] and nonlinear polymerization [266–273], has been proposed. So far, this technique has been applied to investigate the kinetic behavior after the nucleation period, where the overall picture of the kinetics is well understood. However, the versatility of the MC method could be used to solve the complex problems of nucleation kinetics.

The MC method is a powerful technique for investigating complicated phenomena that are difficult to solve by the conventional differential equation approach. In the MC approach, all one needs are the individual probabilities of various kinetic events. It is easy to understand the advantages of applying the MC method to emulsion polymerization if we note that it is possible to simulate the formation processes of all polymer molecules in each polymer particle directly because the volume of the reaction locus is very small. One

unique characteristic of emulsion polymerization is that high molecular weight polymers are produced without decreasing the polymerization rate, and this is due to the compartmentalization of polymerization reactions inside the polymer particles, resulting in the isolation of macroradicals. Usually, the loci of polymerization is made up of 10^{16} to 10^{18} polymer particles per liter. As a consequence, the number of monomeric units in each reaction locus is limited to about 10^5 to 10^8. For example, suppose the diameter of a polymer particle at 100% conversion is 0.1 μm, the density of the polymer is 1 g/cm^3, and the molecular weight of a monomeric unit is 100. In this case, the total number of monomeric units in this polymer particle is 3×10^6. If the number average chain length is 10^4, which is not unusually large in emulsion polymers, each polymer particle consists of only 300 polymer molecules at 100% conversion. For such a small number of polymer molecules, one can readily simulate the formation processes of all polymer molecules using an MC method in a straightforward manner.

In this section we discuss unique MWDs formed via linear emulsion polymerization, while the kinetics of branched and crosslinked polymer formation are considered in Sect. 4.2.

Before the MC simulation method was proposed, theoretical analyses of the MWDs from linear emulsion polymerizations had been conducted on the basis of kinetic population balance equations [274–277] and Markovian statistics [278–280]. These approaches have clarified that the MWD of polymer molecules formed in emulsion polymerization is fundamentally different to that from corresponding bulk polymerization. However, due to the complex heterogeneous nature of the polymerization system, in which entry and desorption of oligomeric radicals are involved, applying these methods to real systems is not straightforward, and analytical solutions are limited to very special cases. Often, the effect of radical desorption on the MWD is taken into account using the first-order chain stoppage reaction [276–280], which does not reflect the real kinetics. Although some approximate methods have been proposed [277, 281], it appears to be a formidable task to correctly account for the chain-length dependence of radical desorption in the conventional approaches.

In MC simulation, any kinetic event can be accounted for, as long as the probability of each kinetic event is represented explicitly. Chain length dependent kinetics can be accounted for in a straightforward manner if the functional form is provided. In conventional MC simulations of molecular build-up processes, the monomeric units are added to each growing polymer molecule one-by-one; therefore, a multitude of random numbers and calculations are required to simulate the formation of each polymer molecule. To get around this problem, a new concept, the *competition technique*, was proposed in order to drastically reduce the amount of calculation required for the simulation [263, 264].

Figure 9 illustrates a case where two polymer radicals exist in a polymer particle.

In this technique, the *imaginary* time (or equivalently, the imaginary chain length, given by $P=k_p[M]_p t$) for a certain event to occur is calculated by using the appropriate probability distribution for each type of event. If the given process

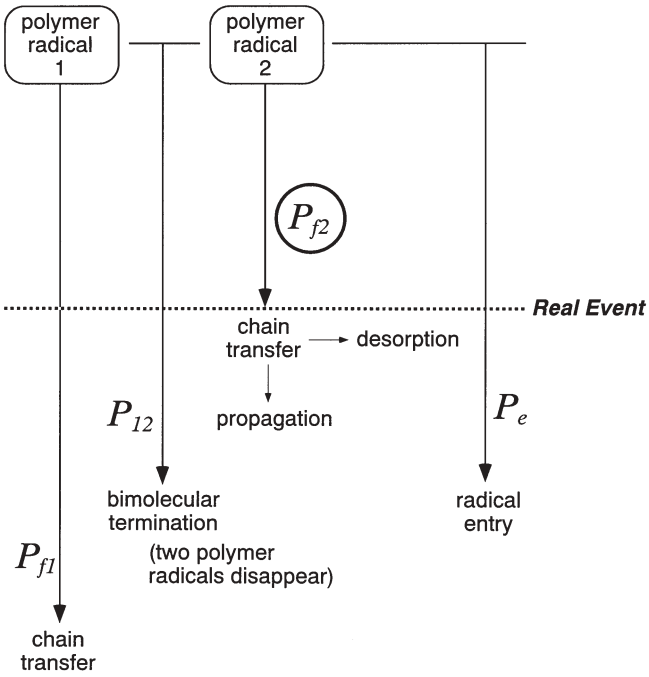

Fig. 9 Schematic drawing illustrating the simulation method based on the competition technique

is considered random and independent of chain-length, one can simply estimate the time for each event to occur by generating one random number that follows the most probable distribution [263, 264]. After calculating the imaginary chain lengths, a kind of event competition is considered, and the shortest "imaginary chain length" is chosen as the "real event". In the figure, P_{f2} is chosen as a real event. If this chain length is 1000, one can add 1000 monomeric units to both polymer radicals by using only four random numbers, not 2000 random numbers as in the conventional type of MC simulations. It is often claimed that MC methods are time-consuming, however, by using a well-designed method, the calculation time can be reduced significantly. In addition, virtually any type of information can be obtained from a set of MC simulations, and significant insights into the complex reaction system can be obtained in a straightforward manner. The MC method is useful for investigating emulsion polymerization kinetics that involve various types of simultaneous kinetic events.

4.1.2 Instantaneous Molecular Weight Distribution

In this part, the instantaneous MWD formed over a very small time interval is considered. This is equivalent to considering the distribution of polymer

chains formed in a certain fixed environment. Note that, because the polymer/monomer ratio is kept approximately constant during Interval II, the instantaneous MWD may be a reasonable approximation for the linear polymers formed during Interval II. This is not the case, however, for nonlinear polymer formation, as discussed later.

Assuming that the polymer particles have a uniform size, a single statistical polymer particle that is representative of the whole population of particles can be considered. This polymer particle is a kind of imaginary micro-reactor that does not modify either the volume or the polymer/monomer ratio, even after polymer chains are produced, so the reaction environment is kept constant except that the number and chain length distribution of the macroradicals are changed stochastically. By producing a large number of polymer molecules consecutively with this imaginary polymer particle, the instantaneous MWD can be determined.

After the nucleation period, three types of kinetic processes determine the kinetics of emulsion polymerization: radical entry, radical desorption, and polymer chain formation in the polymer particles. The kinetics of emulsion polymerization are fully described by the following five dimensionless parameters:

1. Radical entry

$$\varepsilon = \frac{\rho_e}{k_p[M]_p N_T} = \frac{1}{k_p[M]_p \bar{t}_e} \tag{73}$$

where ρ_e is the rate of radical entry into polymer particles, including the reentry of desorped radicals, N_T is the number of polymer particles, and $\bar{t}_e$ is the average time interval between radical entry.

Assuming a random entry of radicals to all polymer particles, the imaginary chain length P_e shown in Fig. 9 follows the most probable distribution, and can be determined by using a random number between 0 and 1, y, as follows [273]:

$$P_e = (1/\varepsilon)\ \ln(1/y) \tag{74}$$

2. Chain transfer

$$C_f = C_m + C_{fCTA}\frac{[CTA]_p}{[M]_p} \tag{75}$$

where C_m is the monomer transfer constant, and C_{fCTA} is the constant of transfer to chain transfer agents.

In the same way as in Eq. 74, the imaginary chain lengths P_{f1} and P_{f2} shown in Fig. 9 can be determined by using a random number between 0 and 1, y, as follows:

$$P_f = (1/C_f)\ \ln(1/y) \tag{76}$$

3. Bimolecular termination

$$\xi = \frac{2k_{tp}}{k_p[M]_p \nu_p N_A} \tag{77}$$

where k_{tp} is the bimolecular termination rate constant, in which the termination rate is represented by $R_t=2k_{tp}[R^*]^2$, not $R_t=k_{tp}[R^*]^2$ used in [263–273]. N_A is Avogadro's number, and ν_p is the volume of a swollen polymer particle. Note that the bimolecular termination rate depends on the particle size in emulsion polymerization, and is larger for smaller polymer particles.

Assuming that the bimolecular terminations are independent of chain-length, the imaginary chain length P_{12} shown in Fig. 9 can be determined by:

$$P_{12} = (1/\xi)\ln(1/y) \tag{78}$$

Note that Eq. 78 must be considered for all possible radical pairs.

4. Radical desorption

$$\delta = \frac{K_0}{k_p[M]_p} \tag{79}$$

where K_0 is the desorption rate coefficient for an oligomeric radical. Any chain-length-dependent radical desorption can be accounted for using the MC method, in principle. However, it is often reasonable to assume that only monomeric radicals can exit. For such cases, the average desorption rate coefficient for all radicals in polymer particles, k_f, which appears in the Smith-Ewart equation [4] can be approximated by [43, 44, 122] $k_f \cong K_0 C_f$. In this article, the simulated results for such simple cases are shown.

If a chain transfer reaction is the actual event, as shown in Fig. 9, a monomeric or a CTA radical is formed. Neglecting the difference between monomeric and CTA radicals, the probability of radical exit when the chain transfer reaction occurs is given by:

$$P_{des} = \frac{\delta}{1 + C_f + (n-1)\xi + \delta} \tag{80}$$

where n is the number of radicals in the polymer particle.

5. Type of bimolecular termination

$$\varphi_c = \frac{k_{tp,c}}{k_{tp,c} + k_{tp,d}} \tag{81}$$

where $k_{tp,c}$ and $k_{tp,d}$ are the bimolecular termination rate constants by combination and by disproportionation, respectively.

If bimolecular termination is the actual event, the probability that the termination is by combination is equal to φ_c.

The MC simulation was performed for 1×10^4 polymer molecules in each condition [264]. It was shown that both the average number of radicals $\bar{n}$ and the distribution of the number of radicals per polymer particle agree completely with the analytical solution derived by O'Toole [119], and it was confirmed that the present MC simulation can be conducted without significant statistical errors [264].

To clarify the unique characteristics of the MWD of emulsion polymers, one of the simplest and most common cases [264], where neither chain transfer (C_f=0) nor radical desorption (δ=0) occurs, is considered here. The magnitude of bimolecular termination (ξ) is changed with a constant radical entry frequency ($\varepsilon=2\times10^{-4}$). Figure 10 shows the calculated number- and weight-average chain lengths and the polydispersity index (PDI= $\bar{P}_w/\bar{P}_n$) as a function of $\bar{n}$.

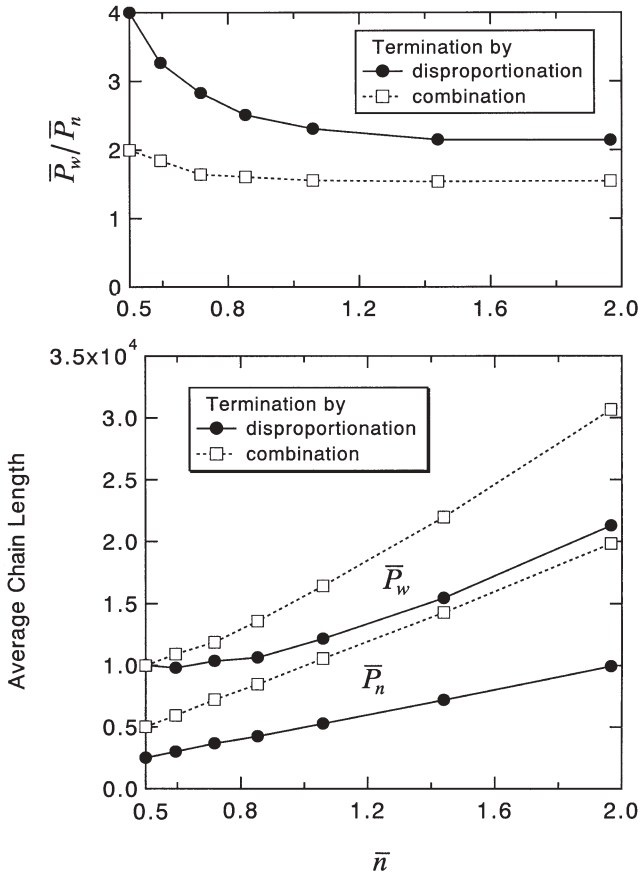

Fig. 10 Calculated number- and weight-average chain lengths as a function of the average number of radicals in a polymer particle, $\bar{n}$, with $\varepsilon=2\times10^{-4}$ and $C_f=\delta=0$

In the present investigation, because the value of $\bar{n}$ increases when the termination rate ξ is decreased, the average chain length becomes larger as $\bar{n}$ increases. As clarified in earlier theoretical investigations [276, 277], the PDI is the largest when $\bar{n}$ =0.5, which could be considered a typical example of emulsion polymerization. At $\bar{n}$ =0.5, PDI=4 if polymer chains are formed solely via bimolecular termination by disproportionation, and PDI=2 when formed by combination. In homogeneous polymerizations, it is well known that PDI=2 when polymer chains are entirely formed by disproportionation, and PDI=1.5 when they are formed solely by combination. Therefore, the PDI of the instantaneous MWD is larger for emulsion polymerization, and as the average number of radicals per polymer particle $\bar{n}$ increases, the PDI approaches that for homogeneous polymerization.

The reason for the broader distribution in a *typical* emulsion polymerization (the so-called zero-one system with $\bar{n}$ =0.5) can be rationalized from the point of view of a very fast termination reaction in a polymer particle. When an oligomeric radical (a monomeric radical is assumed in the present simulation) enters a polymer particle that contains a macroradical, the bimolecular termination occurs before the oligomeric radical grows to a sufficient chain length. An investigation of the MWD produced makes it easier to understand the origin of this behavior. Figure 11 shows the chain length distribution formed by disproportionation (solid curve) and by combination (broken curve).

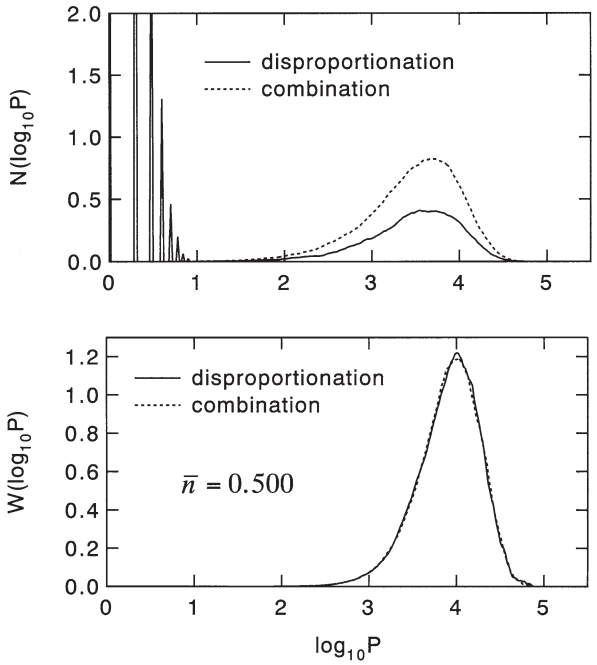

Fig. 11 Calculated chain length distribution on a number and weight basis, for $\bar{n}$=0.500

The independent variable is the logarithm of chain length ($\log_{10}P$), which is usually employed in size exclusion chromatography (SEC) analysis. The upper figure shows the chain length distribution on a number basis, while the lower figure shows that on a weight basis. The chain length distribution formed by disproportionation is the same as the distribution of radicals that cause bimolecular termination. When polymer chains are formed by bimolecular termination from disproportionation, very large peaks appear at smaller chain lengths in the number fraction distribution ($N(\log_{10}P)$). These discrete peaks correspond to integral numbers of monomer units in the chain lengths: 1, 2, 3, ... In the present case, half of the polymers formed by disproportionation are oligomeric chains from very fast bimolecular termination. When polymers are formed via bimolecular termination by combination, on the other hand, the chain length of the radical that has just entered is so small that the dead polymer distribution obtained is almost the same as the macroradical distribution in the polymer particles, which is given by the most probable distribution (PDI=2).

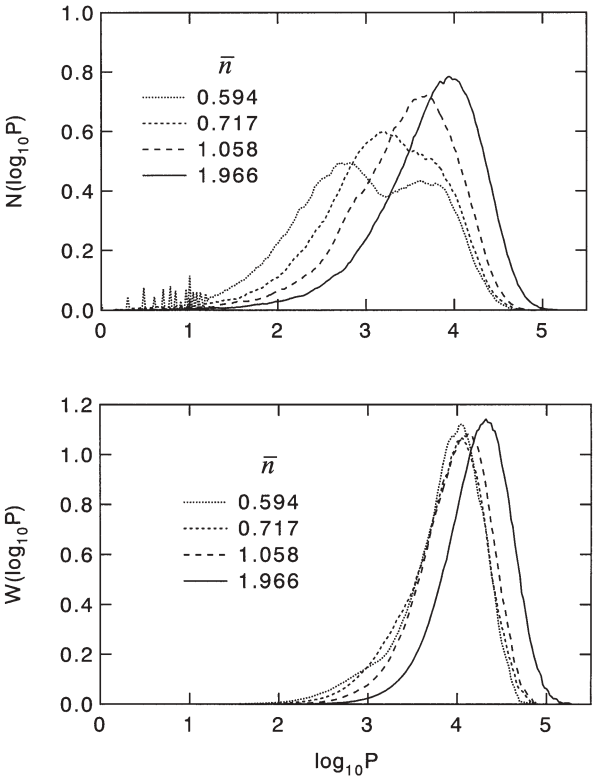

Fig. 12 Instantaneous chain length distribution on a number and weight basis, where dead chains are formed by disproportionation termination. The value of $\bar{n}$ is increased by decreasing the bimolecular termination rate

In addition, because the weight fraction of the oligomeric chains formed by disproportionation is very small, differences between the termination modes cannot be found in the weight fraction distributions obtained via usual SEC techniques, as shown in the lower figure of Fig. 11. Therefore, one needs to pay careful attention to the measurement of the MWD, especially when the effect of bimolecular termination by disproportionation cannot be neglected. If the oligomeric peaks cannot be determined accurately, the obtained PDI drops from 4 to 2, and it is expected that these oligomeric molecules are neglected in usual SEC analysis.

As $\bar{n}$ increases, the unique characteristics of the MWD formed in emulsion polymerization are lost, as shown in Fig. 12.

The smaller and larger peaks in the $N(\log_{10}P)$ formed via bimolecular termination by disproportionation merge as $\bar{n}$ increases. On the other hand, such drastic MWD change cannot be observed in the weight based distributions $W(\log_{10}P)$ that are usually measured by SEC. When $\bar{n}=2$, the MWD formed has already become very close to that for homogeneous polymerization, and in terms of the MWD, pseudobulk polymerization kinetics would be a reasonable approximation. Because $\bar{n}$ increases with particle size, the MWD changes with the particle size. This would be of special interest in cases with broad particle size distributions, as in the case of a continuous emulsion polymerization using a stirred tank reactor.

In our illustrative calculated results, chain transfer reactions are neglected in order to highlight unique characteristics of emulsion polymerization. However, the radical entry rate into a polymer particle is often much smaller than the chain transfer frequency; $\varepsilon \ll C_f$ in emulsion polymerization usually. In such cases, dead polymer chain formation is dominated by chain transfer reactions, and the instantaneous weight fraction distribution is given by the following most probable distribution:

$$N(P) = C_f \exp(-C_f P) \tag{82a}$$

$$W(P) = C_f^2 P \exp(-C_f P) \tag{82b}$$

4.1.3 Effect of Chain-Length-Dependent Bimolecular Termination

The bimolecular termination reaction in free-radical polymerization is a typical example of a diffusion controlled reaction, and is chain-length-dependent [282–288]. When pseudobulk kinetics applies, the MWD formed can be approximated by that resulting from bulk polymerization, and it can be solved numerically [289–291]. As in the other extreme case where no polymer particle contains more than one radical, the so-called zero-one system, the bimolecular termination reactions occur immediately after the entrance of second radical, so unique features of chain-length-dependence cannot be found. Assuming that the average time interval between radical entries is the same for all particles and that the weight contribution from oligomeric chains formed

via disproportionation termination can be neglected, the weight fraction distribution is given by the following most probable distribution:

$$W(P) = (C_f + \varepsilon)^2 P \exp\{-(C_f + \varepsilon)P\} \quad (83)$$

On the other hand, however, it is not straightforward to calculate the MWDs for intermediate cases using the conventional approach. A notable advantage of using an MC simulation technique is that it can be applied to virtually any type of emulsion polymerization, and can account for the chain-length-dependent bimolecular termination reactions in a straightforward manner [265]. Sample simulation results for instantaneous MWDs were shown [265] that were obtained using parameters for styrene polymerization that were reported by Russell [289].

When the bimolecular terminations are highly diffusion controlled, the termination reactions are dominated by interactions between radicals with short and long chain lengths even in bulk polymerization, and the MWD of the longer polymer radicals tends to follow the most probable distribution [287, 292]. Under such conditions, oligomeric chains that can be observed only in the number fraction distribution may be formed via disproportionation termination irrespective of particle size. Figure 13 shows the effect of particle size on the instantaneous chain length distribution where the bimolecular terminations are from disproportionation [265].

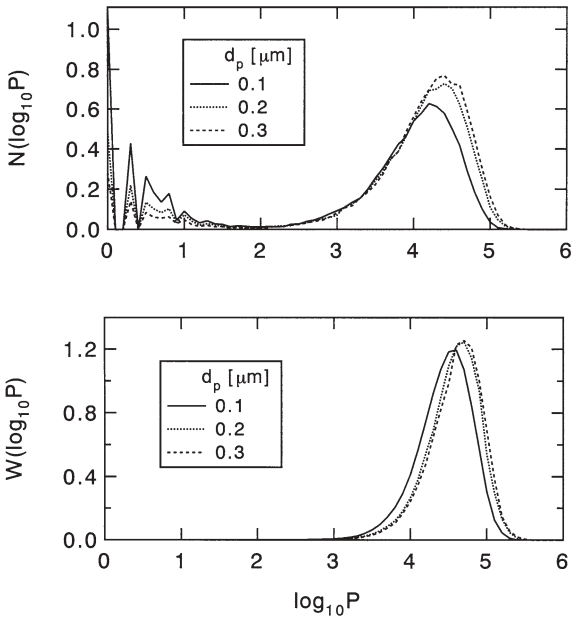

Fig. 13 Effect of particle size on the instantaneous chain length distribution, where bimolecular terminations are chain-length dependent and are by disproportionation

As the particle size increases, the bimolecular termination rate decreases. For cases with chain-length independent bimolecular termination, the oligomeric peak in the number fraction distribution moves toward larger chain length, as shown in Fig. 12. On the other hand, if the bimolecular terminations are highly diffusion controlled, the oligomeric peak location does not move, but the peak height becomes smaller due to an increased amount of dead polymer formation from chain transfer to the monomer, which is accounted for in this simulation. Note that we should not expect these oligomeric peaks to be detected via usual SEC analysis, represented on the basis of the weight fraction distribution, as shown in the lower panel of Fig. 13. The termination mode may not be distinguished from the SEC data.

The chain-length-dependence of bimolecular termination reactions needs to be taken into account in order to be able to accurately estimate the MWD formed, except when very small polymer particles are formed and/or chain transfer reactions dominate over dead polymer chain formation.

4.1.4 Accumulated Molecular Weight Distribution

In a deterministic approach, the instantaneous MWDs are calculated first, and then the accumulated MWD is obtained by integrating the instantaneous MWDs. However, in MC simulations, we can follow the reaction history of each polymer particle directly, and the full MWD is obtained by simulating a large number of polymer particles [263]. Therefore, highly complex reaction kinetics can be simulated directly in a straightforward manner.

During emulsion polymerization, the polymer concentration in the polymer particle that is the locus of polymer chain formation is larger than that in corresponding bulk polymerization. Therefore, the possibility of chain transfer reactions to the polymer occurring is higher, even when the monomer conversion to polymer is not very large. Besides these branching reactions (which will be discussed in Sect. 4.2), another accidental branching may occur during emulsion polymerization. In emulsion polymerization, the time interval between radical entries is usually large, and chain transfer to monomer tends to be the dominant chain termination mode, in the absence of other chain transfer agents. Depending on the mechanism of the chain transfer reaction, active terminal double bonds may be formed by the monomer transfer reaction, which may lead to terminal double bond polymerization (TDBP) [263]. Active terminal double bonds may not be formed during styrene polymerization [293]; however, in order to investigate the potential importance of the TDBP in general, a simulation that incorporates TDBP was conducted using kinetic parameters for the styrene polymerization.

Figure 14 shows the development of the weight fraction distribution with and without TDBP [263].

The parameter K shown in the figure represents the reactivity of the terminal double bonds, defined by $K=k'_p/k_p$, and k'_p is the rate constant of TDBP. The

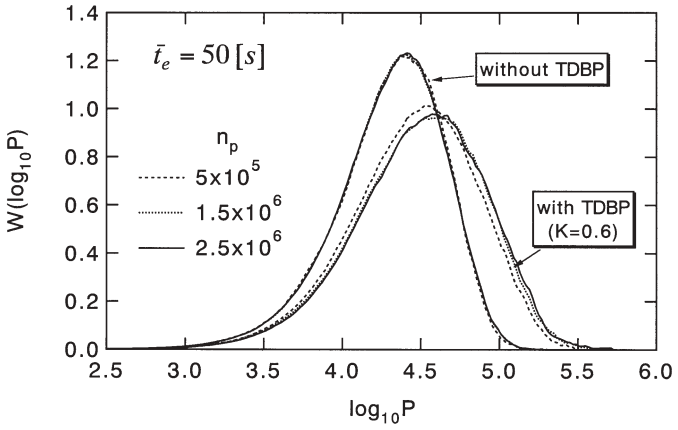

Fig. 14 Accumulated weight fraction distribution development with and without terminal double bond polymerization

average time interval between entries for radicals generated in the water phase (excluding reentry of desorped radicals) is 50 s. The value of n_p is the total number of monomeric units bound into polymer chains in a polymer particle, and therefore, n_p increases as the reaction proceeds. In the simulation, the polymer/monomer ratio in the polymer particle is kept constant. Both with and without TDBP, the MWD profiles do not change significantly during polymerization (as long as monomer droplets exist); however, much larger polymer molecules can be formed by the TDBP and this can change the MWD profile significantly. In emulsion polymerization, the enhanced accidental branching caused by a higher polymer concentration cannot be neglected, even for reaction systems in which the branching reactions are not significant in the bulk polymerization.

4.1.5 Determination of Monomer Transfer Constants from MWD

The traditional method of determining the monomer transfer constant C_m is the Mayo method [294, 295], where the inverse of the number average chain length $\bar{P}_n$ is extrapolated to zero polymerization rate. To obtain reliable C_m values, one needs to measure rather large $\bar{P}_n$ values to high precision that can then be extrapolated to zero polymerization rate. In addition, linear extrapolation is not guaranteed if bimolecular termination reactions are chain-length-dependent [296].

A simple alternative method was proposed by Gilbert et al. [296, 297] to determine the chain transfer constants based on the chain length distribution (CLD). If the dominant chain termination mechanism is chain transfer to monomer, the instantaneous numerical MWD (the number fraction distribution) is given by:

$$N(P) = C_m \exp(-C_m P) \tag{84}$$

In many emulsion polymerizations, the monomer/polymer ratio is kept constant during Interval II, and the accumulated MWD is approximately equal to the instantaneous distribution. Equation 84 shows that the C_m value can be determined from the slope of the $\ln N(P)$ versus P plot.

In a zero-one system in which a radical has just entered a polymer particle containing one polymer radical, and is terminated instantaneously, the number fraction distribution in the absence of a polymer transfer reaction is given by:

$$N(P) = (C_m + \varepsilon) \exp\{-(C_m + \varepsilon)P\} \tag{85}$$

where $\varepsilon = 1/(k_p[M]_p \bar{t}_e)$, as given by Eq. 73.

It is evident from Eq. 85 that the condition $\varepsilon = 1/(k_p[M]_p \bar{t}_e) \ll C_m$ is needed to apply the CLD method to emulsion polymerization. Note that the radical entry rate may be increased through the radical exit. Even when these conditions are satisfied, a higher polymer concentration than for the corresponding bulk polymerization may result in more occurrences of the polymer transfer reaction.

The effect of the polymer transfer reaction on the applicability of the CLD method can be examined by applying the MC simulation method [298]. Figure 15 shows the MC simulation results for the condition $C_m = 5\times10^{-5}$, $\varepsilon = 1/(k_p[M]_p \bar{t}_e) = 5\times10^{-7}$, and for the polymer transfer constant $C_{fp} = 5\times10^{-5}$, when the total number of monomeric units bound into polymer chains in a polymer particle $n_p = 1\times10^6$.

The upper panel of Fig. 15 shows the weight fraction distribution obtained by taking the logarithm of chain length as an independent variable, as in an SEC analysis. The distribution is clearly much broader than without the polymer transfer reactions, as shown in [298]. The lower panel shows the plot of $\ln(N(P))$ versus P, which is clearly curved although a straight regression line could be drawn around the peak region of the $W(\log P)$ curve. The slope obtained for this case is -5.102×10^{-5}, and therefore $\varepsilon + C_m = 5.102\times10^{-5}$. If we use $\varepsilon = 5\times10^{-7}$, we obtain $C_m = 5.052\times10^{-5}$, which is sufficiently close to the true monomer transfer constant, 5×10^{-5}. Note that the MC simulation inevitably involves a small amount of statistical error, and the slope changes slightly if the same simulation is repeated. However, an important conclusion from these kinds of simulations [298] is that, although the MWD is affected significantly by the polymer transfer reactions, the CLD method is still considered applicable as a reasonable approximation for many systems. The C_m value can be estimated reasonably well from the plot of $\ln(N(P))$ versus P, by taking the slope around the peak region of the $W(\log P)$ curve, as long as the polymer transfer constant is not too large.

The MC simulation method can be used to find the experimental conditions where the CLD method can be used to determine the monomer transfer constant.

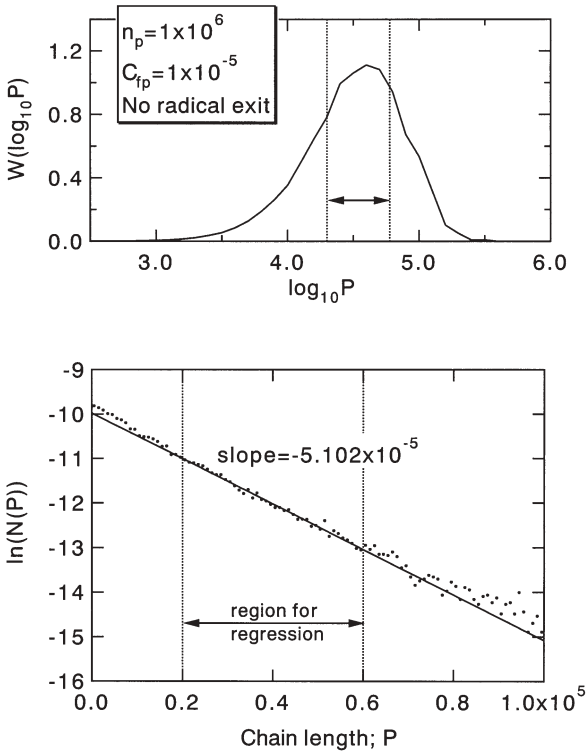

Fig. 15 Monte Carlo simulation results for emulsion polymerization that involves polymer transfer reactions, under the conditions C_m=5×10^{-5}, ε=5×10^{-7} and C_{fp}=5×10^{-5}, without radical desorption

4.2 Branched and Crosslinked Polymer Formation

4.2.1 Long-Chain Branched Polymers

Nonlinear polymer formation in emulsion polymerization is a challenging topic. Reaction mechanisms that form long-chain branching in free-radical polymerizations include chain transfer to the polymer and terminal double bond polymerization. Polymerization reactions that involve multifunctional monomers such as vinyl/divinyl copolymerization reactions are discussed separately in Sect. 4.2.2. For simplicity, in this section we assume that both the radicals and the polymer molecules that formed are distributed homogeneously inside the polymer particle.

In nonlinear emulsion polymerization, a comprehensive mathematical model must account for the following unique characteristics of emulsion polymeriza-

tion: (a) compartmentalization of radicals, (b) higher polymer concentration effects, and (c) limited space effects.

4.2.1.1 Compartmentalization of Radicals

Compartmentalization of radicals into polymer particles may yield a unique MWD for the linear chains, as discussed in Sect. 3.1, except when the dominant chain termination mode is the chain transfer reaction. Branched polymer molecules are assemblies of linear polymer chains (called primary chains), and compartmentalization effects on the primary chain length distribution must be properly accounted for.

The compartmentalization of radicals may produce another important effect when large-sized branched polymer molecules are formed by chain transfer to polymer plus combination termination. As clarified in Sect. 4.1, when the $\bar{n}$ value is small, the frequency of bimolecular termination reactions between large polymer radicals drops significantly compared to models that do not account for compartmentalization of radicals. From this fact, it is easy to see that the size of branched polymer molecule is smaller than that calculated without considering compartmentalization effects [281].

4.2.1.2 Higher Polymer Concentration Effects

The mechanism of emulsion polymerization ensures that the polymer concentration at the polymerization locus is semidilute or concentrated, which results in a greater probability of branch chain formation [299, 300]. This effect produces unique average branching densities and unique distributions of branching densities, that are significantly different from corresponding bulk polymerization [266, 301].

Figure 16a shows the development of average branching density in emulsion polymerization and in a corresponding bulk polymerization, both of which involve the polymer transfer reactions [301].

In bulk polymerization, the average branching density increases with the as the polymerization progresses, while it is fairly high even from a very early stage of the emulsion polymerization. This difference in behavior can be explained by the different polymer concentrations at the locus of each type of polymerization. In bulk polymerization, the polymer concentration at low conversions is very low. Because the branches are formed by the reaction between a polymer molecule and a polymer radical, a lower polymer concentration results in a lower frequency of branch formation and the branching density increases as the polymer concentration increases. On the other hand, in emulsion polymerization, the polymer concentration at the locus of polymerization (in the polymer particle) is high, even just after the formation of polymer particles. A higher polymer concentration results in a higher branching reaction rate. If

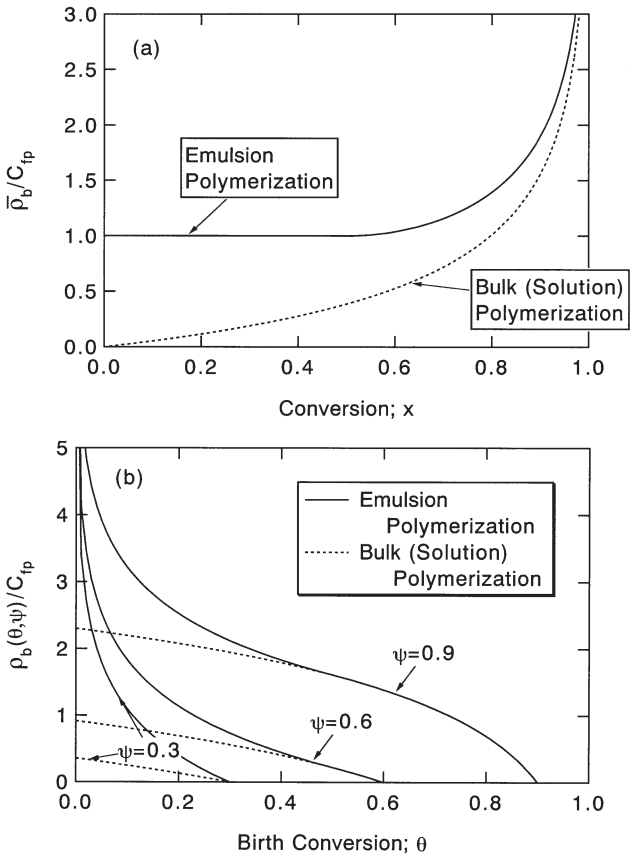

Fig. 16 Development of the average branching density **a** and the branching density distribution **b** for emulsion and bulk polymerizations. The conversion at which monomer droplets disappear in emulsion polymerization is x_c=0.5

the polymer concentration stays the same during the lifetimes of the monomer droplets, the ratio of the branching and propagation reaction rates is kept constant, resulting in a constant average branching density until the depletion of the monomer droplets, as shown in Fig. 16a. Emulsion polymerizations enhance the frequency of branching and crosslinking reactions due to the higher polymer concentration associated with the existence of monomer droplets.

Figure 16b shows the development of the branching density distribution, where $\rho_b(\theta,\psi)$ shows the expected branching density of the primary polymer molecule born at conversion $x=\theta$, when the conversion at the present time is $x=\psi$. The primary chains formed in the early stages of polymerization are subjected to branching reactions for a longer period of time, and therefore, the expected branching density is higher than those chains formed in the later

stages of polymerization. This is the reason that we obtain decreasing functions for both emulsion and bulk polymerization. However, the heterogeneity of the branched structure is more significant for emulsion polymers, as shown in Fig. 16b. Note that the fact that the average branching density does not change as long as monomer droplets exist, as shown in Fig. 16a, does not mean that a homogeneous branched structure is formed during that period.

4.2.1.3 Limited Space Effects

Considerations of "radical compartmentalization" and "higher polymer concentration effects" are not sufficient to describe the processes that build branched polymer molecules in emulsion polymerization, and the effects of limited space must be properly taken into account [266–269].

The locus of polymerization is confined to a very small space, which not only limits the highest molecular weight attainable but can also change the whole MWD profile significantly. The MC simulation technique [266–269] is the only method that can currently take the effects of limited space into account. If the effects of limited space are ignored, the calculated molecular weight may exceed the molecular weight of a whole polymer particle. For example, when the crosslinks – the bridges that connect chains – are formed, conventional deterministic models that do not account for the effects of limited space may predict that the second order moment of the MWD goes to infinity, which is clearly wrong, because the maximum molecular weight is limited by the particle size. In general, those models that do not include the particle size as a parameter when describing the formation of branched chains are illogical.

The limited space effects present rather difficult problems to account for in the conventional deterministic approach. The problem can be highlighted by considering the following hypothetical example. Suppose that there are three polymer chains and three radicals ($R^{\bullet}$), and that polymer transfer reactions are about to occur [269]. Within these polymer chains, suppose that one chain is much larger than the other two, as shown in Fig. 17.

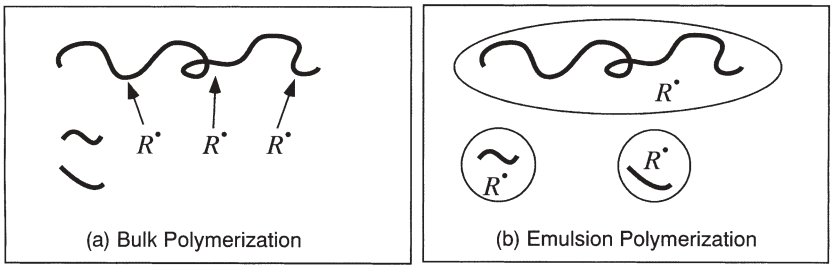

Fig. 17 Hypothetical example that illustrates the differences between the polymer transfer reactions that occur in bulk polymerization **a** and in emulsion polymerization **b**

If all of these species exist in the same reaction locus as in Fig. 17a, it would be highly probable that all of the radicals would attack the largest chain. In other words, the chain transfer rate of the polymer chain with chain length P, v_{fp,P_P}, is proportional to its chain length:

$$v_{fp,P_P} = k_{fp}[R^*]\, r[P_P] \tag{86}$$

where k_{fp} is the rate constant for chain transfer to polymer, $[R^\bullet]$ is the total radical concentration, and $[P_P]$ is the concentration of polymer molecules with chain length P in the whole reaction mixture.

On the other hand, suppose that each of these polymer molecules is isolated into different particles, and that each particle contains one radical, as shown in Fig. 17b. If the radical causes the polymer transfer reaction, the partner must be the polymer molecule that happens to exist in the same particle (so it cannot partner a larger polymer molecule that exists in a different polymer particle). As a consequence, the expected size of the polymer molecule attacked by a radical is smaller for emulsion systems than for the homogeneous model shown in Fig. 17a.

Equation 86 is commonly used for homogeneous reaction systems, but it is not exact in emulsion polymerization. The value of $[P_P]$ is different for each polymer particle, and the value obtained for $[P_P]$ when all of the particles are combined cannot be used either. Strictly, one needs to determine a discrete distribution function of polymer molecules in each polymer particle.

Figure 18 shows the simulated MWD profiles that clearly demonstrate the effects of limited space [273].

Because the total number of monomeric units bound into polymer molecules is $n_p=4\times10^5$ for the present calculation, the high molecular tail can never exceed 4×10^5. Figure 18 shows that the model that does not account for the effects of

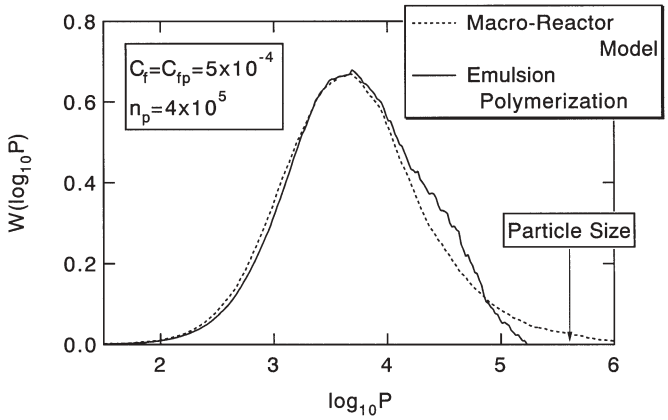

Fig. 18 Comparison of the calculated weight fraction distribution with $C_f=C_{fp}=5\times10^{-4}$ and $x_c=0.5$. For the emulsion polymerization model, the total number of polymerized monomeric units in a polymer particle $n_p=4\times10^5$, which is equal to the size of a dried polymer particle

limited space (the macro-reactor model) is incorrect, because the formation of polymer molecules that are too large to fit in a polymer particle is predicted. More details on the effects of limited space can be found in [268, 269].

The MC simulation method can account for the effects of limited space in a straightforward manner, because the kinetics of polymer formation inside each polymer particle is simulated directly in the MC method. The analytical solution for the development of the weight-average DP was also derived for a simpler case [268], but for more detailed information one needs to resort to the MC method. In MC simulations, one can investigate the structure of each polymer molecule directly, so that highly detailed information can be obtained. Figure 19 shows an example of the branched structure formed during emulsion polymerization that involves chain transfer to polymer, where the primary chains follow the most probable distribution with a number average of 1000.

As we can see, a rather large number of smaller branches exist, which is obviously not what we might expect from the term *long*-chain branches! The 3-D

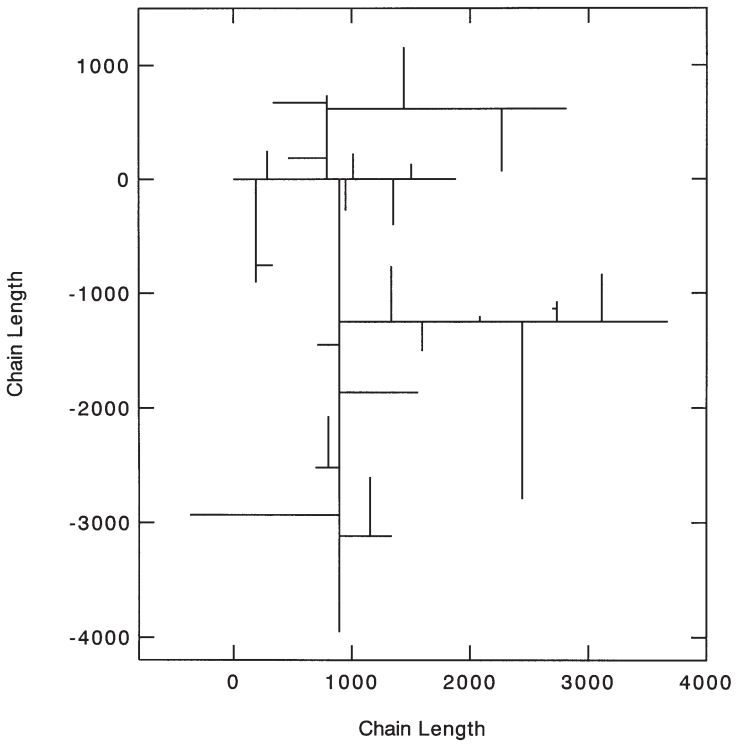

Fig. 19 Example of a branched polymer molecule formed in a model emulsion polymerization. The probability that the chain end is connected to a backbone chain is P_b=0.7. The primary chains follow the most probable distribution with a number-average chain length of 1000

structure of each nonlinear polymer molecule can be estimated, most simply in a θ solvent, using the structural information shown in Fig. 19. By determining the hydrodynamic size of each polymer molecule, we can also estimate the size exclusion chromatography (SEC) elution curve [302–306].

4.2.1.4 Formation of the Bimodal Molecular Weight Distribution

The bimodal MWDs of emulsion-polymerized polyethylenes, which are significantly different from those formed in bulk polymerization, have been reported experimentally [307–309]. An MC simulation was conducted for the experimental conditions reported in [307], and an example is shown in Fig. 20 [310].

The kinetic parameters used were mostly taken from the literature, and an important assumption made was that the particle diameter is about 80 nm (=1.4×10^8 g/mol in molecular weight, which is shown by an arrow in Fig. 20). In [307], it was reported that (1) the particle size is about 50 nm, and that (2) the weight of such a particle is close to the molecular weight of the high molecular weight, narrow distribution component. However, the weight of a low-density polyethylene particle 50 nm in diameter is 6×10^{-17} g, which is 3.6×10^7 g/mol in molecular weight. This molecular weight is too small to contain the polymers in the high molecular weight tail, whose molecular weight can be as large as 8×10^7 g/mol, and so the value of 1.4×10^8 g/mol (≈80 nm in diameter) was used in the MC simulation.

According to the MC simulation, the high molecular weight, narrow distribution component consists of the largest polymer molecule in each polymer particle, and the bimodal MWD is formed because of the limited space effects.

Assuming a simple zero-one system during Interval II, a model analysis was conducted to clarify the conditions needed to form bimodal MWD through the effects of limited space [311].

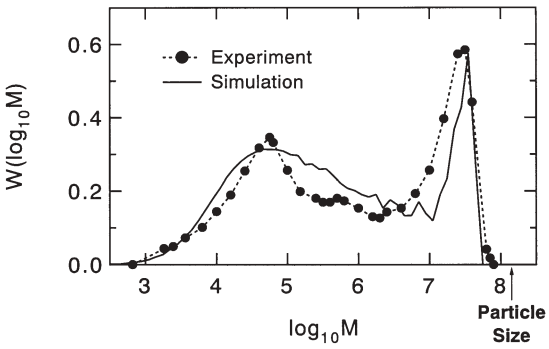

Fig. 20 MWD of emulsion-polymerized polyethylene. The experimental conditions are discussed in detail in [307], and the simulation method is described in [310]

The instantaneous MWD of the primary chains formed during Interval II in a zero-one system (assuming combination termination) is given by the most probable distribution, whose number fraction distribution is given by:

$$N_{pc}(P) = \tau \exp(-\tau P) \tag{87}$$

$$\tau = C_m + C_{fp}\frac{x_c}{(1-x_c)} + C_{fCTA} + \frac{[CTA]_p}{[M]_p} + \frac{1}{k_p[M]_p\bar{t}_e} \tag{88}$$

where x_c is the weight fraction of polymer in the polymer particle, which is kept approximately constant during Interval II, and is often equal to X_{Mc}.

The probability that a newly-formed primary chain starts growing from a radical center on a backbone chain (in other words, the probability that a primary chain end is connected to a backbone chain), P_b, is given by:

$$P_b = \frac{C_{fp}x_c/(1-x_c)}{C_m + C_{fp}x_c/(1-x_c) + C_{fCTA}[CTA]_p/[M]_p + 1/(k_p[M]_p\bar{t}_e)} \tag{89}$$

A model analysis was conducted, which assumed that (1) both τ and P_b do not change during polymerization, (2) all polymer particles are formed instantaneously, and (3) the number of primary chains in a polymer particle, n_{pc}, is the same for all particles. Important conclusions were that (i) bimodal MWDs (represented in terms of $W(\log P)$) are formed if P_b is larger than 0.5, and (ii) for $P_b>0.5$, the weight-average molecular weight increases without limits over the whole course of polymerization. Note that the second conclusion does not indicate that gelation occurs. Figure 21 shows the calculated development of the weight-average chain length [311].

For $P_b<0.5$, the weight-average chain length reaches a constant value that is given by $\bar{P}_w = \bar{P}_{wp}/(1-2P_b)$, where $\bar{P}_{wp}$ is the weight-average chain length of the primary chains. On the other hand, the weight-average molecular weight increases without limit for $P_b>0.5$, but it increases very gradually and it takes an infinitely long time to reach an infinitely large polymer molecule. It was found [313] that the formed MWD is a power-law distribution [312] that possesses fractal characteristics is formed.

For the emulsion-polymerized polyethylene shown in Fig. 20, which clearly shows a bimodal MWD, $P_b=0.813>0.5$. For another example investigated in [311], $P_b=0.711>0.5$, and the MWD is bimodal.

On the other hand, for the emulsion polymerization of vinyl acetate, Friis et al. reported that (i) the weight-average molecular weight does not increase significantly until the monomer droplets are depleted, and that (ii) the MWDs are unimodal [314, 315]. They considered the TDBP in addition to the polymer transfer reactions; however, the contribution of the TDBP is minor and a qualitative discussion on the MWD shape could be made without needing to involve the TDBP. The parameters they used are $C_m=2.32\times10^{-4}$, $C_{fp}=3.98\times10^{-4}$ and $x_c=0.2$, which gives $P_b=0.3$. With $P_b=0.3$, the theoretical analysis in [311] showed

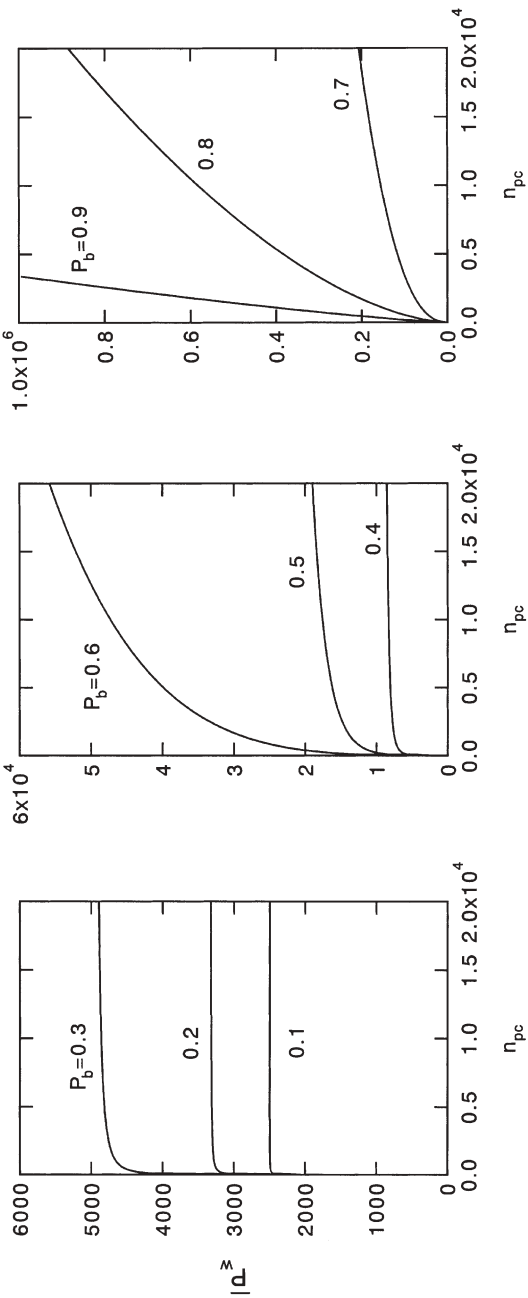

Fig. 21 Calculated development of the weight-average chain length during the model emulsion polymerization

that (i) the weight-average chain length reaches a steady state value rather quickly, and that (ii) the MWDs formed are unimodal, both of which agree with experimental observations.

Although the kinetic behavior during Interval III was not considered in [311], P_b=0.5 is an important consideration when we look at the possibility of forming bimodal MWDs in emulsion polymerization that involves chain transfer to polymer.

4.2.2 Crosslinked Polymers

4.2.2.1 Crosslinked Structure

Assuming that classical chemical kinetics are valid and that the crosslinking reaction rate is proportional to the concentrations of polymer radicals and pendant double bonds, it was shown theoretically that the crosslinked polymer formation in emulsion polymerization differs significantly from that in corresponding bulk systems [270, 316]. To simplify the discussion, it is assumed here that the comonomer composition in the polymer particles is the same as the overall composition in the reactor, and that the weight fraction of polymer in the polymer particle is constant as long as the monomer droplets exist. These conditions may be considered a reasonable approximation to many systems, as shown both theoretically [316] and experimentally [271, 317]. First, consider Flory's simplifying assumptions for vinyl/divinyl copolymerization [318]; that: (1) the reactivities of all types of double bonds are equal, (2) all double bonds

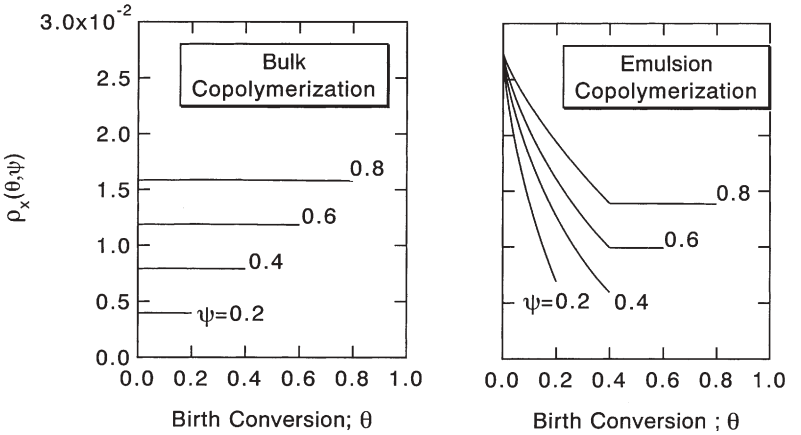

Fig. 22 Crosslinking density distribution development during bulk and emulsion polymerization under Flory's simplifying assumptions, where the initial mole fraction of divinyl monomer is 0.01, and x_c=0.4 for emulsion polymerization

react independently, and (3) there are no cyclization reactions in finite molecules. Under these simplifying assumptions, a completely homogeneous network is formed in homogeneous batch polymerization [319].

Figure 22 shows the calculated results for the expected crosslinking density of primary chains formed at conversion θ when the conversion at the present time is ψ, under Flory's simplifying assumptions for bulk and emulsion copolymerization.

The expected crosslinking density is the same for all primary chains at any stage of polymerization in a bulk system, indicating that a statistically homogeneous network is formed. On the other hand, the crosslinking density distribution is completely different in emulsion polymerization. In particular, the crosslinking densities of the primary chains formed in the earlier stages of polymerization are very high, and the variance of the crosslinking density distribution is significant in emulsion polymerization. The bending at θ=0.4 occurs because the conversion at which monomer droplets disappear is assumed to be 0.4 in these calculations. Homogeneous networks cannot be formed, even under Flory's simplifying assumptions in emulsion crosslinking copolymerization.

Figure 23 shows the average crosslinking density development under Flory's simplifying assumptions.

The average crosslinking density is higher for emulsion polymerization due to the higher polymer concentration effects inside the polymer particles, which are the loci of polymerization. The fact that the average crosslinking density is high even from a very early stage of polymerization has been confirmed experimentally, and this agrees with theoretical calculations adequately [271,

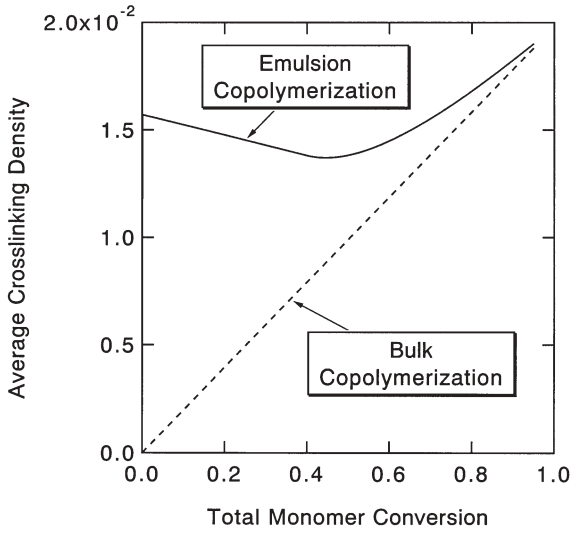

Fig. 23 Average crosslinking density development under Flory's simplifying assumptions

272, 317]. The fact that the average crosslinking densities in some emulsion polymerizations may not change much during emulsion polymerization, as shown in Fig. 23, is sometimes misunderstood as producing a homogeneous polymer network [320]. However, this argument may not be true, as shown in the crosslinking density distribution profile shown in Fig. 22.

4.2.2.2 Unique Molecular Weight Distributions

It has long been recognized that microgels formed in emulsion polymerization possess only supermolecular size and weight [321]. It is known that a reaction system with divinyl monomer makes the particle size smaller compared to the cases without crosslinker [97, 322]. Assuming that the final particle diameter is 50 nm, the molecular weight of this particle is about 4×10^7 g/mol. Such microgels could be soluble in a good solvent, and the MWD could be determined by

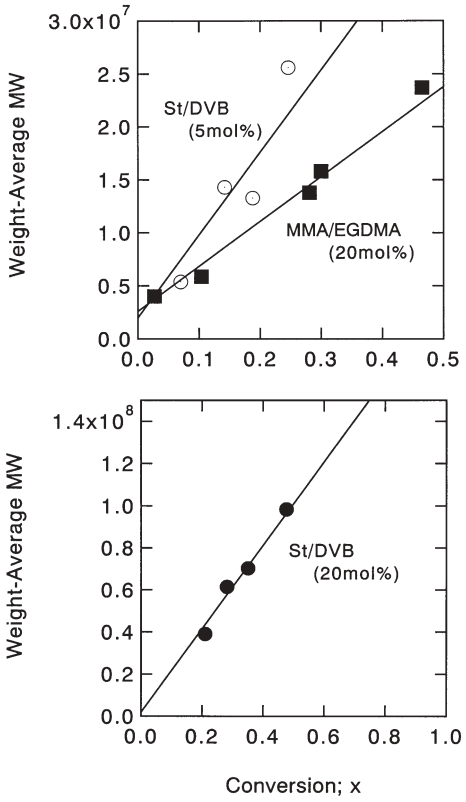

Fig. 24 Experimental results for the weight-average molecular weight development during the emulsion crosslinking copolymerization of styrene (St)/divinylbenzene (DVB) and methyl methacrylate (MMA)/ethylene glycol dimethacrylate (EGDMA). Data from [323]

using SEC even when each polymer particle forms a single crosslinked polymer molecule.

In a typical recipe for microgel formation, a sufficient amount of crosslinker is used. Because the crosslinking density tends to be high from a very early stage of polymerization, the MC simulation results showed [270, 271] that each polymer particle tends to consist of a single large crosslinked polymer molecule even from the early stage of polymerization. In such cases, it was shown [270, 271] that (1) the weight-average molecular weight grows linearly with conversion, and (2) the MWD formed is narrow and the distribution shifts to larger molecular weights, preserving the narrow profile, as polymerization proceeds.

Experimental data [323–325] in which the MWDs are measured by SEC with on-line multiangular laser light scattering (MALLS) show the above trend [326]. Figure 24 shows some examples of the weight-average molecular weight development, which show linear increases with respect to conversion.

The *y*-intercept might approximately correspond to the weight-average molecular weight of primary chains. It was further confirmed [326] that the MWD of polymer molecules and that of whole polymer particles are the same, showing that each polymer particle essentially consists of one crosslinked polymer molecule. Figure 25 shows such an example, and the MWD formed agrees reasonably well with the particle size distribution represented in terms of molecular weights.

On the basis of the MC simulation results [270], it is expected that if the amount of divinyl monomer is reduced to the level of, say, several crosslinkers per primary chain, a bimodal MWD (as shown in Fig. 26) may result.

The arrows indicate the molecular weight of a dried polymer particle, which gives an upper limit to the molecular weight of the polymers attainable. Qualitatively speaking, the high molecular weight peaks are formed because the crosslinked polymer molecules want to grow further due to the higher chain

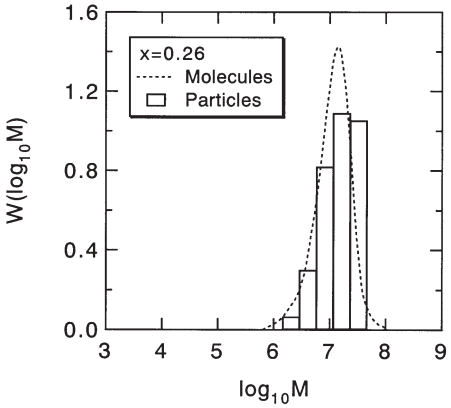

Fig. 25 MWD of polymer molecules and dried polymer particles in the emulsion copolymerization of St and DVB (20 mol%) [326]

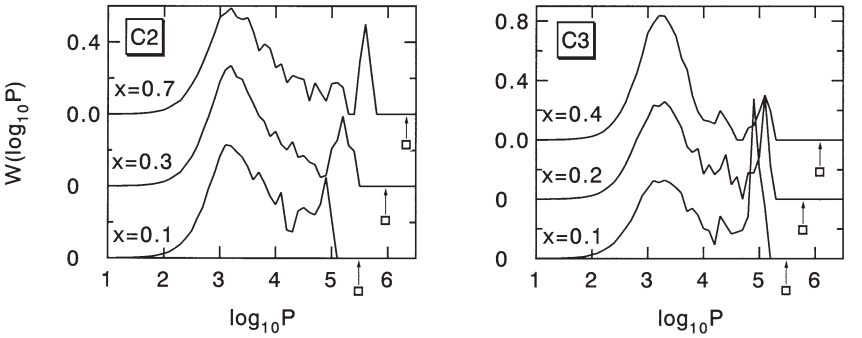

Fig. 26 MC simulation results that show bimodal MWDs in the emulsion copolymerization of vinyl/divinyl monomers [270]

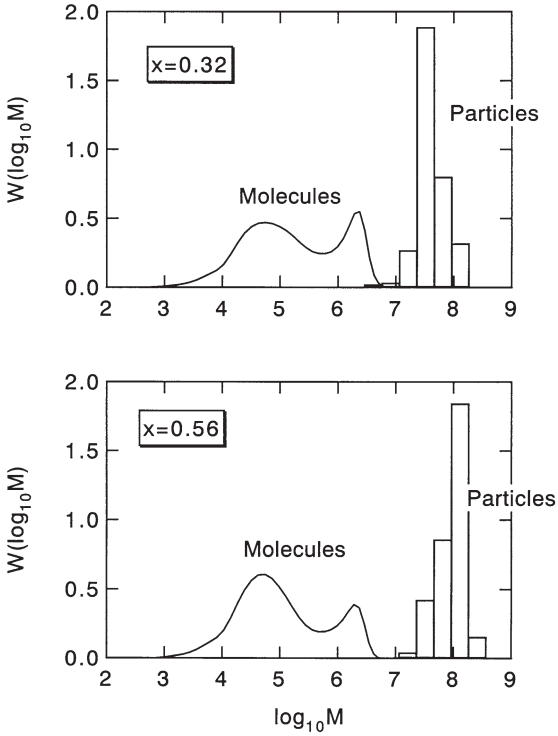

Fig. 27 Experimentally obtained MWD developments of polymer molecules and particles for the emulsion copolymerization of St and DVB [327]

connectivity, but they cannot because of the limitation of a small particle size. Experimentally, such unique bimodal distributions were obtained in the styrene/divinyl benzene system [327] by setting the number of divinylbenzene molecules per chain to ~5. An example of a bimodal MWD, together with the particle size distribution [327], is shown in Fig. 27.

It was found that the locations of these peaks can be controlled independently. The location of a high molecular weight peak is mainly controlled by the particle size, and the location of a low molecular weight peak is controlled by the chain lengths of the primary polymer molecules.

The MC simulation method is particularly suitable for investigating emulsion polymerization that involves various simultaneous kinetic events with a very small locus of polymerization. The MC simulation method will become a standard mathematical tool for the analysis of complex reaction kinetics, both for linear and nonlinear emulsion (co)polymerization.

5
Continuous Emulsion Polymerization

Continuous emulsion polymerization processes are industrially important for the large-scale production of synthetic polymer latexes, and have been used particularly where the solid polymer is to be recovered by coagulating the polymer latex. St-Bu rubber latex was one of the earliest latex products manufactured using continuous emulsion polymerization processes consisting of a number of stirred-tank reactors in series (CSTRs). Since the 1940s, continuous emulsion polymerization processes have been developed for a variety of products and with different reactor configurations [328]. This is because these continuous reactor systems have several advantages, such as [329]:

- Economical production of large-volume or closely-related products
- Uniform product quality
- Full utilization of heat transfer capability
- Fewer problems with wall polymer build-up and coagulation.

However, these systems have also potential disadvantages, such as [329]:

- Less flexibility in terms of the operation and control of product characteristics
- Possible production of off-specification material during start-up or product change-overs
- Difficulties with the direct development of continuous processes based on the information from batch and semi-batch R&D.

Reflecting the importance of continuous emulsion polymerization processes, numerous investigations have been carried out to date, which are categorized into three groups: (1) studies on the reactor configuration (stirred-tank reactors, tubular type reactors such as a simple tubular reactors, pulsed tubular reactors

and loop-tubular reactors, pulsed packed column reactors, Couett-Taylor vortex flow reactors and combinations of these reactors); (2) studies on operational techniques (pre-reactor concept [330] and split-feed operation [331–333]), and; (3) studies on the kinetics and mechanisms of particle formation and growth in a given reactor system. Research work carried out before ~1990 was introduced in a compact but excellent review article [328], which also included those cited in a review article published in 1977 [334]. The present review, therefore, mainly refers to the research work that has been published since ~1990, but also includes any historically important works reported before ~1990.

The stirred-tank reactor and the tubular reactor are two basic reactors used for continuous processes, so much of the experimental and theoretical studies published to date on continuous emulsion polymerization have been conducted using these reactors. The most important elements in the theory of continuous emulsion polymerization in a stirred-tank reactor or in stirred-tank reactor trains were presented by Gershberg and Longfield [330]. They started with the S-E theory for particle formation (Case B), employing the same assumptions as stated in Sect. 3.3, and proposed the balance equation describing the steady-state number of polymer particles produced as:

$$dN_T/dt = \rho_w[A_m/(A_m + A_p)] - N_T/\theta = 0 \tag{90}$$

where θ is the mean residence time of a single CSTR. Introducing the relation, $A_m+A_p=a_sS_0$ into Eq. 90 yields

$$N_T = \rho_w[1 - (A_p/a_sS_0)] \tag{91}$$

where S_0 is the emulsifier concentration in the feed. The residence time distribution for polymer particles in a perfectly mixed CSTR is given by $E(t)dt= dN_T/N_T=(1/\theta)\exp(-t/\theta)dt$. The total surface area of polymer particles per unit volume of water A_p is obtained by the integration

$$A_p = \int_0^{N_T} a_p dN_T = (36\pi)^{1/3} \int_0^{N_T} v_p^{2/3} dN_T = (36\pi)^{1/3} N_T \int_0^{\infty} (\mu t)^{2/3} E(t)\, dt \tag{92}$$

where a_p is the surface area of a polymer particle and $E(t)$ is the residence time distribution function. Combining Eqs. 91 and 92 gives

$$N_T = \frac{\rho_w \theta}{1 + (4.36 \rho_w \mu^{2/3} \theta^{5/3} a_s S_0)} \tag{93}$$

Thus, the rate of polymerization R_p can be predicted using Eqs. 1, 51 and 93.

Omi et al. [335] and Nomura et al. [163] pointed out that Eq. 93 suggests the existence of a maximum number of polymer particles $N_{T,max}$ at the optimum residence time θ_{max}, which is given by

$$\theta_{max} = 0.53(a_sS_0/\rho_w\mu^{2/3})^{3/5} \tag{94}$$

$$N_{T,max} = 0.21(\rho_w/\mu)^{0.4}(a_SS_0)^{0.6} \tag{95}$$

By comparing Eq. 31 with Eq. 95, they also pointed out that $N_{T,max}$ is only 58% of that produced in a batch operation with the same recipe and temperature, and also that

$$\theta_{max} = 0.83 t_c \tag{96}$$

where t_c is the time at which particle formation stops due to complete depletion of micelles in the water phase, in a batch operation with the same recipe as that used in a continuous operation.

Gershberg and Longfield [330] carried out the continuous emulsion polymerization of St at 70 and 100 °C in a train of three CSTRs, and compared the experimental results with theoretical predictions. They presented the following conclusions and suggestions;

1. The theoretical equation $N_T \propto R_p \propto \rho_w^0 S_0^{1.0} \theta^{-2/3}$, derived from Eqs. 1 and 93, correctly predicts the effect of the operating variables upon the rate of polymerization in the stirred-tank reactors at any stage at 70 °C for large θ values.
2. The number of polymer particles produced at 70 °C (and hence, the rate of polymerization) was higher than that at 100 °C, as Eq. 93 predicted.
3. The theory and the experimental data from this study demonstrates that in a train of CSTRs, essentially all of the particles form in the first reactor. Therefore, it is possible to maximize the monomer conversion in the latex leaving the first reactor by keeping the temperature and the residence time at the first reactor as low as possible in order to produce the maximum number of polymer particles and so increase the rate of polymerization in the succeeding stages. This is the so-called "*pre-reactor*" concept.
4. $N_{T,max}$ certainly occurs at low θ, as the theory predicts.
5. Sustained oscillation can take place in the monomer conversion.
6. The residence time in the first stage should be long enough to overcome the retarding effects of traces of oxygen and/or impurities in the feed-stream upon particle formation and growth.

Poehlein and Degraff [336] extended the derivation of Gershberg and Longfield [330] to the calculation of both molecular weight and particle size distribution in the continuous emulsion polymerization of St in a CSTR. On the other hand, Nomura et al. [163] carried out the continuous emulsion polymerization of St in a cascade of two CSTRs and developed a novel model for the system by incorporating their batch model [14], which introduced the concept that the radical capture efficiency of a micelle relative to a polymer particle was much lower than that predicted by the diffusion entry model ($\rho \propto d^{1.0}$). The assumptions employed were almost the same as those of Smith and Ewart (Sect. 3.3), except that the model did not assume a constant value of μ. The elementary reactions and their rate expressions employed in the first stage are as follows:

1. Particle formation by radical entry into a micelle (Eq. 32):

$$R^* + m_s \rightarrow N^*, k_{em} m_s [R_w^*] \tag{32}$$

2. Formation of dead particles by entry of a radical into an active particle containing a radical (Eq. 33):

$$R^* + N^* \rightarrow N_0, k_{ep} N^* [R_w^*] \tag{33}$$

3. Formation of active particles by entry of a radical into a dead particle containing no radical (Eq. 34):

$$R^* + N_0 \rightarrow N^*, k_{ep} N_0 [R_w^*] \tag{34}$$

where m_s is the concentration of monomer-swollen micelles, $[R_w^*]$ is the concentration of free radicals in the water phase, N^* is the concentration of active particles containing a radical, N_0 is the concentration of dead particles that contain no radicals, k_{em} is the rate constant for the entry of radicals into micelles, and k_{ep} is the rate constant for the entry of radicals into particles. If these rate expressions are used, then the balance equation describing the steady-state number of polymer particles produced becomes

$$dN_T/dt = \rho_w [k_1 m_s R^*/(k_1 m_s R^* + k_2 N_T R^*)] - N_T/\theta = 0 \tag{97}$$

where $N_T = N^* + N_0$. Then Eq. 97 is rearranged to give

$$N_T = \rho_w \theta/[1 + (k_2 N_T/k_1 m_s)] = \rho_w \theta/(1 + \varepsilon N_T/S_m) \tag{98}$$

where $\varepsilon = (k_2/k_1) M_m$; M_m is the aggregation number per micelle and S_m is the concentration of emulsifier forming micelles, given by $S_m = S_0 - (A_p/a_s)$. Rearranging Eq. 98 along with the steady-state balance equations for the monomer and the number of active particles finally yields

$$\varepsilon N_T^2/(\rho_w \theta - N_T) = S_0 - k_v (K M_0/2)[\rho_w \theta/(\rho_w \theta - N_T/2)]^{2/3} N_T \theta^{2/3} \tag{99}$$

where k_v and K are the constants associated with the adsorption area of the emulsifier on the particles' surface and the particle growth rate, respectively, and M_0 is the concentration of the monomer in the feed. Equation 99 can be used to calculate the relationship between N_T and θ, and that between $N_{T,max}$ and θ_{max}. A comparison of the experimental data and theoretical predictions for the dependence of N_T on θ is presented in Fig. 28 [163, 331].

The experimental data showed much better agreement with the results predicted using Eq. 99 than the results calculated using the Gershberg and Longfield model (Eq. 93), which gave a higher value of $N_{T,max}$ and a smaller value of θ_{max}. The reason for this may be that the rate of radical entry into a micelle must be less than that predicted by the collision entry model, given by $\rho_w [d_m^2/(d_m^2 + d_p^2)]$.

Gerrens and Kuchner [337] investigated the continuous emulsion polymerization kinetics in a cascade of three CSTRs, and with St and MA as monomers with different solubilities in water. They showed that the experimental results obtained with St agreed with the predictions from the Gershberg and Longfield

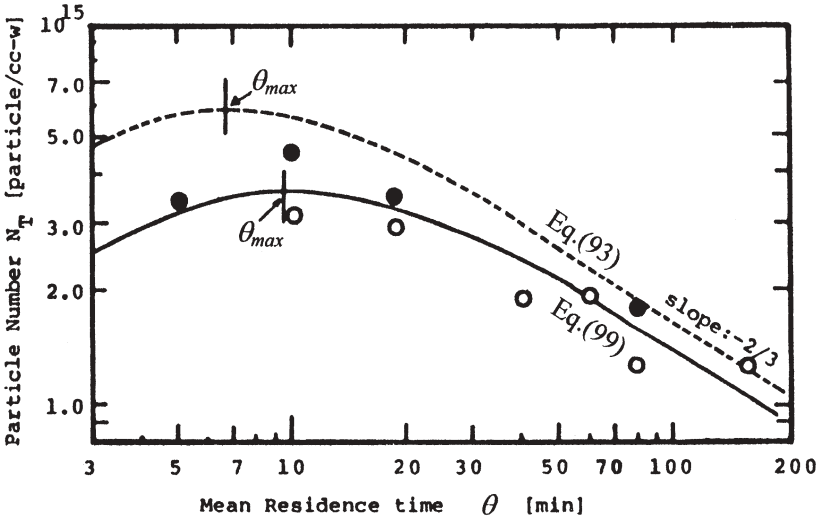

Fig. 28 Effect of the mean residence time in the first reactor θ on the number of polymer particles produced (S_0 (NaLS)=12.5 g/dm^3-water, I_0 (KPS)=1.25 g/dm^3-water, M_0 (St)= 500 g/dm^3-water; 50 °C. Experimental data: empty circles, first reactor; filled circles, second reactor

model, but for MA only the particle number varied in the manner predicted by the Gershberg and Longfield model. This showed that a relatively water-soluble monomer does not correlate with the model based on S-E theory. The existence of multiple steady-states for the isothermal operation of continuous emulsion polymerization in a CSTR was first demonstrated by Gerrens et al. [338, 339]. It is now well understood from a kinetic point of view that this phenomenon takes place as a consequence of the so-called "*gel-effect*" (the Trommsdorff-Norrish effect).

Oscillations in the number of polymer particles, the monomer conversion, and the molecular weight of the polymers produced, which are mainly observed in a CSTR, have attracted considerable interest. Therefore, many experimental and theoretical studies dealing with these oscillations have been published [328]. Recently, Nomura et al. [340] conducted an extensive experimental study on the oscillatory behavior of the continuous emulsion polymerization of VAc in a single CSTR. Several researchers have proposed mathematical models that quantitatively describe complete kinetics, including oscillatory behavior [341–343]. Tauer and Müller [344] proposed a simple mathematical model for the continuous emulsion polymerization of VCl to explain the sustained oscillations observed. Their numerical analysis showed that the oscillations depend on the rates of particle growth and coalescence. However, it still seems to be difficult to quantitatively describe the kinetic behavior (including oscillations) of the continuous emulsion polymerization of monomers, especially those with relatively high solubility in water. This is mainly because the kinetics and mech-

anisms of particle formation in systems containing such monomers are not completely understood yet. It is now known that oscillations in the monomer conversion and the molecular weight of the polymer produced occur due to oscillations in the number of polymer particles. Since oscillatory behavior is undesirable in practice from the standpoint of stable operation and product quality problems, a variety of techniques have been proposed to eliminate the oscillations in the number of polymer particles. The simplest but most effective technique among them would be to add a small continuous tubular type reactor – a pre-reactor with plug flow, operating as a seed generator (a seeding reactor), located upstream of the main CSTRs [331, 345].

To meet the growing demand for the large-scale production of latex with narrow PSD and consistent quality, it was initially recognized that continuous emulsion polymerization in a tubular reactor might be advantageous from the standpoint of higher performance (compared to a CSTR), greater heat transfer, better quality control and lower equipment costs [346]. Nevertheless, very little research work has been done with tubular reactors compared to CSTRs. Feldon et al. [346] successfully performed the continuous emulsion copolymerization of St and Bu in a continuous tubular reactor. It was originally thought that the polymerization needed to be conducted in the turbulent flow regime in order to obtain satisfactory heat transfer and mixing. However, it was found that this turbulent flow gave rise to the formation of a pre-coagulum, which resulted in an accumulation of polymer particles on the reactor wall which eventually plugged the reactor. Therefore, the stable and long-term operation of a continuous tubular reactor (CTR) is usually a very difficult task [346]. In addition, when the rate of polymerization is low, as it often is in such reactors, a very long tube is necessary to achieve high monomer conversion. This is not practical because it is difficult to transport a highly viscous latex product through a long tube.

In order to make full use of the advantages of a tubular reactor while avoiding its drawbacks, the use of a continuous loop-tubular reactor (CLTR) has been proposed. Background on this discovery, as well as a discussion of the main characteristics of the continuous loop-tubular reactor, was first provided by Geddes [347]. He studied the changes in properties during emulsion copolymerization in a continuous loop reactor, with particular reference to particle size distribution. Cycling of properties similar to that observed in CSTRs was found [348]. Bataille and co-workers [349, 350] carried out the emulsion homopolymerizations of St and VAc using a batch loop-tubular reactor. They found that a limiting conversion, lower than that obtained in a stirred-tank batch reactor, occurred for all cases, and that the value of the limiting conversion was a maximum at the laminar-turbulent transition point. Lee et al. [351–352] carried out the continuous emulsion polymerization of St in a continuous loop-tubular reactor with recycling. The effects of the emulsifier, initiator, and monomer concentrations, temperature, and mean residence time on the monomer conversion, average particle diameter, the number of polymer particles produced and, in some cases, the average molecular weight, were ex-

amined to clarify the characteristics of a CLTR. Overshoots in both monomer conversion and the number of polymer particles were observed, but these diminished at about three times the mean residence time. Neither oscillations nor multiple steady-states were observed. The steady-state number of polymer particles was independent of the mean residence time. Asua and co-workers [21, 353–356] carried out the redox-initiated emulsion copolymerization of VAc and Veoba 10 in a CLTR. They studied the effect of the flow rate on shear-induced coagulation and the effect of the start-up strategy on the smoothness of the operation and on the amount of off-specification product, as well as proposing a mathematical model for the process [353, 354]. They compared the performance of a CLTR with that of a CSTR operating under similar conditions, and concluded that, in most cases, both reactors showed a similar performance, but under exigent conditions, the CSTR was prone to thermal runaway, whereas the CLTR was much safer [355]. Moreover, the effects on the reactor performance of both macromixing (residence time distribution) and micromixing (the degree of monomer distribution in polymer particles) in the reaction mixture were examined and the macromixing was characterized by means of tracer response experiments [356]. They also showed that when the recycle ratio (the ratio of the flow rate inside the reactor to the feed flow rate) was increased, the behavior of the reactor approached that of a CSTR, and that when the feed was pre-emulsified, the state of micromixing was substantially improved because the rate of monomer diffusion from the monomer droplets into the polymer particles was enhanced. Araújo et al. [21] developed a detailed dynamic mathematical model that described the evolution of PSDs during the emulsion copolymerization of VAc and Veova 10 in a CLTR and compared the calculated results with their experimental data.

With the aim of improving the performance of a continuous tubular reactor by decreasing its backmixing, a pulsed tubular (PT) reactor [357], a pulsed packed column (PPC) reactor [358], and a pulsed sieve plate column (PSPC) reactor [19] have been proposed as continuous reactors with near-plug flow. These reactors are considered to be modified versions of a tubular reactor, but with less backmixing than a simple tubular reactor. Paquet and Ray [357] successfully conducted the continuous emulsion polymerization of MMA in a PT reactor. When they performed the first four runs without any pulsation, only one of the runs was successful; the other three plugged. They found, therefore, that the use of a pulsation source eliminated the reactor fouling and plugging problem that has frequently occurred in continuous tubular reactors. Also, no oscillatory behavior was observed. The exit conversion remained constant for three residence times and was close to that observed in a corresponding batch reactor. No clear dependence of the pulsation rate on monomer conversion was revealed.

Mayer et al. [358] investigated the performance of a PPC reactor in the continuous emulsion polymerization of St. They found that the number of polymer particles produced in the PPC reactor depended strongly on the residence time distribution (RTD) – in other words, on the pulsation conditions – and that it had a value between those recorded for the batch and the CSTR processes.

They developed a mathematical model based on a micellar nucleation hypothesis and plug flow with axial dispersion, and showed that there was a good agreement between the model predictions and the experimental results. On the other hand, Scholtens et al. [359] extended the Mayer model and predicted the effect of RTD on the intermolecular chemical composition distribution (CCD) of copolymers produced in the continuous emulsion polymerization of St and MA in a PPC reactor with side feed streams. They concluded that the PPC reactor was a good continuously operated alternative to a semi-batch process that produces latexes with a predicted CCD. Sayer et al. [19] utilized a PSPC reactor for the continuous emulsion polymerization of VAc and developed a dynamic mathematical model to simulate the experimental results, showing that the continuous PSPC reactor could be described by an axial dispersion model that covered the entire range between the plug flow and perfectly mixed stirred-tank reactors. Another possible way of producing a plug flow is to use a reactor system with a cascade of CSTR trains. Certainly, the larger the number of stages, the closer the flow pattern will approach plug flow. However, an increase in the number of stages is not necessarily desirable because of the probability of shear-induced latex coagulation, caused by the increased exposure of latex particles to stirring.

As an alternative to a cascade of CSTR trains, a novel continuous reactor with a Couette-Taylor vortex flow (CTVF) has been proposed, which can realize any flow pattern between plug and perfectly mixed flows [361–366]. A continuous Couette-Taylor vortex flow reactor (CCTVFR) consists of two concentric cylinders with the inner cylinder rotating and with the outer cylinder at rest. Figure 29 shows a typical flow pattern caused by the rotation of the inner cylinder.

Nomura et al. [360, 364] first utilized a Couette-Taylor vortex flow reactor (CTVFR) for the continuous emulsion polymerization of St to clarify its char-

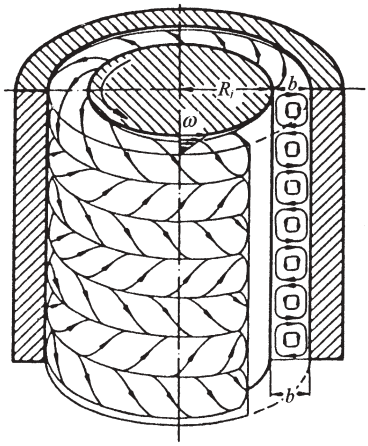

Fig. 29 Taylor vortices between two concentric cylinders (Couette-Taylor vortices): inner cylinder rotating, outer cylinder at rest

acteristics as a continuous emulsion polymerization reactor, and developed a model for the continuous emulsion polymerization of St in a single CCTVFR that incorporated their batch model. The flow pattern is governed by the dimensionless number called the Taylor number, T_a, defined by

$$T_a = \left(\frac{\omega b R_i}{\nu}\right)\left(\frac{b}{R_i}\right) \tag{100}$$

where R_i is the inner cylinder radius, b is the radial clearance between two concentric cylinders, ν is the kinematic viscosity, and ω is the angular velocity of the inner cylinder. When the Taylor number exceeds a certain value between 46 and 60, called the critical Taylor number, T_{ac}, a transition occurs from pure Couette flow to a flow regime in which toroidal vortices are regularly spaced along the cylinder axis, as shown in Fig. 29, which is the so-called "Couette-Taylor vortex flow". They adopted the tank-in-series model that has only one parameter, N, the number of tanks in series, to characterize the deviation of the flow in the CCTVFR from plug flow. The relationship between the number of tanks N and the Taylor number T_a was determined by using a stimulus-response method. Figure 30 shows an interesting example of the monomer con-

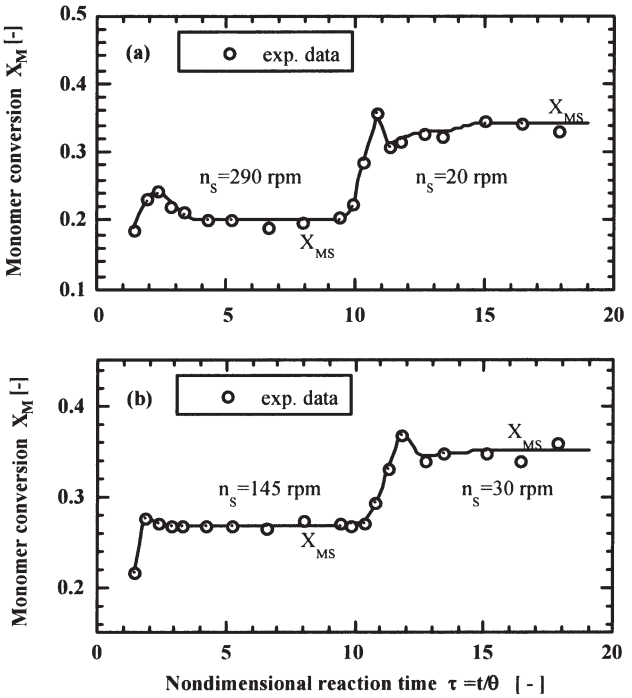

Fig. 30 Effect of rotational speed of inner cylinder on steady-state monomer conversion (S_0 (NaLS)=6.25 g/dm^3-water, I_0 (KPS)=1.25 g/dm^3-water, M_0 (St)=100 g/dm^3-water; 50 °C)

version versus reaction time, where the steady-state monomer conversion was increased from 27 to 35% simply by decreasing the rotational speed of the inner cylinder from 145 to 30 rpm.

This can be explained by the fact that the flow in the CCTVFR became closer to plug flow as the Taylor number was dropped closer to T_{ac}. Therefore, the steady-state particle number and the steady-state monomer conversion could be arbitrarily varied by simply varying the rotational speed of the inner cylinder. Moreover, no oscillations were observed, and the rotational speed of the inner cylinder could be kept low, so that the possibility of shear-induced coagulation could be decreased. Therefore, a CCTVFR with these characteristics is considered to be highly suitable as a pre-reactor for a continuous emulsion polymerization process. In the case of the continuous emulsion polymerization of VAc carried out with the same CCTVFR, however, the situation was quite different [365]. Oscillations in monomer conversion were observed, and almost no appreciable increase in steady-state monomer conversion occurred even when the rotational speed of the inner cylinder was decreased to a value close to T_{ac}. Why the kinetic behavior with VAc is so different to that with St cannot be explained at present.

Ohmura et al. [361, 362] carried out the continuous emulsion polymerization of St and of VAc in a single CCTVFR from the standpoint of controlling the particle size distribution of the latex produced. They also observed no oscillations in the monomer conversion for the St system, but did observe them in the system with VAc. They concluded that a self-sustained oscillation would be useful for controlling the size of latex particles and for raising the monomer conversion. On the other hand, Schmidt et al. [363] studied the continuous emulsion polymerization of *n*-BA in a single CCTVFR. The special flow pattern and residence time distributions of the reactor were investigated at different flow conditions. Both the hydrodynamics and the monomer conversion of the CCTVFR were modeled using computational fluid dynamics simulations. The model predictions were in good agreement with experimental results.

In order to increase the performance and the productivity of the whole continuous reactor system, it has been suggested that a pre-reactor operating as a seed generator (a seeding reactor) should be placed upstream of a reactor train. Even when it is optimized to have the mean residence time as θ_{max}, the steady-state number of polymer particles in a continuous stirred-tank pre-reactor, reaches only 58% of the number produced in an ideal plug flow reactor or in a batch reactor using the same recipe and temperature conditions [163, 335]. Therefore, it is generally desirable to place a pre-reactor with plug flow behavior (such as tubular, PSPC, PPC and CTVF reactors) upstream of the main reactors, because this can produce a similar number of polymer particles to that produced in a batch reactor if properly operated. Instead of incorporating a pre-reactor, Nomura et al. [331, 332] have devised an operational technique called "*split-feed operation*", by which the number of polymer particles produced could be increased to much higher than that in a batch reactor under

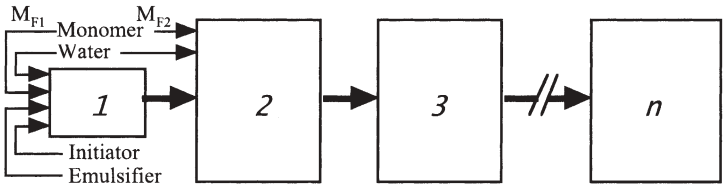

Fig. 31 Schematic diagram of split-feed operation in continuous emulsion polymerization

the same recipe conditions. Figure 31 indicates the general concept of the split-feed operation.

In a batch emulsion polymerization of St, they found that the number of polymer particles produced increased when the amount of initially charged monomer was decreased below a critical value, M_c, as shown in Fig. 32, where the solid line shows the values predicted by

$$N_T = (a_s^3 \rho_p^2 / 36\pi) S_0^3 M_0^{-2} I_0^0 \tag{101}$$

where ρ_p is the polymer density, and S_0, M_0 and I_0 are the emulsifier, monomer and initiator concentrations, respectively.

When a monomer split-feed operation based on the experimental result shown in Fig. 32 was applied, for example, to a continuous tubular pre-reactor with some backmixing, the number of polymer particles increased by about 30% at M_{F1}=0.02 g/cm^3-water, compared to the number produced in a batch reactor, as shown in Fig. 33.

The monomer split-feed operation was also shown to work in a continuous stirred-tank pre-reactor. When certain conditions are fulfilled, the split-feeds

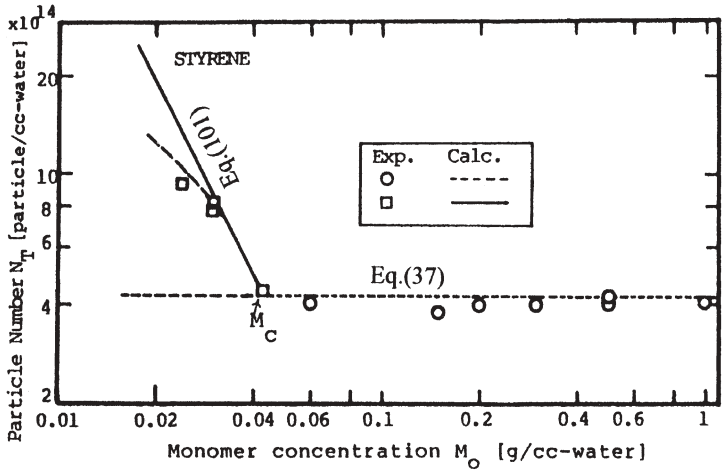

Fig. 32 Effect of lowering the initial monomer concentration on particle formation in the batch emulsion polymerization of St (S_0 (NaLS)=6.25 g/dm^3-water, I_0 (KPS)=1.25 g/dm^3-water, M_0 (St)=variable; 50 °C)

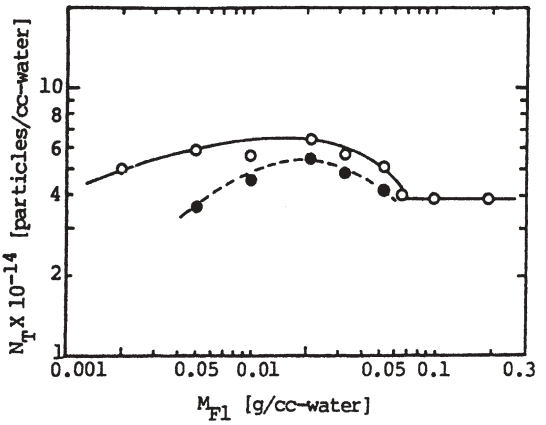

Fig. 33 Effect of monomer concentration M_{F1} fed to the first tubular seeding reactor with back mixing on the number of polymer particles produced (S_0 (NaLS)=6.25 g/dm^3-water, I_0 (KPS)=1.25 g/dm^3-water, M_{F1} (St)=variable; 50 °C. Experimental data: empty circles, particle number observed at t=40 min in a batch reactor; filled circles, steady-state particle number observed in the first tubular seeding reactor operated with mean residence time τ=40 min)

of emulsifier, initiator and water could effectively increase the number of polymer particles produced. The split-feed operation has additional advantages in that the volume of a pre-reactor can be made smaller, and oscillations can be eliminated when it is applied to a continuous stirred-tank pre-reactor. Penlides et al. [333] have also discussed the advantages of the split-feed operation.

Despite the industrial importance, very little work on the kinetics of continuous emulsion copolymerization has been reported. Poehlein et al. [366, 367] carried out the continuous emulsion copolymerization of St-AM and St-AN using a continuous reactor system comprised of a tubular reactor followed by one or two stirred-tank reactors, and developed a steady-state model by employing the kinetic model proposed by Nomura et al. [14] for batch emulsion copolymerization. Their model could predict the latex particle size distribution, average number of radicals per particle, rate of copolymerization, and copolymer composition. They also investigated the continuous emulsion copolymerization of a moderately water-soluble monomer, ethyl acrylate, with a completely water-soluble monomer, methacrylic acid. Several continuous processes involving a tubular reactor and/or a CSTR were designed and utilized so as to produce a latex product with properties similar to the batch product [368, 369]. Nomura et al. [370] carried out the continuous emulsion copolymerization of a sparingly water-soluble monomer, St, with a moderately water-soluble monomer, MMA, in a single CSTR, in order to experimentally elucidate how the kinetic behavior of the continuous emulsion homopolymerization of a sparingly water-soluble monomer changes when it is copolymerized with a moderately water-soluble monomer.

6 Concluding Remarks

The kinetics and mechanisms of particle growth and polymer structure development are comparatively well understood compared to those of particle nucleation. Therefore, the rate of polymerization and the properties of the polymer produced can be (roughly) estimated as long as the number of polymer particles produced is known (for example, in seeded emulsion polymerization). However, the prediction of the number of polymer particles produced is still far from being an established technique. Therefore, further efforts are needed to qualitatively and quantitatively clarify the effects of numerous factors that affect the process of particle formation in order to gain a more quantitative understanding of emulsion polymerization.

References

1. Gilbert RG (1995) Emulsion polymerization: A mechanistic approach. Academic, London
2. Lovell PA, El-Aasser MS (eds)(1997) Emulsion polymerization and emulsion polymers. Wiley, New York
3. Fitch RM (1997) Polymer colloids: A comprehensive introduction. Academic, London
4. Smith WV, Ewart RH (1948) J Chem Phys 16:592
5. Harkins WD (1947) J Am Chem Soc 69:1428
6. Leslie GL, Napper DH, Gilbert RG (1992) Aust J Chem 45:2057
7. Yeliseeva VI (1982) In: Piirma I (ed) Emulsion polymerization. Academic, New York, p 247
8. Gardon JL (1968) J Polym Sci A1 6:623
9. Ugelstad J, Hansen FK (1976) Rubber Chem Technol 49:536
10. Penboss IA, Napper DH, Gilbert RG (1983) J Chem Soc Farad T 1 79:1257
11. Maxwell IA, Morrison BR, Napper DH, Gilbert RG (1991) Macromolecules 24:1629
12. López de Arbina L, Barandiaran MJ, Gugliotta LM, Asua JM (1996) Polymer 37:5907
13. Gardon JL (1968) J Polym Sci A1 6:643
14. Harada M, Nomura M, Kojima H, Eguchi W, Nagata S (1972) J Appl Polym Sci 16:811
15. Hansen FK, Ugelstad J (1978) J Polym Sci Pol Chem 16:1953
16. Hansen FK (1992) ACS Sym Ser 492:12
17. Hansen FK (1993) Chem Eng Sci 48:437
18. Unzueta E, Forcada J (1997) J Appl Polym Sci 66:445
19. Sayer C, Palma M, Giudici R (2002) Ind Eng Chem Res 41:1733
20. Nomura M, Harada M, Eguchi W, Nagata S (1976) ACS Sym Ser 24:102
21. Araujo PHH, de la Cal JC, Asua JM, Pinto JC (2001) Macromol Theor Simul 10:769
22. Herrera-Ordóñez J, Olayo R (2000) J Polym Sci Pol Chem 38:2201
23. Dong Y, Sundberg DC (2002) Macromolecules 35:8185
24. Hawkett BS, Gilbert RG, Napper DH (1980) J Chem Soc Farad T 1 76:1323
25. Colombie D, Sudol ED, El-Aasser MS (2000) Macromolecules 33:4347
26. Marestin C, Guyot A, Claverie J (1998) Macromolecules 31:1686
27. Schoonbrood HAS, German AL, Gilbert RG (1995) Macromolecules 28:34
28. Liotta V, Georgakis C, Sudol ED, El-Aasser MS (1997) Ind Eng Chem Res 36:3252

29. Tauer K, Deckwer R (1998) Acta Polym 49:411
30. Adams ME, Trau M, Gilbert RG, Napper DH, Sangster DF (1988) Aust J Chem 41:1799
31. Penboss IA, Gilbert RG, Napper DH (1986) J Chem Soc Farad T 1 82:2247
32. Kusters JMH, Napper DH, Gilbert RG (1992) Macromolecules 25:7043
33. Wang X, Boya B, Sudol ED, El-Aasser MS (2001) Macromolecules 34:8907
34. Coen EM, Lyons RA, Gilbert RG (1996) Macromolecules 29:5128
35. Cheong IW, Kim JH (1997) Colloid Polym Sci 275:736
36. Vorwerg L, Gilbert RG (2000) Macromolecules 33:6693
37. Leemans L, Jerome R, Teyssie P (1998) Macromolecules 31:5565
38. Ohtsuka Y, Kawaguchi H, Sugi Y (1981) J Appl Polym Sci 26:1637
39. Nomura M, Ichikawa H, Fujita K, Okaya T (1997) J Polym Sci Pol Chem 35:2689
40. Nomura M, Suzuki K (2004) Prog Coll Pol Sci 124:7
41. Ugelstad J, Mørk PC, Dahl P, Rangnes P (1969) J Polym Sci C27:49
42. Nomura M, Harada M, Eguchi W, Nagata S (1971) J Chem Eng Jpn 4:54
43. Nomura M (1982) In: Piirma I (ed) Emulsion polymerization. Academic, New York, p 191
44. Nomura M, Harada M (1981) J Appl Polym Sci 26:17
45. Nomura M, Yamamoto K, Horie I, Fujita K, Harada M (1982) J Appl Polym Sci 27:2483
46. Casey BS, Morrison BR, Maxwell IA, Gilbert RG, Napper DH (1994) J Polym Sci Pol Chem 32:605
47. Nomura M, Kubo M, Fujita K (1983) J Appl Polym Sci 28:2767
48. Adams M, Napper DH, Gilbert RG, Sangster DF (1986) J Chem Soc Farad T 1 82:1979
49. Asua JM, Sudol ED, EL-Aasser MS (1989) J Polym Sci Pol Chem 27:3903
50. Barandiaran MJ, Asua JM (1996) J Polym Sci Pol Chem 34:309
51. Asua JM (1998) Polymer 39:2061
52. Morrison BR, Casey BS, Lacik I, Leslie GL, Sangster DF, Gilbert RG, Napper DH (1994) J Polym Sci Pol Chem 32:631
53. Kim JU, Lee HH (1996) Polymer 37:1941
54. Fang S-J, Wang K, Pan Z-R (2003) Polymer 44:1385
55. López de Arbina L, Barandiaran MJ, Gugliotta LM, Asua JM (1997) Polymer 38:143
56. Forcada J, Asua JM (1990) J Polym Sci Pol Chem 28:987
57. Barudio I, Guillot, Fevotte G (1998) J Polym Sci Pol Chem 36:157
58. Saldivar E, Dafniotis P, Ray WH (1998) J Macromol Sci R M C 38:207
59. Saldiver E, Araujo O, Giudici R, López-Barrón C (2001) J Appl Polym Sci 79:2380
60. Araujo O, Giudici R, Saldivar E, Ray WH (2001) J Appl Polym Sci 79:2360
61. Vega JR, Gugliotta LM, Bielsa RO, Brandolini MC, Meira GR (1997) Ind Eng Chem Res 36:1238
62. Gugliotta LM, Brandolini MC, Vega JR, Iturralde EO, Azum JL, Meira GR (1995) Polym React Eng 3:201
63. Barandiaran MJ, López de Arbina L, de la Cal JC, Gugliotta LM, Asua JM (1995) J Appl Polym Sci 55:231
64. Nomura M, Harada M, Nakagawara K, Eguchi W, Nagata S (1971) J Chem Eng Jpn 4:160
65. Hansen FK, Ugelstad J (1979) Makromol Chem 180:2423
66. Fitch RM (1981) ACS Sym Ser 165:1
67. Hansen FK, Ugelstad J (1982) In: Piirma I (ed) Emulsion polymerization. Academic, New York, p 51
68. Tauer K, Kuhn I (1995) Macromolecules 28:2236
69. Kuhn I, Tauer K (1995) Macromolecules 28:8122
70. Lichti G, Gilbert RG, Napper DH (1983) J Polym Sci Pol Chem 21:269
71. Feeney PJ, Napper DH, Gilbert RG (1984) Macromolecules 17:2520
72. Richards JR, Congalidis JP (1989) J Appl Polym Sci 37:2727

73. Sütterlin N (1980) In: Fitch RM (ed) Polymer colloids II. Plenum, New York, p 583
74. Nomura M, Fujita K (1994) Polym React Eng 2:317
75. Nomura M, Kodani T, Ojima J, Kihara Y, Fujita K (1998) J Polym Sci Pol Chem 36:1919
76. Morrison BR, Maxwell IA, Gilbert RG, Napper DH (1992) In: Daniels ES, Sudol ED, El-Aasser MS (eds) Polymer Latexes. ACS Symp Ser. 492. Am Chem Soc, Washington DC, p 28
77. Sajjadi S, Brooks BW (1999) J Polym Sci Pol Chem 37:3957
78. Nomura M, Sakai H, Kihara Y, Fujita K (2002) J Polym Sci 40:1275
79. Yuan X-Y, Dimonie VL, Sudol ED, Roberts JE, El-Aasser MS (2002) Macromolecules 35:8356
80. Herrera-Ordóñez J, Olayo R (2000) J Polym Sci Pol Chem 38:2219
81. Herrera-Ordóñez J, Olayo R (2001) J Polym Sci Pol Chem 39:2547
82. Varela de la Rosa L, Sudol ED, EL-Aasser MS, Klein A (1996) J Polym Sci Pol Chem 34:461
83. Varela de la Rosa L, Sudol ED, EI-Aasser MS, Klein A (1999) J Polym Sci Pol Chem 37:4066
84. Varela de la Rosa L, Sudol ED, EI-Aasser MS, Klein A (1999) J Polym Sci Pol Chem 37:4073
85. Nomura M, Satpathy US, Kouno Y, Fujita K (1988) J Polym Sci Pol Lett 26:385
86. Nomura M, Takahashi K, Fujita K (1990) Makromol Chem–M Symp 35/36:13
87. Chern C-S, Lin C-H (1998) Polymer 40:139
88. Chern C-S, Lin C-H (2000) Polymer 41:4473
89. Wang Z, Paine AJ, Rudin A (1995) J Polym Sci Pol Chem 33:1597
90. Morrison BR, Gilbert RG (1995) Macromol Symp 92:13
91. Coen EM, Gilbert RG, Morrison BR, Leube H, Peach S (1998) Polymer 39:7099
92. Prescott SW, Fellows CM, Gilbert RG (2002) Macromol Theor Simul 11:163
93. Butucea V, Sarbu A, Georgescu C (1998) Angew Makromol Chem 255:37
94. Cheong I-W, Kim J-H (1998) Macromol Theor Simul 7:49
95. Sajjadi S (2000) J Polym Sci Pol Chem 38:3612
96. Sajjadi S (2001) J Polym Sci Pol Chem 39:3940
97. Nomura M, Fujita K (1993) Polym Int 30:483
98. Sajjadi S (2002) J Polym Sci Pol Chem 40:1652
99. Ozdeger E, Sudol ED, El-Aasser MS, Klein A (1997) J Polym Sci Pol Chem 35:3813
100. Ozdeger E, Sudol ED, El-Aasser MS, Klein A (1997) J Polym Sci Pol Chem 35:3827
101. Ozdeger E, Sudol ED, El-Aasser MS, Klein A (1997) J Polym Sci Pol Chem 35:3837
102. Lin S-Y, Capek I, Hsu T-J, Chern C-S (1999) J Polym Sci Pol Chem 37:4422
103. Unzueta E, Forcada J (1995) Polymer 36:4301
104. Chen L-J, Lin S-Y, Chern C-S, Wu S-C (1997) Colloid Surface A 122:161
105. Lin S-Y, Capek I, Hsu T-J, Chern C-S (2000) Polym J 32:932
106. Colombie D, Sudol ED, El-Aasser MS (2000) Macromolecules 33:7283
107. Asua JM, Schoonbrood HAS (1998) Acta Polym 49:671
108. Amalvy JI, Unzue MJ, Schoonbrood HAS, Asua JM (1998) Macromolecules 31:5631
109. Wang X, Sudol ED, El-Aasser MS (2001) J Polym Sci Pol Chem 39:3093
110. Wang X, Sudol ED, El-Aasser MS (2001) Macromolecules 34:7715
111. Cochin D, Laschewsky A, Nallet F (1997) Macromolecules 30:2278
112. Ayoub MMH, Nasr HE, Rozik NN (1998) J Macromol Sci Pure 35:1415
113. Ayoub MMH (1998) J Elastom Plast 30:207
114. Wang X, Sudol ED, El-Aasser MS (2001) Langmuir 17:6865
115. Kato S, Nomura M (1999) Colloid Surface A 153:127
116. Cheong I-W, Nomura M, Kim J-H (2001) Macromol Chem Phys 202:2454

117. Piirma I (1993) Polymer surfactants (Surfactant Science Series No 42). Marcel Dekker, New York
118. Capek I (2002) Adv Colloid Interfac 99:77
119. O'Toole JT (1965) J Appl Polym Sci 9:1291
120. Ugelstad J, Mørk PC, Aasen JO (1967) J Polym Sci A1 5:2281
121. Stockmayer WH (1957) J Polym Sci 24:314
122. (a) Nomura M, Fujita K (1985) Makromol Chem Suppl 10/11:25, (b) Nomura M (1987) Kobunshi Kagaku 36:680
123. Sakai H, Kihara Y, Fujita K, Kodani T, Nomura M (2001) J Polym Sci Pol Chem 39:1005
124. Asua JM, Adams ME, Sudol ED (1990) J Appl Polym Sci 39:1183
125. Mendoza J, de la Cal JC, Asua JM (2000) J Polym Sci Pol Chem 38:4490
126. Kiparissides C, Achilias CDS, Frantzikinakis CE (2002) Ind Eng Chem Res 41:3097
127. de la Cal JC, Asua JM (2001) J Polym Sci Pol Chem l39:585
128. Gilmore CM, Poehlein GW, Schork FJ (1993) J Appl Polym Sci 48:1449
129. Gilmore CM, Poehlein GW, Schork FJ (1993) J Appl Polym Sci 48:1461
130. Budhlall BM, Sudol ED, Dimonie VL, Klein A, El-Aasser MS (2001) J Polym Sci Pol Chem 39:3633
131. Shaffie KA, Moustafa AB, Mohamed ES, Badran AS (1997) J Polym Sci Pol Chem 35:3141
132. Bruyn HD, Gilbert RG, Ballard MJ (1996) Macromolecules 29:8666
133. Chern C-S, Poehlein GW (1987) J Appl Polym Sci 33:2117
134. Bruyn HD, Miller CM, Bassett DR, Gilbert RG (2002) Macromolecules 35:8371
135. Matsumoto A, Kodama K, Aota H, Capek I (1999) Eur Polym J 35:1509
136. Ballard MJ, Napper DH, Gilbert RG (1981) J Polym Sci Pol Chem 19:939
137. Nomura M, Kubo M, Fujita K (1981) Mem Fac Eng Fukui Univ 29:167
138. Storti G, Carra S, Morbidelli M, Vita G (1989) J Appl Polym Sci 37:2443
139. Tobita H, Hamielec AE (1989) Macromolecules 22:3098
140. Nomura M, Horie I, Kubo M, Fujita K (1989) J Appl Polym Sci 37:1029
141. Chen S-A, Wu K-W (1988) J Polym Sci Pol Chem 26:1487
142. Giannetti E (1989) Macromolecules 22:2094
143. Saldivar E, Ray WH (1997) Ind Eng Chem Res 36:1322
144. Dube MA, Penlidis A, Mutha RK, Cluett WR (1996) Ind Eng Chem Res 35:4434
145. Martinet F, Guillot J (1999) J Appl Polym Sci 72:1627
146. Vicente M, Leiza JR, Asua JM (2001) AIChE J 47:1594
147. Vega JR, Gugliotta LM, Meira GR (2002) Polym React Eng 10:59
148. Shoaf GL, Poehlein GW (1991) J Appl Polym Sci 42:1213
149. Yang B-Z, Chen L-W, Chiu W-Y (1997) Polym J 29:744
150. Yang B-Z, Chen L-W, Chiu W-Y (1997) Polym J 29:737
151. Slawinski M, Schellekens MAJ, Meuldijk J, Herk AMV, German AL (2000) J Appl Polym Sci 76:1186
152. Wang PH, Pan C-Y (2001) Colloid Polym Sci 279:98
153. Santos AMD, Mckenna TF, Guillot J (1997) J Appl Polym Sci 65:2343
154. Yan C, Cheng S, Feng L (1999) J Polym Sci Pol Chem 37:2649
155. Henton DE, Powell C, Reim RE (1997) J Appl Polym Sci 64:591
156. Xu Z, Yi C, Cheng S, Zhang J (1997) J Appl Polym Sci 66:1
157. Fang S-J, Fujimoto K, Kondo S, Shiraki K, Kawaguchi H (2000) Colloid Polym Sci 278:864
158. Kostov GK, Petrov PC (1994) J Polym Sci Pol Chem 32:2229
159. Petrov PC, Kostov GK (1994) J Polym Sci Pol Chem 32:2235
160. Noel LFJ, Altveer JLV, Timmermans MDF, German AL (1996) J Polym Sci Pol Chem 34:1763

161. Urretabizkaia A, Asua JM (1994) J Polym Sci Pol Chem 32:1761
162. Ge X, Ye Q, Xu X, Chu G, Zhang Z (1998) J Appl Polym Sci 67:1005
163. Nomura M, Kojima H, Harada M, Eguchi W, Nagata S (1971) J Appl Polym Sci 15:675
164. Morton M, Kaizerman S, Altier MW (1954) J Colloid Sci 9:300
165. Gardon JL (1968) J Polym Sci A1 6:2859
166. Maxwell IA, Kurja J, Doremaele GHV, German AL, Morrison BR (1992) Makromol Chem 193:2049
167. Antonietti M, Kasper H, Tauer K (1996) Langmuir 12:6211
168. Vanzo E, Marchessault RH, Stannett V (1965) J Colloid Sci 20:62
169. Ugelstad J, Mørk PC, Mfutakamba HR, Soleimany E, Nordhuus I, Schmid R, Berge A, Ellingsen T, Aune O, Nustad K (1983) In: Pohelein GW, Ottewill RH, Goodwin JW (eds) Science and technology of polymer colloids, vol 1 (NATO ASI Ser E:67). Martinus Nijhoff, Boston, MA, p 51
170. Maxwell IA, Kurja J, van Doremaele GHJ, German AL (1992) Makromol Chem 193:2065
171. Schoonbrood HAS, German AL (1994) Macromol Rapid Commun 15:259
172. Noël LFJ, Maxwell IA, German AL (1993) Macromolecules 26:2911
173. Schoonbrood HAS, Boom MATVD, German AL, Hutovic J (1994) J Polym Sci Pol Chem 32:2311
174. Noël LFJ, van Zon JMAM, Maxwell IA, German AL (1994) J Polym Sci Pol Chem 32:1009
175. Gugliotta LM, Arzamendi G, Asua JM (1995) J Appl Polym Sci 55:1017
176. Karlsson O, Wesslen B (1998) J Appl Polym Sci 70:2041
177. Mathey P, Guillot J (1991) Polymer 32:934
178. Nomura M, Liu X, Ishitani K, Fujita K (1994) J Polym Sci Pol Phys 32:2491
179. Liu X, Nomura M, Fujita K (1997) J Appl Polym Sci 64:931
180. Liu X, Nomura M, Liu Y-H, Ishitani K, Fujita K (1997) Ind Eng Chem Res 36:1218
181. Aerdts AM, Boei MWA, German AL (1993) Polymer 34:574
182. Said ZFM, Fataftah ZA (1996) Polym Int 40:307
183. Tognacci R, Storti G, Bertucco A (1996) J Appl Polym Sci 62:2341
184. Varela de la Rosa L, Sudol ED, EI-Aasser MS, Klein A (1999) J Polym Sci Pol Chem 37:4054
185. Cheong I-W, Kim J-H (1999) Colloid Surface A 153:137
186. BenAmor S, Colombie D, McKenna T (2002) Ind Eng Chem Res 41:4233
187. Tauer K, Muller H, Schellenberg C, Rosengarten L (1999) Colloid Surfuce A 153:143
188. López de Arbina L, Gugliotta LM, Barandiaran MJ, Asua JM (1998) Polymer 39:4047
189. de Buruaga IS, Arotcarena M, Armitage PD, Gugliotta LM, Leiza JR, Asua JM (1996) Chem Eng Sci 51:781
190. de Buruaga IS, Echevarria A, Armitage PD, de la Cal JC, Leiza JR, Asua JM (1997) AIChE J 43:1069
191. Gugliotta LM, Leiza JR, Arotcarena M, Armitage PD, Asua JM (1995) Ind Eng Chem Res 34:3899
192. Nomura M, Ashizawa N (1998) US Patent 5 762 879, assigned to Todoroki Sangyo Co, Fukui, Japan
193. Breitenbach VJW, Edelhauser H (1961) Macromol Chem 44–47:196
194. van der Hoff BME (1960) J Polym Sci 48:175
195. Al-Shahib WAG, Dunn AS (1980) Polymer 21:429
196. Barton J, Karpatyova A (1987) Makromol Chem 188:693
197. Il'menev PY, Litvinenko GI, Kaminskii VA, Gritskova IA (1988) Polym Sci USSR 30:826
198. Nomura M, Fujita K (1989) Makromol Chem Rapid Commun 10:581
199. Nomura M, Yamada A, Fujita S, Sugimoto A, Ikoma J, Fujita K (1991) J Polym Sci Pol Chem 29:987

200. Nomura M, Ikoma J, Fujita K (1992) ACS Sym Ser 492:55
201. Nomura M, Fujita K (1992) DECHEMA Monogr 127:359
202. Nomura M, Ikoma J, Fujita K (1993) J Polym Sci Pol Chem 31:2103
203. Asua JM, Rodriguez VS, Sudol ED, El-Aasser MS (1989) J Polym Sci Pol Chem 27:3569
204. Alduncin JA, Forcada J, Barandiaran MJ, Asua JM (1991) J Polym Sci Pol Chem 29:1265
205. Vaskova V, Renoux D, Bernard M, Selb J, Candau F (1995) Polym Advan Technol 6:441
206. Mørk PC (1995) J Polym Sci Pol Chem 33:2305
207. Mørk PC, Ugelstad J, Aasen JO (1995) J Polym Sci Pol Chem 33:1759
208. Mørk PC, Makame Y (1997) J Polym Sci Pol Chem 35:2347
209. Suzuki K, Goto A, Takayama M, Muramatsu A, Nomura M (2000) Macromol Symp 155:99
210. Nomura M, Suzuki K (1997) Macromol Chem Phys 198:3025
211. Capek I (2001) Adv Colloid Interfac 91:295
212. Biggs S, Grieser F (1995) Macromolecules 28:4877
213. Ooi SK, Biggs S (2000) Ultrason Sonochem 7:125
214. Cooper C, Grieser F, Biggs S (1996) J Colloid Interf Sci 184:52
215. Bradley M, Grieser F (2002) J Colloid Interf Sci 251:78
216. Chou HCJ, Stoffer JO (1999) J Appl Polym Sci 72:797
217. Chou HCJ, Stoffer JO (1999) J Appl Polym Sci 72:827
218. Liao Y, Wang Q, Xia H, Xu X, Baxter SM, Slone RV, Wu S, Swift G, Westmoreland DG (2001) J Polym Sci Pol Chem 39:3356
219. Xia H, Wang Q, Liao Y, Xu X, Baxter SM, Slone RV, Wu S, Swift G, Westmoreland DG (2002) Ultrason Sonochem 9:151
220. Nomura M, Harada M, Eguchi W, Nagata S (1972) J Appl Polym Sci 16:835
221. Penlidis A, Macgegor JF, Hamielec AE (1988) J Appl Polym Sci 35:2023
222. Cunningham MF, Geramita K, Ma JW (2000) Polymer 41:5385
223. Bruyn HD, Gilbert RG, Hawkett BS (2000) Polymer 41:8633
224. Kokthoff IM, Harris WE (1947) J Polym Sci 2:49
225. Whang BCY, Lichti G, Gilbert RG, Napper DH (1980) J Polym Sci Pol Lett 18:711
226. Nomura M, Minamino Y, Fujita K, Harada M (1982) J Polym Sci Pol Chem 20:1261
227. Lichti G, Sangster DF (1982) J Chem Soc Farad T 1 78:2129
228. Maxwell IA, Morrison BR, Napper DH, Gilbert RG (1992) Makromol Chem 193:303
229. Weerts PA, van der Loos JLM, German AL (1991) Makromol Chem 192:2009
230. Huo BP, Campbell JD, Penlidis A, Macgregor JF, Hamielec AE (1987) J Appl Polym Sci 35:2009
231. Kemmere MF, Mayer MJJ, Meuldijk J, Drinkenburg AAH (1999) J Appl Polym Sci 71:2419
232. Barton J, Juranicova V (1991) Makromol Chem Rapid Commun 12:669
233. Echevarria A, Leiza JR, de la Cal JC, Asua JM (1998) AIChE J 44:1667
234. Salazar A, Gugliotta LM, Vega JR, Meira GR (1998) Ind Eng Chem Res 37:3582
235. Sayer C, Lim EL, Pinto JC, Arzamendi G, Asua LM (2000) J Polym Sci Pol Chem 38:1100
236. Sayer C, Lima EL, Pinto JC, Arzamendi G, Asua JM (2000) J Polym Sci Pol Chem 38:367
237. Plessis C, Arzamendi G, Leiza JR, Alberdi JM, Schoonbrood HAS, Charmot D, Asua JM (2001) J Polym Sci Pol Chem 39:1106
238. Gugliotta LM, Salazar A, Vega JR, Meira GR (2001) Polymer 42:2719
239. Nomura M, Suzuki H, Tokunaga H, Fujita K (1994) J Appl Polym Sci 51:21
240. Okaya T, Suzuki A, Kikuchi K (2000) Macromol Symp 150:143
241. Bataille P, Dalpe J-F, Dubuc F, Lamoureux L (1990) J Appl Polym Sci 39:1815
242. Shunmukham SR, Hallenbeck VL, Guile RL (1951) J Polym Sci 6:691
243. Schoot CJ, Bakker J, Klaassens KH (1951) J Polym Sci 7:657
244. Evans CP, Hay PM, Marker L, Murray RW, Sweeting OJ (1961) J Appl Polym Sci 5:39

245. Omi S, Shiraishi Y, Sato H, Kubota H (1969) J Chem Eng Jpn 2:64
246. Weerts PA, van der Loos JLM, German AL (1991) Makromol Chem 192:1993
247. Arai K, Arai M, Iwasaki S, Saito S (1981) J Polym Sci Pol Chem 19:1203
248. Kim CU, Lee JM, Ihm SK (1999) J Appl Polym Sci 73:777
249. Ozdeger E, Sudol ED, El-Aasser MS, Klein A (1998) J Appl Polym Sci 69:2277
250. Brooks BW (1971) Brit Polym J 3:269
251. Zubitur M, Asua JM (2001) J Appl Polym Sci 80:841
252. Soares JBP, Hamielec AE (1997) In: Asua JM (ed) Polymeric dispersions (NATO ASI Ser E:335). Kluwer Academic, London, p 289
253. Cunningham MF, Ma JW (2000) J Appl Polym Sci 78:217
254. Ma JW, Cunningham MF (2000) Macromol Symp 150:85
255. Zubitur M, Mendoza J, de la Cal JC, Asua JM (2000) Macromol Symp 150:13
256. Rimmer S, Tattersall P (1999) Polymer 40:5729
257. Rimmer S (2000) Macromol Symp 150:149
258. Leyrer RJ, Machtle W (2000) Macromol Chem Phys 201:1235
259. Lau W (1994) US Patent 5 521 266, assigned to Rohm and Haas Co, Philadelphia, PA, USA
260. Vanderhoff JW (1981) ACS Sym Ser 165:199
261. Lowry V, El-Aasser MS, Vanderhoff JW, Klein A (1984) J Appl Polym Sci 29:3925
262. Matejicek A, Ditl P, Pivonkova A, Kaska J, Formanek L (1988) J Appl Polym Sci 35:583
263. Tobita H, Takada Y, Nomura M (1994) Macromolecules 27:3804
264. Tobita H, Takada Y, Nomura M (1995) J Polym Sci Pol Phys 33:441
265. Tobita H (1995) Macromolecules 28:5128
266. Tobita H (1994) Polymer 35:3023
267. Tobita H (1994) Polymer 35:3032
268. Tobita H (1997) J Polym Sci Pol Phys 35:1515
269. Tobita H, Nomura M (1999) Colloid Surface A 153:119
270. Tobita H, Yamamoto K (1994) Macromolecules 27:3389
271. Tobita H, Uemura Y (1996) J Polym Sci Pol Phys 34:1403
272. Tobita H, Yoshihara Y (1996) J Polym Sci Pol Phys 34:1415
273. Tobita H (1995) Acta Polym 46:185
274. Min KW, Ray HW (1974) J Macromol Sci R M C 11:177
275. Lin CC, Chiu WY (1979) J Appl Polym Sci 23:2049
276. Lichti G, Gilbert RG, Napper DH (1980) J Polym Sci Pol Chem 18:1297
277. Lichti G, Gilbert RG, Napper DH (1982) In: Piirma I (ed) Emulsion polymerization. Academic, New York, p 93
278. Katz S, Shinnar R, Saidel GM (1969) Adv Chem Ser 91:145
279. Giannetti E, Storti G, Morbidelli M (1988) J Polym Sci Pol Chem 26:1985
280. Storti G, Polotti G, Cociani M, Morbidelli M (1992) J Polym Sci Pol Chem 30:731
281. Ghielmi A, Storti G, Morbidelli M (1998) Macromolecules 31:7172
282. Benson SW, North AM (1962) Am Chem Soc 84:935
283. Ito K (1974) J Polym Sci Pol Chem 12:1991
284. Mahabadi HK (1985) Macromolecules 18:1319
285. Olaj OF, Zifferer G, Gleizner G (1986) Makromol Chem 187:977
286. Russell GT, Gilbert RG, Napper DH (1992) Macromolecules 25:2459
287. O'Shaughnessy B, Yu J (1994) Macromolecules 27:5067
288. Buback M, Egorov M, Kaminsky V (1999) Macromol Theor Simul 8:520
289. Russell GT (1994) Macromol Theor Simul 3:439
290. Clay PA, Gilbert RG (1995) Macromolecules 28:552
291. Wulkow M (1996) Macromol Theor Simul 5:393

292. Tobita H (1995) Macromolecules 28:5119
293. Olaj OF, Kauffmann HF, Breitenbach JB (1977) Makromol Chem 178:2707
294. Mayo FR (1943) J Am Chem Soc 65:2324
295. Mayo FR, Gregg RA, Matheson MS (1951) J Am Chem Soc 73:1691
296. Christie DI, Gilbert RG (1996) Macromol Chem Phys 197:403
297. Buback M, Gilbert RG, Russell GT, Hill DJT, Moad G, O'Driscoll KF, Shen J, Winnik MA (1992) J Polym Sci Pol Chem 30:851
298. Tobita H, Shiozaki H (2001) Macromol Theor Simul 10:676
299. Morton M, Salatiello PP (1951) J Polym Sci 6:225
300. Britton D, Heatley F, Lovell PA (1998) Macromolecules 31:2828
301. Tobita H (1993) Polym React Eng 1:357
302. Tobita H, Saito S (1999) Macromol Theor Simul 8:513
303. Tobita H, Hamashima N (2000) J Polym Sci Pol Phys 38:2009
304. Tobita H, Hamashima N (2000) Macromol Theor Simul 9:453
305. Tobita H (2001) J Polym Sci Pol Phys 39:2960
306. Tobita H, Kawai H (2002) E-Polymers 048
307. Starkweather WH Jr, Han MC (1992) J Polym Sci Pol Chem 30:2709
308. Senrui S, Suwa T, Takehisa M (1974) J Polym Sci Pol Chem 12:93
309. Senrui S, Suwa T, Takehisa M (1974) J Polym Sci Pol Chem 12:105
310. Tobita H (2002) J Polym Sci Pol Chem 40:3426
311. Tobita H (2003) Bimodal molecular weight distribution formed in emulsion polymerization with long-chain branching. Polym React Eng 11:855
312. Barabasi A-L, Albert R (1999) Science 286:509
313. Tobita H (2004) Scale-free power-law distribution of emulsion-polymerized nonlinear polymers: Free-radical polymerization with chain transfer to polymer. Macromolecules 37:585
314. Friis N, Goosney D, Wright JD, Hamielec AE (1974) J Appl Polym Sci 18:1247
315. Friis N, Hamielec AE (1975) J Appl Polym Sci 19:97
316. Tobita H (1992) Macromolecules 25:2671
317. Tobita H, Kimura K, Fujita K, Nomura M (1993) Polymer 34:2569
318. Flory PJ (1953) Principles of polymer chemistry. Cornell University Press, Ithaca, NY
319. Tobita H, Hamielec AE (1989) In: Reichert K-H, Geiseler W (eds) Polymer reaction engineering. VCH, Weinheim, Germany, p 43
320. Ding ZY, Ma S, Kriz D, Aklonis JJ, Salovey R (1992) J Polym Sci Pol Phys 30:189
321. Baker WO (1949) Ind Eng Chem 41:511
322. Obrecht W, Seitz U, Funke W (1976) ACS Sym Ser 24:92
323. Nakamura K, Imoto A, Aota H, Matsumoto A (1994) The 8th Polymeric Microsphere Symposium, Fukui, Japan, p 37
324. Matsumoto A, Mori Y, Takahashi S, Aota H (1995) Netsukokasei-Jushi (J Thermoset Plast Jpn) 16:131
325. Matsumoto A, Kodama K, Mori Y, Aota H (1998) Pure Appl Chem A35:1459
326. Tobita H, Kumagai M, Aoyagi N (2000) Polymer 41:481
327. Tobita H, Aoyagi N, Takamura S (2001) Polymer 421:7583
328. Hamielec AE, Tobita H (1992) In: Ulmann's encyclopedia of industrial chemistry, vol A21. VCH, Weinheim, Germany, p 305
329. Pohelein G (1997) In: Lovell PA, El-Aasser MS (eds) Emulsion polymerization and emulsion polymers. Wiley, New York, p 277
330. Gershberg DB, Longfield JE (1961) Symp Polym Kinetics and Catalyst Systems, Preprint 10, 45th AIChE Meeting, New York
331. Nomura M (1981) ACS Sym Ser 165:121

332. Nomura M (1986) In: Reichert K-H, Geisler W (eds) Polymer eeaction engineering. Hüthig & Wepf, Basel, p 41
333. Penlidis A, MacGregor JF, Hamielec AE (1989) Chem Eng Sci 44:273
334. Poehlein GW, Dougherty DJ (1977) Rubber Chem Technol 50:601
335. Omi S, Ueda T, Kubota H (1969) J Chem Eng Jpn 2:193
336. Degraff AW, Poehlein GW (1971) J Polym Sci A2 9:1955
337. Gerrens H, Kuchner K (1970) Brit Polym J 2:18
338. Gerrens H, Kuchner K, Ley G (1971) Chem Ing Tech 43:693
339. Gregor L, Gerrens H (1974) Macromol Chem 175:563
340. Nomura M, Sasaki S, Xue W, Fujita K (2002) J Appl Polym Sci 86:2748
341. Kiparissides C, MacGregor JF, Hamielec AE (1979) J Appl Polym Sci 23:401
342. Rawlings JB, Ray WH (1988) Polym Eng Sci 28:237
343. Rawlings JB, Ray WH (1988) Polym Eng Sci 28:257
344. Tauer K, Muller I (1995) DECHEMA Monogr 131:95
345. Greens RK, Gonzalez RA, Poehlein GW (1976) ACS Sym Ser 24:341
346. Feldon M, McCann RF, Laundrie RW (1953) India Rubber World 128:51
347. Geddes K (1983) Chem Ind 21:223
348. Geddes KR (1989) Brit Polym J 21:443
349. Rollin AL, Patterson I, Huneault R, Bataille P (1977) Can J Chem Eng 55:565
350. Iabbadene A, Bataille P (1994) J Appl Polym Sci 51:503
351. Lee D-Y, Kuo J-F, Wang J-H, Chen C-Y (1990) Polym Eng Sci 30:187
352. Lee D-Y, Wang J-H, Kuo J-F (1992) Polym Eng Sci 32:198
353. Abad C, de la Cal JC, Asua JM (1995) Polymer 36:4293
354. Abad C, de la Cal JC, Asua JM (1994) Chem Eng Sci 49:5025
355. Abad C, de la Cal JC, Asua JM (1995) J Appl Polym Sci 56:419
356. Abad C, de la Cal JC, Asua JM (1995) DECHEMA Monogr 131:87
357. Paquet DA Jr, Ray WH (1994) AIChE J 40:73
358. Mayer MJJ, Meuldijk J, Thoenes D (1996) Chem Eng Sci 51:3441
359. Scholetens CA, Meuleijk J, Drinkenburg AAH (2001) Chem Eng Sci 56:955
360. Imamura T, Saito K, Ishikura S, Nomura M (1993) Polym Int 30:203
361. Kataoka K, Ohmura N, Kouzu M, Okubo Y (1995) Chem Eng Sci 50:1409
362. Ohmura N, Kataoka K, Watanabe S, Okubo M (1998) Chem Eng Sci 53:2129
363. Schmidt W, Kossak S, Langenbuch J, Moritz H-U, Herrmann C, Kremeskötter J (1998) DECHEMA Monogr 134:509
364. Wei X, Takahashi H, Sato S, Nomura M (2001) J Appl Polym Sci 80:1931
365. Xue W, Yoshikawa K, Oshima A, Nomura M (2002) J Appl Polym Sci 86:2755
366. Mead RN, Poehlein GW (1988) Ind Eng Chem Res 27:2283
367. Mead RN, Poehlein GW (1989) Ind Eng Chem Res 28:51
368. Shoaf GL, Poehlein GW (1989) Polym Plast Tech Eng 28:289
369. Poehlein GW (1995) Macromol Symp 92:179
370. Fang S-J, Xue W, Nomura M (2003) Polym React Eng 11:815

Received: February 2004